

**NEW INSIGHTS FROM STUDYING INSULIN-LIKE GROWTH FACTOR
(IGF)-BINDING PROTEIN-5 IN ZEBRAFISH : ROLE OF IGF SIGNALING IN
EPITHELIAL CALCIUM ABSORPTION**

by

Wei Dai

A dissertation submitted in partial fulfillment
of the requirements for the degree of
Doctor of Philosophy
(Molecular, Cellular and Developmental Biology)
in The University of Michigan
2011

Doctoral Committee:

Professor Cunming Duan, Chair
Professor Steven E. Clark
Professor John Y. Kuwada
Assistant Professor Jiandie Lin
Assistant Professor Haoxing Xu

© Wei Dai

2011

DEDICATION

To my parents
and my husband
for their love, support, and encouragement

ACKNOWLEDGEMENTS

The Ph.D. training at the University of Michigan has been an exciting and challenging journey in my life, and I would like to thank all the people who have helped me during the past five and a half years.

I owe the deepest gratitude to my mentor Dr. Cunming Duan for the education, guidance, and support he provided to me during the five years in his lab. Now I can still remember the mini-journal club that he did with me during my rotation, the congratulation gift he sent me when I passed my preliminary exam, the comforting words he said to me when I made a careless mistake in my experiment, the compliments he made when I solved a problem after a long-term struggle, the excitement he expressed when I showed him an unexpected result, and the whole-hearted support he provided throughout the years. More importantly, his insight, devotion, persistence, and optimism will continue to benefit me in my future career.

I am grateful to my committee members: Dr. Steven Clark, Dr. John Kuwada, Dr. Jiandie Lin, and Dr. Haoxing Xu for their constant encouragement and valuable suggestions for my research project. I also want to express my gratitude to Dr. Steven Clark and Dr. Matthew Chapman for providing me with the opportunity to do rotations in their labs.

I feel grateful to all the Duan lab members who have worked with me. I wish to offer special thanks to Dr. Hiroyaso Kamei, Dr. Wei Xia, Dr. Yang Zhao, and Ms. Lisa

Hebda. I thank the Denver lab, Xu lab, Cadigan lab, Raymond lab, Kuwada lab, Hume lab, and Chapman lab for sharing facilities and reagents and providing valuable technical assistance. I also want to thank Dr. Li Qian and Dr. Shenghui He for their suggestions and support as senior graduate students.

Last but not least, I am truly thankful to my family and friends for their care and support. Most importantly, I thank my parents and my husband for their unconditional love.

TABLE OF CONTENTS

DEDICATION	ii
ACKNOWLEDGEMENTS	iii
LIST OF FIGURES	viii
LIST OF TABLES	x
ABSTRACT	xi
CHAPTER 1 Background and Introduction	1
1.1 Introduction	1
1.2 IGF signaling	2
1.2.1 Components of the IGF system	2
1.2.2 Function of IGF signaling	5
1.2.3 IGFBP5	8
1.2.4 Function of IGFBP5	10
1.3 Epithelial calcium absorption	13
1.3.1 Calcium homeostasis	13
1.3.2 Epithelial calcium absorption	15
1.3.3 TRPV5/TRPV6 channels	17
1.3.4 Function of TRPV5/TRPV6	19
1.3.5 Dietary regulation	20
1.4 IGF and calcium homeostasis	22
1.4.1 Role of IGF signaling in calcium homeostasis	22
1.4.2 Role of calcium in regulating growth factor signaling	24
1.5 The zebrafish model	25
1.5.1 General features of the zebrafish model	25
1.5.2 Zebrafish as a model to study IGF signaling	26
1.5.3 Zebrafish as a model to study epithelial calcium transport	28
1.6 Project summary	29
CHAPTER 2 Duplicated zebrafish insulin-like growth factor binding protein-5 genes with split functional domains: Evidence for evolutionarily conserved IGF binding, nuclear localization, and transactivation activity	36

2.1 Abstract.....	36
2.2 Introduction.....	37
2.3 Result	39
2.3.1 Identification of two <i>igfbp-5</i> genes in zebrafish and other teleost fish species	39
2.3.2 The duplicated <i>igfbp-5</i> genes exhibit distinct expression patterns	40
2.3.3 Both IGFBP-5a and -5b are secreted proteins and they both bind to IGF and modulate IGF actions	41
2.3.4 Both IGFBP-5a and -5b are localized in the nucleus, but only IGFBP-5b has transactivation activity	42
2.3.5 Several unique residues in the IGFBP-5 N-domain are critical for the transactivation activity	43
2.4 Discussion.....	45
2.5 Materials and Methods.....	48
2.6 Acknowledgements.....	52
CHAPTER 3 Expression and functional characterization of Igfbp5a in the <i>trpv6</i> -expressing ionocytes in zebrafish embryos.....	68
3.1 Abstract.....	68
3.2 Introduction.....	68
3.3 Result	71
3.3.1 Overlapping spatial and temporal expression patterns of <i>igfbp5a</i> and <i>trpv6</i> ...	71
3.3.2 <i>igfbp5a</i> mRNA colocalizes with <i>trpv6</i> but not <i>atp6v1al</i>	72
3.3.3 The number of <i>trpv6</i> -expressing ionocytes increases in Igfbp5a morphants ..	72
3.3.4 Igfbp5a affects development rather than function of the <i>trpv6</i> -expressing ionocytes.	74
3.4 Discussion.....	75
3.5 Materials and Methods.....	77
3.6 Acknowledgements.....	81
CHAPTER 4 Insulin-like growth factor (IGF) signaling is required for proliferation of the <i>trpv6</i> -expressing Na ⁺ -K ⁺ -ATPase-rich (NaR) cells in response to insufficient calcium supply in zebrafish	90
4.1 Abstract.....	90
4.2 Introduction.....	90
4.3 Result	93
4.3.1 Low-Ca ²⁺ acclimation results in a dramatic increase in the NaR cells and a correlated increase in <i>igfbp5a</i> mRNA expression	93
4.3.2 The increased NaR cells in low-Ca ²⁺ water is due to elevated cell proliferation during the larval stage.....	94

4.3.3 Low Ca ²⁺ acclimation increases <i>trpv6</i> gene expression in addition to the NaR cell number change	95
4.3.4 Low Ca ²⁺ acclimation activates Akt but not MAPK signaling in the NaR cells through an IGF1R-dependent mechanism	96
4.3.5 IGF1R and Akt signaling is required for the low-Ca ²⁺ induced increase in NaR cell proliferation.....	97
4.3.6 <i>Igfbp5a</i> modulates local Igf actions in the NaR cells in low-Ca ²⁺ water.....	98
4.3.7 IGF signaling is also required for the low-Ca ²⁺ induced increase of the NaR cells in adult zebrafish gills.....	99
4.4 Discussion.....	100
4.5 Materials and Methods.....	102
4.6 Acknowledgements.....	106
CHAPTER 5 Conclusions and future directions	123
5.1 Summary of contributions.....	123
5.1.1 Two zebrafish <i>igfbp5s</i> : gene duplication and functional diversification	123
5.1.2 <i>Igfbp5a</i> in the <i>trpv6</i> -expressing NaR cells: a new regulator of calcium homeostasis	124
5.1.3 The IGF system in low-calcium acclimation: growth factor signaling in environmental adaptation.....	124
5.2 Future directions	125
5.2.1 Understand how low-calcium water activates IGF signaling.....	125
5.2.2 Explore how IGF signaling functions in low-calcium acclimation	127
5.3 Conclusions and perspectives	128
REFERENCES	132

LIST OF FIGURES

Figure 1.1 IGF1R signal transduction pathways.....	32
Figure 1.2 Proposed mechanisms of IGFBP5 actions	33
Figure 1.3 Mechanism of Ca ²⁺ homeostasis	34
Figure 1.4 Mechanism of epithelial Ca ²⁺ absorption	35
Figure 2.1 There are two <i>igfbp-5</i> genes in zebrafish and other teleost fish.....	55
Figure 2.2 Zebrafish <i>igfbp-5a</i> and <i>-5b</i> exhibit distinct spatial and temporal expression pattern	57
Figure 2.3 Both zebrafish IGFBP-5a and -5b can bind IGF-1 and regulate its biological activity.....	58
Figure 2.4 Nuclear localization and TA activities of zebrafish IGFBP-5a and -5b.....	59
Figure 2.5 Two unique amino acid changes in the IGFBP-5a N domain are responsible for its lack of TA activity.....	61
Figure 2.6 Proposed model for the gene expression and functional divergence of <i>igfbp-5</i> genes in teleost fish.....	62
Figure 2.7 (supplementary to Figure 2.5.) Sequence alignment of several mammalian and teleost IGFBP-5 N-domains.....	63
Figure 3.1 Overlapping temporal expression pattern of <i>igfbp5a</i> and <i>trpv6</i>	82
Figure 3.2 Similar spatial expression patterns of <i>igfbp5a</i> and <i>trpv6</i>	83
Figure 3.3 <i>igfbp5a</i> mRNA colocalizes with <i>trpv6</i> but not <i>atp6v1al</i>	84
Figure 3.4 Translation-blocking of <i>Igfbp5a</i> results in an increase in the number of <i>trpv6</i> - expressing ionocytes	86
Figure 3.5 Splice-inhibiting of <i>Igfbp5a</i> results in an increase in the number of <i>trpv6</i> - expressing ionocytes	88
Figure 3.6 Knockdown of <i>Igfbp5a</i> results in an increase in Ca ²⁺ influx and content.....	89
Figure 4.1 Low Ca ²⁺ acclimation results in a dramatic increase in the NaR cells and a correlated increase in <i>igfbp5a</i> mRNA expression	108
Figure 4.2 The increase in the NaR cells in low-Ca ²⁺ water is due to elevated cell proliferation during the larval stage.....	110
Figure 4.3 Low Ca ²⁺ acclimation increases <i>trpv6</i> gene expression in addition to the NaR cell number change	112

Figure 4.4 Low Ca^{2+} acclimation activates Akt but not MAPK signaling in NaR cells through an IGF1R-dependent mechanism	114
Figure 4.5 IGF1R and Akt signaling are required for the low- Ca^{2+} induced increase in NaR cell proliferation	116
Figure 4.6 Igfbp5a modulates local Igf actions in the NaR cells in low- Ca^{2+} water	117
Figure 4.7 IGF signaling is also required for the low- Ca^{2+} induced increase of the NaR cells in adult zebrafish gills.....	119
Figure 4.8 (supplementary to Figure 4.7.) Expression analysis of components in the IGF system in zebrafish larvae and adult gill.....	120
Figure 5.1 Model for how epithelial Ca^{2+} absorption increased in acclimation to low environmental Ca^{2+} supply (data, prediction):.....	129
Figure 5.2 pAkt staining of 3 dpf larvae acclimated to normal- or low- Ca^{2+} water for 8 hr. RR, Ruthenium red.	130
Figure 5.3 mRNA levels in 5 dpf larvae acclimated to water with different Ca^{2+} levels.	131

LIST OF TABLES

Table 2.1 Accession numbers of the IGFBP sequences used for the phylogenetic analyses	64
Table 2.2 NCBI or Ensembl Gene ID of the genes used for the conserved synteny analysis	65
Table 2.3 Oligonucleotide primers used for plasmid construction in Chapter 2	66
Table 2.4 Sequence identities between zebrafish IGFBP-5a/-5b and IGFBPs in human and mouse.....	67
Table 4.1 Nominal ion concentrations and osmolarity of the fish media	121
Table 4.2 Oligonucleotide primers used Chapter 4	122

ABSTRACT

Insulin-like growth factors (IGFs) are potent regulators of development and homeostasis. IGF-binding proteins (IGFBPs) are important modulators of IGF signaling. In this study, I took advantage of the zebrafish model to investigate the *in vivo* function of the IGF system, in particular IGFBP5. Two zebrafish *igfbp5* genes were identified, exhibiting functional diversification both in expression patterns and biochemical properties. One of them, *igfbp5a*, is specifically expressed in the *trpv6*-expressing NaR cells in the yolk skin of zebrafish embryos and larvae. These cells mediate epithelial Ca^{2+} absorption from the water, and are functionally equivalent to the enterocytes in the mammalian intestinal epithelium. Morpholino knockdown of *igfbp5a* increased the number of the NaR cells and elevated Ca^{2+} content and Ca^{2+} influx in the embryos, suggesting that *Igfbp5a* functions as a regulator of Ca^{2+} homeostasis by negatively modulating the population of the NaR cells. In zebrafish larvae, *igfbp5a* and *trpv6* co-expressing NaR cells increase their number dramatically in low- Ca^{2+} water. IGF1R downstream Akt signaling is specifically activated upon low- Ca^{2+} treatment. Pharmacological inhibition of IGF1R or PI3K abolished the low- Ca^{2+} induced cell proliferation. These findings suggest that IGF signaling is required for the increase of the NaR cells during low- Ca^{2+} acclimation. Taken together, this study reveals previously unknown roles of IGF and IGFBP5 in epithelial Ca^{2+} transport. It also provides new insight into the molecular regulation of growth factor signaling during development and physiological adaptation.

CHAPTER 1

Background and Introduction

1.1 Introduction

Tissue growth and renewal are not only determined by the intrinsic clock, but they are also subject to environmental modulations. The cellular and molecular processes that can fine-tune cell growth in adaption to environmental changes are of great importance to maintain homeostatic physiological status. Both genetic defects and unfavorable environments may disrupt such homeostasis and cause diseases. Therefore, studying the mechanisms of how internal signaling pathways respond to external alterations not only addresses a fundamental biological question, but it may also contribute to health care and disease treatment.

Hormones and growth factors are critical players in regulating growth and maintaining homeostasis. Insulin like growth factor (IGF), discovered in the 1950s as a potent mitogen to stimulate cartilage growth (Salmon and Daughaday, 1957), is one such player that can function both as an endocrine hormone to control whole body growth and as a local growth factor to exert pleiotropic roles (Le Roith et al., 2001). The activity of IGF can be modulated by IGF-binding proteins (IGFBPs), and recent studies suggest that IGFBP can regulate IGF bioavailability in response to environmental changes (Kajimura et al., 2005).

Nutrient availability is one of the key environmental factors that affect growth. The vertebrate transport epithelia, in close contact with the environment, are tissues actively remodeled by the nutrient status. Ca^{2+} , one of the essential mineral nutrients, is a major component for the bone, an important enzyme cofactor in body fluid, and a second messenger for multiple intracellular signaling pathways. Regulation of Ca^{2+} homeostasis is of critical importance to health.

Recently, the transient receptor potential (TRP) channels, ion channels involved in multiple cellular processes, show emerging roles as cellular sensors in response to environmental stimuli (Clapham, 2003). TRPV5 and TRPV6 are epithelial Ca^{2+} channels involved in epithelial Ca^{2+} transport (Hoenderop et al., 2005). They play important roles in maintaining Ca^{2+} homeostasis. They are also highly responsive to Ca^{2+} availability in external resources.

In this review, background information of the IGF system and epithelial Ca^{2+} absorption will be introduced. Studies suggesting potential links between IGF signaling and Ca^{2+} homeostasis will be reviewed. Questions to be addressed in the thesis study will be summarized.

1.2 IGF signaling

1.2.1 Components of the IGF system

The central IGF axis is composed of two extracellular ligands, IGF1 (Rinderknecht and Humbel, 1978a) and IGF2 (Rinderknecht and Humbel, 1978b), a plasma membrane receptor, IGF1R (Ullrich et al., 1986), and six extracellular IGFBP1-6 (Binkert et al., 1989; Brinkman et al., 1988; Shimasaki et al., 1991a; Shimasaki et al., 1991b; Shimasaki et al., 1990; Wood et al., 1988).

IGFs are so-called insulin-like growth factors because they are structurally similar to and evolutionally conserved with insulin. The A- and B-domains of IGFs are homologous to those of insulin. Unlike insulin, which cleaves off the C-domain of proinsulin to form a mature protein containing the A-domain and B-domain linked by disulfide bonds, IGFs retain their C-domain. In addition, they have D- and E-domains in extension to the carboxy-terminal A-domain. The E-domain is removed in the mature protein (Hylka et al., 1985).

IGF1R is a cell surface tyrosine kinase receptor in a heterotetrameric β - α - α - β form linked by disulfide bonds. The propeptide containing one α - and one β -subunit encoded by the *IGF1R* gene is glycosylated, dimerized, and cleaved to yield α - and β -subunits (Ullrich et al., 1986). The α -subunits contain the ligand binding site (Garrett et al., 1998), and the β -subunits contain the transmembrane domain and intracellular tyrosine kinase domain. IGF1 binds to IGF1R with 0-4 fold higher affinity than IGF2 in different experiments (Danielsen et al., 1990; Forbes et al., 2002; Pandini et al., 2002).

Despite the overall agreement that IGF1R is the main receptor for IGF signaling, involvement of other receptors has been implied. Insulin receptor (INSR), homologous to IGF1R, has two isoforms, IR-A and IR-B, due to alternative splicing of exon 11 encoding 12 amino acids at the carboxy (C)-terminus of the extracellular receptor α -subunit (Seino and Bell, 1989). IGF2, but not IGF1, can bind IR-A with similar affinity as insulin, but it induces a cellular response different from insulin (Frasca et al., 1999; Sciacca et al., 2002). In addition, hybrid receptors resulting from heterodimerization of IGF1R and INSR hemireceptors are proposed to bind IGFs and function in signal transduction (Pandini et al., 2002; Pandini et al., 1999). IGF2R (Morgan et al., 1987), a structurally

different receptor that possesses binding sites for diverse ligands, including IGF2 and mannose-6-phosphate (M6P), functions in sequestering IGF2 and targeting it for lysosomal degradation (Oka et al., 1985). IGF2R binds IGF1 with very low affinity and does not bind insulin (Tong et al., 1988).

IGFBPs, initially identified from serum, amniotic fluid, and other biological resources as high affinity IGF binding proteins, bind IGFs with equal or even stronger affinity than IGF1R (Clemmons, 1997). All *IGFBP* genes contain four coding exons that encode proteins with common domain organizations. After removal of the secretory signal peptide, the mature proteins contain conserved amino (N)- and carboxyl (C)-domains, but variable central linker (L)-domains. Conserved cysteine residues, 12 in the N-domain (except for 10 in IGFBP6) and 6 in the C-domain, form intra-domain disulfide bonds. Both the N- and C-domain contribute to ligand binding. Despite the structural similarities, different IGFBPs vary in expression patterns, biochemical properties, and functions (Duan and Xu, 2005; Firth and Baxter, 2002).

Binding of IGFs to IGF1R induces receptor autophosphorylation, and the signaling is transmitted to a series of downstream cascades (Fig. 1.1). Three tyrosine residues (Tyr1131, Tyr1135 and Tyr1136) within the kinase domain are the earliest major autophosphorylation sites essential for signal transduction (Gronborg et al., 1993; Murakami and Rosen, 1991; White et al., 1988b). Phosphorylation on other tyrosine residues has also been detected. Tyr1251 in the C-terminus of the receptor is required for transforming activity (Miura et al., 1995) and cell proliferation (Blakesley et al., 1998). Tyr950, located in the IGF1R juxtamembrane region, serves as a docking site for several receptor substrates (White et al., 1988a), including the insulin receptor substrates (IRS) 1-

4 and the Src homology collagen (Shc). Once activated, IRS and Shc bind to growth factor receptor-bound protein 2 (Grb2), which in turn recruits the guanine-nucleotide-exchange factor (Sos). This leads to activation of the Ras/Raf/mitogen-activated protein kinase kinase (MEK)/mitogen-activated protein kinase (MAPK) pathway.

Phosphorylated IRS also binds to p85, the regulatory subunit of phosphatidylinositol 3-kinases (PI3K). PI3K activates phosphoinositol-dependent kinases (PDKs), which subsequently phosphorylate Akt at Ser473 and Thr308. Akt activation can phosphorylate multiple downstream targets, including mTOR, GSK3, Bad, and nuclear targets. IGF1R phosphorylation can also activate two other MAPK families, p38 and JNK (Dupont et al., 2003; Samani et al., 2007).

1.2.2 Function of IGF signaling

Broadly expressed in fetuses and adults, the IGF system is involved in embryonic development, postnatal growth, and adult homeostasis.

IGF signaling is important for both prenatal and postnatal growth. In humans, a homozygous partial deletion of the *IGF1* gene was associated with prenatal and postnatal growth failure (Woods et al., 1996). Mutations in the *IGF1R* gene, resulting in decreased function or expression, were associated with retarded intrauterine growth and subsequent growth (Abuzzahab et al., 2003). *Igf1* heterozygous mutant mice have lower levels of IGF1 and weigh 10-20% less than normal adults due to a decrease in organ, muscle, and bone mass. *Igf1* homozygous mutant mice weigh 70% less than normal adults and have defects in brain, bone, muscle, lung, and skin. Single *Igf1* or *Igf2* null mutants have 60% of normal birthweight. *Igf1r* null mutants exhibit a more severe growth deficiency (45% of normal birthweight) and die invariably at birth of respiratory failure. *Igf1* and *Igf1r*

double mutants show the same phenotype as *Igf1r* single mutants, while *Igf2/Igf1r* and *Igf1/Igf2* double mutants show further exacerbated growth deficiency (30% of normal birthweight) (Baker et al., 1993; DeChiara et al., 1990; Liu et al., 1993; Powell-Braxton et al., 1993). IGF2 is also important for placental growth. Combinational knockout (KO) of *Igf1*, *Igf2*, and *Igf1r* in mice showed that placental growth is served exclusively by an IGF2-XR interaction (Baker et al., 1993). The XR was later suggested to be IR-A (Frasca et al., 1999). Mice with an *Igf2r* null allele from their mother (but not father) have 25-30% fetal overgrowth, elevated levels of circulating IGF2, and die around birth (Lau et al., 1994).

The development and function of a broad range of organs and tissues are affected by IGF signaling. β -cell-specific KO of *Igf1r* in mice affects β -cell differentiation, but not growth and development, leading to defective insulin secretion and glucose tolerance (Kulkarni et al., 2002; Ueki et al., 2006). IGF1 has neuroprotective effects in Huntington's disease patients by inhibiting mutant huntingtin-induced cell death and reducing the formation of intranuclear inclusions of mutant huntingtin through the Akt pathway (Humbert et al., 2002). Muscle-specific overexpression of *Igf1* in mice results in myocyte hypertrophy and preserves muscle function in Duchenne muscular dystrophy (Barton et al., 2002; Musaro et al., 2001). In vascular growth, low IGF1 levels are associated with a lack of vessel growth in premature infants (Hellstrom et al., 2001), and vascular endothelial cell-specific KO of *Igf1r* in mice causes a 34% reduction in neovascularization following hypoxia (Kondo et al., 2003). The IGF system is also important for reproduction and gonad development. Mice with null mutations of *Igf1* are infertile (Baker et al., 1993). XY mice mutant for the *Ir*, *Igf1r*, and *Irr* develop ovaries

and exhibit a female phenotype, indicating that the insulin receptor tyrosine kinase family is required for male sexual differentiation (Nef et al., 2003).

Emerging evidence reveals a function of IGF signaling in stem cells. Age-associated changes in stem cell supportive niche cells deregulate haematopoiesis through dysfunction of haematopoietic stem cells. These defects in niche cells can be reversed by neutralization of IGF1 in the marrow (Mayack et al., 2010). Human ES cells and autologously derived human ES fibroblast-like cells (hdFs) are defined by IGF-dependence. IGF1R is expressed exclusively in ES cells, and FGFR1 is expressed in hdFs. Survival of ES cells is reduced when the IGF2/IGF1R pathway is blocked (Bendall et al., 2007).

Recent studies demonstrate IGF signaling as a critical player in aging. A positive role in local tissues and a negative role in the whole body have been proposed. IGF is generally considered neuroprotective, and its decline in the brain is associated with reduced cognitive functions (Aleman et al., 1999) and increased brain amyloid β levels (Carro et al., 2002) in old-aged people. Studies in model organisms in worm, fly (Clancy et al., 2001; Wessells et al., 2004), and mouse (Holzenberger et al., 2003) consistently show that reduced IGF signaling prolongs lifespan.

Dysregulation of the IGF system leads to, or associates with, a plethora of human diseases including cancer. Overexpression of *IGF2* is associated with Beckwith-Wiedemann syndrome (Weksberg et al., 1993), overgrowth disorder (Morison et al., 1996), and Silver-Russell Syndrome hypomethylation (Bartholdi et al., 2009). Elevated IGF1 or IGF2 levels are observed in a variety of cancers and tumors in humans. Breast cancer risk correlates with circulating IGF1 (Hankinson et al., 1998). IGF2 level is

elevated in Wilms tumors (Reeve et al., 1985; Scott et al., 1985), rhabdomyosarcoma (Pedone et al., 1994), intestinal tumor (Sakatani et al., 2005), and colorectal cancer (Cui et al., 2003).

1.2.3 IGFBP5

IGFBP5 has a secretory signal peptide of 20 amino acids (aa). The mature protein contains 252 aa and consists of three domains of similar length. The N- and C-domain are highly conserved while the L-domain is more variable.

The primary IGF binding site is located in the N-domain (Shand et al., 2003). Nuclear magnetic resonance spectroscopy of mini-IGFBP5, comprising residues A40 to I92, revealed residues V49, Y50, P62, and K68 to L75 as the primary IGF2 binding site (Kalus et al., 1998). Mutations in five residues (K68N/P69Q/L70Q/L73Q/ L74Q) in the N-domain caused a 1,000 fold reduction in the affinity for IGF1 (Imai et al., 2000). The N-domain also contains several acidic residues and prolines that are critical for transcriptional activation activity (Zhao et al., 2006). The C-domain of IGFBP5 has a stretch of basic nucleotides (R201-R218) that are involved in IGF binding (G203K/Q209A and the basic residues) (Allan et al., 2006; Bramani et al., 1999), ALS binding (K211N/R214A/K217A/R218A) (Firth et al., 2001), extracellular matrix (ECM) binding (R207A/R214A) (Parker et al., 1998), heparin binding (R201L/K202E/K206Q/R214A) (Song et al., 2000), and nuclear transport (K206N/K208N/K217A/R218A) (Xu et al., 2004). The L-domain contains several confirmed and predicted sites for proteolysis, phosphorylation, and glycosylation (Firth and Baxter, 2002).

IGFBP5 is a secreted protein that can enter blood circulation. Similar to IGFBP3, IGFBP5 can complex with IGF and the acid-labile subunit (ALS) in a 1:1:1 molar ratio (Baxter and Martin, 1989; Twigg and Baxter, 1998). Such complex formation is proposed to restrict IGFs in circulation (Binoux and Hossenlopp, 1988), prolong the half-life of IGFs (Lewitt et al., 1994; Ueki et al., 2000), and prevent the potential hypoglycemic effect of IGFs activating the insulin receptor (Daughaday and Kapadia, 1989).

Secreted IGFBP5 can also bind to ECM components. Studies with cultured human fetal fibroblasts suggest that such binding can protect IGFBP5 from degradation and potentiate the biological actions of IGF1 (Jones et al., 1993).

IGFBP5 has also been shown to localize in the nucleus in a number of studies. The nuclear localization signal (NLS) in the C-domain was first recognized as having strong homology to known bipartite NLS (Radulescu, 1994), and this was later confirmed by mutagenesis (Schedlich et al., 1998; Xu et al., 2004). The route for nuclear entry is suggested to result from endocytosis of the secreted protein (Schedlich et al., 1998; Xu et al., 2004). Alternatively, using transfected IGFBP5, another route of retrograde trafficking from the ER has been proposed (Zhao, 2007). Nuclear import is mediated by importin β (Schedlich et al., 2000). Nuclear IGFBP5 was found to interact with FHL2 (four and a half LIM domains 2) (Amaar et al., 2002) and the vitamin D receptor (VDR) (Schedlich et al., 2007), although the function of such interaction is not clear. However, using immunohistochemistry to detect the endogenous protein, or using fluorescent-labeled IGFBP5 in endocytosis assays, IGFBP5 was detected in the vesicular compartment of mammary epithelial cells in culture, but not in the nucleus (Jurgeit et al.,

2007). The discrepancy may be due to different experimental procedures or cell type specificity.

IGFBP5 expression can be regulated by growth hormone (GH) and IGF1 at transcriptional and posttranslational levels. In old-aged people, stimulating GH secretion increased serum IGF1, IGFBP3, and IGFBP5 protein levels (Bowers et al., 2004). Transgenic overexpression of *Igf1* in the brain causes a 2-3 fold increase of IGFBP5 mRNA and protein in the IGF1 overexpression regions (Ye and D'Ercole, 1998). In porcine vascular smooth muscle cells, cell density regulates IGFBP5 level. Sparse culture expresses more IGFBP5 mRNA and protein due to IGF1 stimulation (Duan and Clemmons, 1998). IGF1 stimulates *IGFBP5* mRNA expression in an IGF1R-dependent manner through the PI3K/Akt/S6K but not MAPK pathway (Duan et al., 1999). In U-2 human osteosarcoma cells and T47D human breast carcinoma cells that secrete IGFBP5, adding IGF1 increased IGFBP5 levels in the culture medium by inhibiting proteolysis but not influencing *IGFBP5* mRNA abundance (Conover and Kiefer, 1993; Shemer et al., 1993).

1.2.4 Function of IGFBP5

Several mechanisms of IGFBP5 actions have been proposed (Fig. 1.2) (Duan and Xu, 2005). In the inhibition model, IGFBP5 sequesters IGFs from their receptors (Rozen et al., 1997). There are two potentiation models, one proposes that IGFBP5 transports IGFs to their site of action through cell surface binding (Jones et al., 1993). Another model states that IGFBP5-specific proteases can cleave the high affinity binding protein into fragments with lower affinity for IGFs, thereby increasing free IGF bioavailability (Imai et al., 1997). Besides modulating IGF function, IGFBP5 also has IGF- and IGF

receptor-independent functions. The different models proposed may be due to cell type specificity resulting from variable ECM components and other binding proteins/ligands/receptors expressed, or because of altered experimental conditions (overexpression or knockdown).

Igfbp5 KO mice show normal whole-body growth, while serum IGFBP3 levels are significantly elevated (Ning et al., 2007). *Igfbp3*, -4, and -5 triple KO results in a significant reduction of serum IGF1 and body weight (78% of wild type adult) (Ning et al., 2006). Overexpression of *Igfbp5* in mice causes a maximum of a 4-fold increase of IGFBP5 and up to a 2-fold increase of total and free IGF1 in circulation. Significantly increased neonatal mortality, reduced female fertility, whole-body growth inhibition, and retarded muscle development are observed (Salih et al., 2004). Interestingly, overexpressing an IGF binding-deficient IGFBP5 also causes significant growth deficiency without interfering with the IGF system, suggesting an IGF1-independent role of IGFBP5 during development (Tripathi et al., 2009).

Detailed studies of the tissue-specific roles of IGFBP5 provide more insight into the *in vivo* function of IGFBP5. However, the effect of IGFBP5 remains controversial. In mammary glands, IGFBP5 levels increase after weaning, and it has been found to inhibit the mitogenic and anti-apoptotic effects of IGF1. Overexpressing IGFBP5 under the control of the mammary-specific β -lactoglobulin promoter induces apoptosis in mice (Tonner et al., 2002). In *Igfbp5* KO mice, mammary gland involution after weaning is delayed, suggesting that endogenous IGFBP5 inhibits the anti-apoptotic role of IGF1 (Ning et al., 2007). In the MCF-7 human breast cancer cell line, vitamin D-related compounds stimulate production of IGFBP5. The growth-promoting activity of IGF1 but

not long R3 IGF1, an analogue with greatly reduced affinity for IGFBPs, is attenuated (Rozen et al., 1997).

In prostate tissues, IGFBP5 is highly upregulated after androgen withdrawal. An adaptive mechanism of IGFBP5 overexpression to potentiate the mitogenic and anti-apoptotic effects of IGF1 has been proposed. Overexpressing IGFBP5 in LNCaP human androgen-dependent prostate cancer cells increased tumor growth after castration (Miyake et al., 2000a). Knockdown of IGFBP5 inhibits the growth of androgen-dependent Shionogi tumor cells in a prostate cancer mouse model (Miyake et al., 2000b).

IGFBP5 levels in bone decline with age (Nicolas et al., 1995). Systemic administration of recombinant IGFBP5, either alone or in combination with IGF1, increases bone formation parameters in mice (Richman et al., 1999). Local administration of recombinant IGF1 with IGFBP5 increases bone mass in rodents, whereas IGF1 or IGFBP5, alone, has weak or no effect (Bauss et al., 2001). However, transgenic mice overexpressing IGFBP5 under the control of the bone-specific osteocalcin promoter show a transient decrease in trabecular bone volume and impaired osteoblastic function (Devlin et al., 2002). In U-2 human osteosarcoma cells, while knockdown of IGFBP5 inhibits cell survival and differentiation, adding IGFBP5 increases apoptosis (Yin et al., 2004).

In skeletal muscle, IGFBP5 expression is induced during myogenesis. Expressing sense RNA of IGFBP5 inhibits differentiation in C2 myoblasts, while antisense RNA results in premature differentiation (James et al., 1996). In C2C12 myoblasts, knockdown of IGFBP5 impairs myogenesis and suppresses IGF2 gene expression. When added with low concentrations of IGF2, wild type, but not an IGF binding-deficient, IGFBP5 restores

IGF2 expression and myogenic differentiation, suggesting an IGF-dependent pro-differentiation role of IGFBP5 (Ren et al., 2008).

1.3 Epithelial calcium absorption

1.3.1 Calcium homeostasis

Ca^{2+} is a major component of the skeleton, and it is important for multiple vital physiological processes. Approximately 99% of the body's Ca^{2+} is stored in the skeleton in the form of Ca^{2+} phosphate salts (Cashman, 2002). The remaining Ca^{2+} in the extracellular fluid functions as a cofactor for many enzyme activities involved in processes such as blood coagulation and ECM assembly (Lorand and Graham, 2003). Intracellular Ca^{2+} functions as a signal for numerous cellular processes including exocytosis, neuronal excitation, muscle contraction, and immune response, as well as gene transcription and cell proliferation (Berridge et al., 2003; Clapham, 2007; Suzuki et al., 2008b). Intracellular Ca^{2+} signaling is mediated by Ca^{2+} movement between the cytosol and the internal stores (endoplasmic reticulum and mitochondria) and/or the external media (Berridge et al., 2003; Clapham, 2007; Suzuki et al., 2008b).

To ensure the function of Ca^{2+} in these activities, the ionized serum Ca^{2+} concentration must be maintained within a narrow range of 1.1-1.3 mM (Suzuki et al., 2008b). Serum total Ca^{2+} concentration is maintained within 2.2-2.6 mM, but it can vary depending on the serum albumin level. Ca^{2+} homeostasis is maintained by concerted actions in three organs: intestine absorption, kidney reabsorption, and bone turnover. In an adult on a normal diet containing 1000 mg of Ca^{2+} per day, about 400 mg is absorbed in the gastrointestinal tract. Meanwhile, about 200 mg is secreted in the digestive juice and leaves the body in feces. Therefore, a net 200 mg/day is absorbed in the intestine.

The kidney excretes approximately 10 g of Ca^{2+} per day in pro-urine and reabsorbs 97-99%, leading to a net loss of 200 mg/day in the urine, which maintains the Ca^{2+} balance. Bone serves as an important storage pool for Ca^{2+} , and its daily turnover (~200 mg) contributes to the maintenance of Ca^{2+} balance between meals (Schrier, 2006).

Ca^{2+} homeostasis is regulated primarily by three hormones (Fig. 1.3): 1,25-(OH)₂D₃ (the active form of vitamin D), parathyroid hormone (PTH), and calcitonin. When the chief cells in the parathyroid gland sense low serum Ca^{2+} concentration through the Ca^{2+} sensing receptor (CaSR), they secrete PTH, which stimulates 1,25-(OH)₂D₃ production in the kidney. Increased 1,25-(OH)₂D₃ works on both the intestine and kidney to increase Ca^{2+} absorption and reabsorption. PTH also acts on the bone to trigger Ca^{2+} release. When serum Ca^{2+} level increases, parafollicular cells in the thyroid gland release calcitonin, a hypocalcemic hormone that stimulates Ca^{2+} deposition in the bone (Hoenderop et al., 2005; Suzuki et al., 2008b).

Dysregulation of serum Ca^{2+} level can be caused by eating disorders and malfunction in the calcitropic hormones and organs. For example, hypercalcemia can be caused by excessive secretion of PTH in primary hyperparathyroidism (Bilezikian et al., 2005) and production of parathyroid hormone-related proteins in malignancy (Clines and Guise, 2005). Hypocalcemia may be due to vitamin D deficiency (Cooper and Gittoes, 2008) and inadequate PTH secretion in hypoparathyroidism (Shoback, 2008).

Although some patients with chronic abnormal levels of ionized serum Ca^{2+} may be asymptomatic, commonly present symptoms affect neuromuscular activities. Hypercalcemia leads to diminished neuromuscular activity, including muscle weakness and mental confusion (Bilezikian et al., 2005). Hypocalcemia can present neuromuscular

symptoms such as twitching and spasms, as well as heart failure and altered mental status (Shoback, 2008). Long-term Ca^{2+} deficiency can lead to rickets and osteoporosis (Suzuki et al., 2008b).

1.3.2 Epithelial calcium absorption

Ca^{2+} absorption occurs in several epithelial tissues, including the intestine, kidney, placenta, and mammary glands, as well as gills in fish. In the vertebrate transport epithelia, Ca^{2+} absorption from lumen to blood happens through two routes. When Ca^{2+} concentration in the lumen is high enough, paracellular transport can work following the transepithelial Ca^{2+} gradient. When the lumen Ca^{2+} level is low, transcellular transport plays a major role in active Ca^{2+} uptake (Hoenderop et al., 2005).

Paracellular transport is a passive process driven by the electrochemical gradient of Ca^{2+} . It is mediated through the selective permeable tight junction between the epithelial cells (Schneeberger and Lynch, 2004; Van Itallie and Anderson, 2006).

The transcellular transport pathway is composed of three steps (Fig. 1.4): Ca^{2+} entry across the apical membrane, Ca^{2+} transport inside of the cell, and Ca^{2+} extrusion across the basolateral membrane.

Apical Ca^{2+} entry is a passive process following the electrochemical gradient because of the extremely low intracellular free Ca^{2+} concentration (~ 100 nM) and hyperpolarization of the membrane. Apical influx is considered rate-limiting because its rate is coupled in a 1:1 ratio to that of transcellular transport (Raber et al., 1997).

Epithelial Ca^{2+} channels TRPV5/TRPV6 (Hoenderop et al., 1999; Peng et al., 1999) mediate the first step. TRPV5 is highly expressed in the kidney. TRPV6 is expressed more in the intestine than in kidney. It is also present in other tissues, including the

pancreas, placenta, skin, mammary, and exocrine glands (Suzuki et al., 2008b). (See 1.3.3 for more information)

Cytosolic Ca^{2+} diffusion is mediated by the Ca^{2+} carrier proteins calbindin- $\text{D}_{9\text{K}}$ / $\text{D}_{28\text{K}}$ (Darwish et al., 1987; Wilson et al., 1985). They belong to the EF-hand Ca^{2+} -binding protein superfamily including calmodulin, troponin C, and S100 protein (Kawasaki et al., 1998). Calbindins are important for keeping the cytosolic free Ca^{2+} level low, so that the apical channels TRPV5/TRPV6 are not inactivated and Ca^{2+} signaling events in the cell are not induced. The binding kinetics of these Ca^{2+} -binding proteins are relatively slow, thus making the rapid intracellular Ca^{2+} signaling independent of the Ca^{2+} transport (Koster et al., 1995). Calbindin- $\text{D}_{9\text{K}}$ is highly expressed in the intestine (as well as the kidney in mouse), while calbindin- $\text{D}_{28\text{K}}$ is present in the kidney, pancreas, placenta, bone, and brain (as well as the intestine in birds) (Hoenderop et al., 2005).

Basolateral Ca^{2+} extrusion is an active process that is energy consumptive. Two proteins, the $\text{Na}^+/\text{Ca}^{2+}$ exchanger (NCX1) (Komuro et al., 1992) and the plasma membrane Ca^{2+} -ATPase (PMCA1b) (Brandt et al., 1992; Strehler and Zacharias, 2001) are thought to function. NCX1 belongs to a family of ion transporters that can mostly extrude 1 Ca^{2+} for 3 extracellular Na^+ , using the Na^+ gradient and the electrical potential across the plasma membrane as an energy source (Blaustein and Lederer, 1999). NCX1 is broadly expressed in many tissues, while NCX2 and NCX3 are only expressed in the brain and skeletal muscle (Lytton, 2007). PMCA1b, resulting from alternative splicing, is the predominant isoform of PMCA1 and is abundantly expressed in the intestine and kidney (Strehler and Zacharias, 2001). NCX1 and PMCA1b work together in basolateral Ca^{2+} extrusion (Hoenderop et al., 2005).

1.3.3 TRPV5/TRPV6 channels

TRPV5 and TRPV6 belong to the transient receptor potential (TRP) channel family, a group of ion channels with sequence homology but diverse functions (Clapham, 2003). By functional expression cloning using a kidney/intestine cDNA library in *Xenopus laevis* oocytes, their cDNAs were identified to encode apical Ca^{2+} influx channels that mediate Ca^{2+} absorption (Hoenderop et al., 1999; Peng et al., 1999). The encoded proteins contain six transmembrane domains (TM) and cytoplasmic N- and C-terminus. The 6TM subunits are assembled as tetramers to form a cation-permeable pore (Hoenderop et al., 2003b). The short hydrophobic stretch between TM5 and TM6 is predicted to be the pore formation region and renders Ca^{2+} selectivity (Nilius et al., 2001b). The N-terminus contains several ankyrin repeats. There are also several PDZ motifs and putative protein kinase A (PKA) and protein kinase C (PKC) phosphorylation sites in the N- and C-terminus.

Three unique features of TRPV5/TRPV6 compared with other TRP channels have been described: 1) highly Ca^{2+} -selective: Most TRP channels are nonselective with $P_{\text{Ca}}/P_{\text{Na}} \leq 10$. However, TRPV5 and TRPV6 show $P_{\text{Ca}}/P_{\text{Na}} > 100$. 2) almost completely inwardly rectifying: Cation flow (positive charge) passes through the channel in the inward direction into the cell. 3) constitutively open: Most TRP channels are inactive until stimulated by the G-protein-coupled receptor and receptor tyrosine kinase, temperature, or mechanical stress. TRPV5/TRPV6, however, are constitutively open in the generally used overexpression systems when intracellular Ca^{2+} concentration is low and cells are hyperpolarized and there is no blockage by Ca^{2+} and Mg^{2+} (Clapham, 2003;

Hoenderop et al., 2005) . These properties support the Ca^{2+} uptake function of TRPV5/TRPV6.

TRPV5/TRPV6 expression can be rapidly regulated by hormones at the transcriptional level. $1,25\text{-(OH)}_2\text{D}_3$ increases TRPV5/TRPV6 expression by transcriptional activation (Hoenderop et al., 2001; Song et al., 2003b; Wood et al., 2001), likely through the vitamin D receptor response elements (VDREs) on the gene promoter (Meyer et al., 2006; Wang et al., 2005). PTH induces TRPV5/TRPV6 expression through a vitamin D-dependent mechanism. It activates 1α -hydroxylase to increase $1,25\text{-(OH)}_2\text{D}_3$ production (Hoenderop et al., 2005). Estrogen upregulates TRPV6 (and to a less degree TRPV5) expression through VDR-independent mechanisms (Van Abel et al., 2002; van Abel et al., 2003; Van Cromphaut et al., 2003). TRPV5/TRPV6 activity is also regulated by posttranslational modification. Klotho activates TRPV5 by hydrolysis of its extracellular N-linked oligosaccharides (Chang et al., 2005). There are several putative PKA and PKC phosphorylation sites in TRPV5/TRPV6 (Hoenderop et al., 1999; Peng et al., 1999). Recent studies show that ATP and phosphorylation regulate channel activity (Al-Ansary et al., 2010; Sternfeld et al., 2007) and membrane abundance (Sopjani et al., 2010). Several associated proteins for TRPV5/ TRPV6, including calmodulin (Niemeyer et al., 2001), S100A10 (van de Graaf et al., 2003), 80K-H (Gkika et al., 2004), BSPRY (van de Graaf et al., 2006c), RGS2 (Schoeber et al., 2006), NHERF4 (van de Graaf et al., 2006b), and cyclophilin B (Stumpf et al., 2008) have been shown to regulate channel function.

1.3.4 Function of TRPV5/TRPV6

Studies in mice provide valuable lessons on how the epithelial Ca^{2+} channels function *in vivo*. *Trpv5* KO mice have normal body weight and ionized serum Ca^{2+} levels on a regular 1% Ca^{2+} diet. However, they show hypercalciuria, reduced bone thickness, and upregulated intestinal TRPV6 expression (Hoenderop et al., 2003a). The hypercalciuria is due to defective renal reabsorption, and it is independent of intestine absorption because it persists on a Ca^{2+} deficient diet. The serum 1,25-(OH) $_2$ D $_3$ level in KO mice is significantly elevated, which may explain the stimulative effect on the intestine to upregulate TRPV6 and calbindin-D $_{9K}$. The reduced bone thickness may be due to abnormal bone reabsorption since TRPV5 is required for osteoclast function (van der Eerden et al., 2005).

Trpv6 KO mice show a more severe phenotype than *Trpv5* KO mice. Although the KO also affects the neighboring gene, EphB6, which is required for T cell function (Luo et al., 2004), the authors claimed that the phenotype observed is not related to EphB6 (Bianco et al., 2007). The animals weigh smaller than wild type adults on a regular 1% Ca^{2+} diet, and they show defective intestine absorption, reduced bone mineral density, and hypercalciuria. The defective intestine absorption is due to failure in active Ca^{2+} absorption, and the animals develop hypocalcemia on a low- Ca^{2+} diet. Their serum PTH and 1,25-(OH) $_2$ D $_3$ levels are higher than the control, which may explain the stimulative effect on bone reabsorption that leads to bone loss. The reason for hypercalciuria is not clear. A possible explanation could be increased bone loss that increases serum Ca^{2+} concentration, or perhaps TRPV6 is also involved in renal reabsorption. Interestingly, 20% of TRPV6 KOs developed alopecia/dermatitis, which

suggests a role of TRPV6 in the skin. TRPV6 KOs also show defective maternal-fetal Ca^{2+} transport in the placenta (Suzuki et al., 2008a).

Studies in *Trpv6* KO mice suggest that other pathways also mediate intestinal Ca^{2+} absorption besides TRPV6. In *Trpv6* KO mice, 1,25-(OH) $_2$ D $_3$ can still stimulate Ca^{2+} absorption *in vivo* (Kutuzova et al., 2008). This may be due to a stimulatory effect of 1,25-(OH) $_2$ D $_3$ on paracellular Ca^{2+} transport. Moreover, using the everted gut sac method, it has been shown that active intestinal Ca^{2+} transport still occurs in TRPV6/calbindin-D $_{9K}$ double-KO mice, albeit at a reduced rate, suggesting that other pathways may be involved in active Ca^{2+} absorption in the intestine (Benn et al., 2008).

Interestingly, TRPV6 is also expressed in tissues other than the intestine, and its level is high in some cancer cells but low in normal cells. Examples for such TRPV6 expression include prostate (Fixemer et al., 2003; Peng et al., 2001b; Wissenbach et al., 2001), breast (Bolanz et al., 2008), and others tissue malignancies (Zhuang et al., 2002). In LNCaP human prostate cancer cells, siRNA knockdown of TRPV6 decreased cell proliferation and increased apoptosis (Lehen'kyi et al., 2007). However, it is not clear whether the upregulation of TRPV6 is a primary cause of the malignancy or a secondary mechanism for maintaining a higher proliferation rate in the cancer cells.

1.3.5 Dietary regulation

Due to the daily loss in renal excretion, adults must gain Ca^{2+} supplement from their diet. The amount of Ca^{2+} in daily food intake may vary, and physiological adaptations occur to accommodate the difference in dietary intake. When mice are raised on a 0.02% low- Ca^{2+} diet compared with a 1.1% normal- Ca^{2+} diet, their serum total Ca^{2+} level shows a 27% reduction. There is a 6-fold increase in TRPV6 expression level in the

intestine, while TRPV5 expression in the kidney does not change (Van Cromphaut et al., 2001). Similar observations have been made in another study: mice raised on a 0.02% low-Ca²⁺ diet showed a 30-fold increase in intestinal TRPV6 expression compared with the group raised on a 1% normal-Ca²⁺ diet, while minor changes occur in renal TRPV5 and TRPV6 (Song et al., 2003b). Both vitamin D-dependent (Song et al., 2003b) and – independent pathways (Song et al., 2003a) have been proposed. The vitamin D-dependent pathway may be explained by the VDREs in the gene promoter (Meyer et al., 2006; Wang et al., 2005), while the independent pathway may be explained by unidentified Ca²⁺ responsive elements in the promoter (Hoenderop et al., 2005). Dietary Ca²⁺ also stimulates intestinal Ca²⁺ absorption through TRPV6-independent mechanisms (Benn et al., 2008).

High dietary Ca²⁺ also has a beneficial effect in correcting vitamin D deficiency-induced hypocalcaemia. 1 α -hydroxylase KO mice (Dardenne et al., 2001) fed a 1.1% normal-Ca²⁺ diet have higher serum PTH and lower serum Ca²⁺. A 2% high-Ca²⁺ diet normalizes serum Ca²⁺ in these mice and upregulates expression of TRPV6 in the intestine (van Abel et al., 2003) as well as TRPV5 in the kidney (Hoenderop et al., 2002). More importantly, rickets and osteomalacia are cured by the 2% high-Ca²⁺ diet in those 1 α -hydroxylase KO mice (Dardenne et al., 2003). *Vdr* KO mice fed a 1.1% normal-Ca²⁺ diet had higher serum PTH and 1,25-(OH)₂D₃, and lower serum Ca²⁺. A 2% high-Ca²⁺ rescue diet normalized serum Ca²⁺ as well as PTH and 1,25-(OH)₂D₃ (Van Cromphaut et al., 2001). In another study, *Vdr* KO mice fed a 0.5% Ca²⁺ diet had higher serum PTH and 1,25-(OH)₂D₃, and lower serum Ca²⁺. A 2% Ca²⁺ rescue diet normalized plasma Ca²⁺ but not PTH or 1,25-(OH)₂D₃ (Song et al., 2003a). In both *Vdr* KO studies, different from

the 1α -hydroxylase KO ones, high- Ca^{2+} diet reduces intestinal TRPV6 expression while renal TRPV5 level does not change significantly.

Dietary Ca^{2+} has been implicated in disease treatments, but its exact role is not well understood. High dietary Ca^{2+} shows a preventive effect on colon tumors (Lamprecht and Lipkin, 2003). However, its effect is complex, since it reduces colon cell proliferation in normal tissue but may become tumor-promoting during carcinogenesis (Whitfield, 2009). A high- Ca^{2+} diet was suggested to reduce the risk of osteoporosis, while a low- Ca^{2+} diet was recommended to avoid kidney stone formation. Recent studies, however, suggest that these recommendations may be wrong (Borghi et al., 2002; Feskanich et al., 2003).

1.4 IGF and calcium homeostasis

1.4.1 Role of IGF signaling in calcium homeostasis

Although studies of IGF signaling in epithelial Ca^{2+} transport in mammalian intestine and kidney are lacking, IGF2 has been implicated in regulating fetal Ca^{2+} supply in the mouse placenta. IGF2 is specifically expressed in the labyrinthine trophoblast of the placenta under its P0 promoter, and P0 deletion leads to reduced of placental growth followed by fetal growth restriction (Constancia et al., 2002). Interestingly, placental-specific *Igf2* KO mouse embryos showed a reduction in total Ca^{2+} content at E17 followed by a compensatory adaptation at E19 (Dilworth et al., 2010).

IGF signaling functions in bone growth and remodeling and has been implicated in osteoporosis (Giustina et al., 2008; Niu and Rosen, 2005). Targeted overexpression of *Igf1* in osteoblasts increases bone volume without affecting the total number of osteoblasts or osteoclasts (Zhao et al., 2000). Osteoblast-specific KO of *Igf1r* leads to a

significant decrease in the rate of bone mineralization despite an unexpected osteoblast and osteoclast hyperactivity (Zhang et al., 2002). *Als* and liver *Igf1* double KO mice exhibit significantly reduced bone thickness and bone mineral density, suggesting that circulating IGF1 is necessary for normal bone growth (Yakar et al., 2002).

A role of IGF1 in regulating ion transport across the epithelia has been proposed in fish studies. GH and IGF1 have been shown to be important for seawater adaptation. When transferred to seawater, their gene expression levels increase, and injecting GH and IGF1 increases salinity tolerance. In fish gills, it has been shown that GH and IGF1 stimulate the number and/or size of chloride cells. GH and IGF1 also increase gill Na^+/K^+ -ATPase activity and/or expression level (Evans, 2002; McCormick, 2001).

IGF1 regulates Ca^{2+} signaling by different mechanisms. In skeletal muscle, local IGF1-induced muscle hypertrophy is mediated through calcineurin, a Ca^{2+} /calmodulin-regulated protein phosphatase. IGF1 activates the calmodulin-binding catalytic subunit, calcineurin A, which then activates the transcription factor NFAT (Musaro et al., 1999; Semsarian et al., 1999). IGF1 may be involved in regulating TRPV5/TRPV6 channel translocation. A number of TRP channel activities are regulated by channel trafficking upon stimuli (Bahner et al., 2002; Singh et al., 2004). IGF1, as well as epidermal growth factor (EGF), triggers TRP channel (TRPV1, TRPV2 and TRPC5) activity by increasing its membrane abundance (Bezzarides et al., 2004; Kanzaki et al., 1999; Van Buren et al., 2005). IGF1 and EGF trigger channel translocation at different speeds, suggesting that the intracellular pathways involved may not be the same. Moreover, Rab11a, a Rab GTPase involved in vesicle trafficking, has been shown to target TRPV5/TRPV6 to the plasma membrane (van de Graaf et al., 2006a).

1.4.2 Role of calcium in regulating growth factor signaling

Ca^{2+} signaling regulates exocytosis and production of some growth factors. Elevation of intracellular Ca^{2+} level stimulates insulin release from the secretory granule in β -cells (Wollheim and Sharp, 1981). In keratinocytes, TRPV3 mediated Ca^{2+} influx stimulates TGF- α release, leading to activation of the EGF receptor (Cheng et al., 2010).

Ca^{2+} influx is also associated with activation of some growth factor receptors and the MAPK or Akt pathway. In PC12 cells, Ca^{2+} influx through voltage-sensitive Ca^{2+} channels leads to MAPK activation (Rosen et al., 1994). In vascular smooth muscle cells, Angiotensin II induces Ca^{2+} -dependent activation of the EGF receptor, leading to MAPK activation (Eguchi et al., 1998). Studies of intracellular Ca^{2+} signaling-induced Akt phosphorylation in cultured cells showed some inconsistent results. In Balb/c-3T3 fibroblasts, depletion of intracellular Ca^{2+} by EGTA pretreatment has no effect on EGF-induced Akt activation, but it completely abolishes S6K stimulation. Induction of intracellular Ca^{2+} by ionomycin or thapsigargin results in a full activation of S6K but little or no change of Akt (Conus et al., 1998). In some breast cancer cells, inhibiting calmodulin by its antagonist W-7 abolishes growth factor stimulated Akt phosphorylation (Coticchia et al., 2009).

Extracellular Ca^{2+} can also change intracellular signaling pathways. A model involving CaSR signaling has been proposed (Lamprecht and Lipkin, 2003; Whitfield, 2009). However, the cellular responses and molecular mechanisms are controversial. Low extracellular Ca^{2+} has been shown to induce cell proliferation in colon cells both *in vitro* and *in vivo* (Buset et al., 1986; Kallay et al., 1997). In rat fibroblasts, high extracellular Ca^{2+} stimulates MAPK phosphorylation and cell proliferation (McNeil et al.,

1998). In H-500 rat Leydig cancer cells, high extracellular Ca^{2+} increases cell proliferation and survival through the PI3K/Akt and p38 MAPK but not MEK/MAPK pathways (Tfelt-Hansen et al., 2004).

1.5 The zebrafish model

1.5.1 General features of the zebrafish model

Zebrafish (*Danio rerio*) is a teleost fish of the minnow family (Cyprinidae) in the class of ray-finned fish (Actinopterygii). They have a life cycle of 3-5 years, reaching sexual maturity in 3-4 months (Kishi et al., 2003). They have several advantageous features as a model organism. First, is their rapid *ex utero* embryogenesis. The embryos hatch within 72 hours post fertilization, and they can consume their yolk ball and remain unfed for 5-7 days. Secondly, embryos are optically transparent, and pigmentation can be inhibited to maintain transparency during the early larval stage. A third feature is their high fecundity (100-200 embryos per mating).

Zebrafish were initially introduced as a model organism by George Streisinger approximately 30 years ago, aiming to establish a vertebrate model that could allow the application of genetic and embryological methods (Streisinger et al., 1981). Early large-scale forward genetics screenings using N-ethyl-N-nitrosourea (ENU)-induced mutagenesis were performed by Christiane Nüsslein-Volhard and Wolfgang Driever and colleagues, yielding 2,000 mutants (1996). Detailed embryonic developmental stages were characterized (Kimmel et al., 1995), and powerful tools such as cell lineage tracing (Kimmel and Warga, 1986), single cell ablation (Eisen et al., 1989), and transplantation (Eisen, 1991) have been developed to study cellular processes during early embryogenesis.

Disadvantages of the zebrafish model are due to its genome complexity and lack of methods for embryonic stem cell-based gene KO. The genome project has reached a nearly completed draft (http://www.sanger.ac.uk/Projects/D_rerio/). Targeted mutagenesis using CEL-I-mediated heteroduplex cleavage (TILLING) and subsequent resequencing (Wienholds et al., 2003) or zinc finger nucleaus (Foley et al., 2009), are being developed. Antisense morpholinos (MOs) can generate valuable information in loss-of-function analysis, especially during the early stages (Eisen and Smith, 2008). siRNAs, however, seem to have largely nonspecific effects (Oates et al., 2000). Furthermore, transgenesis is made much easier using the transposable elements (Urasaki et al., 2006).

Taking advantage of the features of the zebrafish model, several powerful methods have been developed. The transparency and *ex utero* development allows non-invasive real-time imaging to monitor the biological events *in vivo* (Lawson and Weinstein, 2002). The great conservation of the signaling pathways and the easy accessibility to a large number of individuals make zebrafish an appealing model for drug discovery (Zon and Peterson, 2005).

1.5.2 Zebrafish as a model to study IGF signaling

Studies in zebrafish have provided valuable lessons on the function of IGF signaling *in vivo*. The components of the IGF system, including the IGF ligands, receptors, and IGFBPs, are conserved in zebrafish (Wood et al., 2005a). Perhaps the most intriguing findings using the zebrafish model come from the studies of IGFBPs. In mice, minor overall growth deficiency is observed in single *Igfbp* KO mice (*Igfbp1*, -2, -3, -4, -5) (Leu et al., 2003; Ning et al., 2007; Wood et al., 2000). This may be due to functional

redundancy and compensation, since single *Igfbp* KO resulted in upregulation of its homolog expression in adult serum (Ning et al., 2007; Wood et al., 2000). Moreover, characterization of early development in mice is difficult due to intrauterine development of the embryos. In zebrafish, however, gene expression pattern during embryogenesis can be characterized in great detail, and their functions can be addressed specifically. For example, zebrafish *Igfbp1a* is expressed throughout the body during early embryogenesis. It is strongly induced in hypoxia, and both gain- and loss-of-function analyses establish its role in causing hypoxia-induced growth retardation (Kajimura et al., 2005). *Igfbp2a* is expressed in lens epithelium and cranial boundary regions during early embryonic development. Targeted knockdown of *Igfbp2a* results in a series of abnormalities, including delayed development, reduced blood circulation, and specific angiogenic defects (Wood et al., 2005b). *Igfbp3* is expressed in migrating cranial neural crest cells, pharyngeal arches and the developing inner ears in zebrafish embryos. MO knockdown and mRNA rescue approaches demonstrate that *Igfbp3* positively regulates pharyngeal skeleton morphogenesis and inner ear development (Li et al., 2005).

A special feature using the zebrafish model to study IGF signaling is that the components of the IGF system are largely duplicated, including IGF1, IGF2, IGF1R, IGFBP1, IGFBP2, and IGFBP6 (Kamei et al., 2008; Schlueter et al., 2006; Wang et al., 2009a; Zhou et al., 2008; Zou et al., 2009). This could be a problem because of the increased complexity. However, it may be potentially beneficial, since functional diversification may have reduced the pleiotropic effect, thus allowing us to dissect the function of a gene with fewer complications.

1.5.3 Zebrafish as a model to study epithelial calcium transport

Zebrafish gill and embryonic skin are functionally equivalent to mammalian transport epithelia. A model of transcellular Ca^{2+} transport in fish similar to that in mammals has been proposed (Flik et al., 1995). However, variations exist between the mammalian and zebrafish model in epithelial Ca^{2+} transport:

First of all, since fish live in an aquatic environment, they face a greater challenge of ion-water balance than their terrestrial counterparts. They have a specialized organ, the gill, for epithelial ion transport (Hwang and Lee, 2007). In freshwater fish, >95% of the whole body Ca^{2+} uptake is estimated to occur in the gill (Flik et al., 1985). In the zebrafish embryos and early larvae when the gill is not developed, cells involved in Ca^{2+} uptake locate on the yolk sac skin (Pan et al., 2005).

Second, the tissue composition and cell types in mammalian and zebrafish transport epithelia are different. In rat intestine, *Trpv6* is expressed higher in the tips of the villi than in the crypts (Peng et al., 1999), suggesting that it is expressed in the enterocytes (also called columnar cells or absorptive cells). Enterocytes and secretory cells originate from the stem cells lying in the crypt base (Crosnier et al., 2006). The stem cells give rise to transit amplifying cells, which generate enterocytes (also contain subtypes) and three classes of secretory cells. Notch signaling mediates the cell fate choice between enterocytes and secretory cells (Crosnier et al., 2005; Jensen et al., 2000). In zebrafish, *trpv6*-expressing cells constitute a subset of Na^+/K^+ -ATPase rich (NaR) cells in the skin (Pan et al., 2005). These NaR cells, together with H^+ -ATPase rich (HR) cells, originate from skin ionocyte precursors during embryogenesis. Bmp, notch-delta

signaling, and Foxi3 transcription factors control the cell fate choice between ionocytes and keratinocytes (Hsiao et al., 2007; Janicke et al., 2007).

Third, divergence in the genome occurred during evolution. In mammals, two genes, *TRPV5* and *TRPV6*, likely originated from a recent gene duplication event because they locate on the same chromosome adjacent to each other. In fish, only one *trpv6* gene has been identified (Pan et al., 2005; Peng et al., 2001a; Qiu and Hogstrand, 2004). In other cases, functional substitution of paralogues may occur. For example, in mammals, PMCA1b is suggested to be involved in basolateral Ca²⁺ extrusion, while in zebrafish, *pmca2*, but not *pmca1a*, co-expresses with *trpv6*.

Due to these differences, zebrafish skin/gill ionocytes serve as an appealing comparative model to study the function of epithelial Ca²⁺ transport: First, it is easy to challenge the water-ion balance. An interesting phenomenon of low-Ca²⁺ water adaptation in fish is that the number of chloride cells/mitochondria-rich cells/*trpv6*-expressing NaR cells increases (McCormick et al., 1992; Pan et al., 2005; Perry and Wood, 1985), although the underlying mechanism is not clear. Second, due to the localization of the NaR cells on the skin of zebrafish embryos and larvae, it is readily accessible for experimental observation and manipulation. Furthermore, due to the more advanced genome and methodologies compared with other fish models, zebrafish are also becoming a good model for studying molecular mechanisms in fish physiology.

1.6 Project summary

In summary, the IGF research field has been active for more than 50 years, and recent studies are continuing to reveal the function of IGF signaling in new areas.

IGFBP5, being the most conserved IGF-binding protein, shows pleiotropic functions *in*

vivo, and its mechanism of action remains elusive. In the thesis study, I initiated with addressing the *in vivo* role of IGFBP5 using the zebrafish model. In chapter II, I characterized expression and biochemical properties of two zebrafish *igfbp5* gene products. I found that *igfbp5a* and *-5b* are expressed in spatially restricted, mostly non-overlapping domains during early development. The IGF binding site is conserved in both zebrafish Igfbp5s, and they are both secreted and capable of IGF binding. Both proteins contain a consensus bipartite nuclear localization signal and were found in the nucleus when introduced into cultured cells. While zebrafish Igfbp5b possesses transactivation activity, zebrafish Igfbp5a lacks this activity. Mutational analysis demonstrated that two unique amino acids in positions 22 and 56 of Igfbp5a are responsible for its lack of transactivation activity. These findings suggest that the duplicated zebrafish *igfbp5s* have evolved divergent regulatory mechanisms and distinct biological properties by partitioning of ancestral structural domains.

In chapter III, I started to unravel the unique expression pattern of *igfbp5a* discovered in Chapter II. I identified the specific cell type that expresses *igfbp5a* to be the *trpv6*-expressing NaR cells, which mediates transcellular Ca^{2+} absorption across the epithelia. I used morpholino-modified antisense oligonucleotides to knockdown Igfbp5a, and I found an increased number of the NaR cells as well as elevated Ca^{2+} content and Ca^{2+} influx in the Igfbp5a morphants. These findings suggest that Igfbp5a functions as a regulator of Ca^{2+} homeostasis by negatively modulating the population of the NaR cells.

The finding that *igfbp5a* is specifically expressed in the *trpv6*-expressing NaR cells prompted me to ask whether IGF signaling may play a role in epithelial Ca^{2+} absorption. In fish, low- Ca^{2+} acclimation triggers the increase of the NaR cells, but the

mechanism is not clear. In chapter IV, I started with the finding that the number of *igfbp5a* and *trpv6* co-expressing NaR cells increases dramatically in low-Ca²⁺ water. Intrigued by this finding, I studied the role of IGF signaling in the NaR cells under low-Ca²⁺ acclimation. I found that the increased cell number in low-Ca²⁺ water results from elevated cell proliferation. IGF1R downstream Akt signaling is specifically activated upon low-Ca²⁺ treatment, while inhibition of IGF1R or PI3K abolished the low-Ca²⁺-induced increase of the NaR cells. Furthermore, low-Ca²⁺ acclimation increases the mRNA levels of one of the IGF1R ligands, *igf2a*. This study revealed a new role of IGF/PI3K/Akt signaling in Ca²⁺ homeostasis by regulating the proliferation of the NaR cells in the vertebrate transport epithelia.

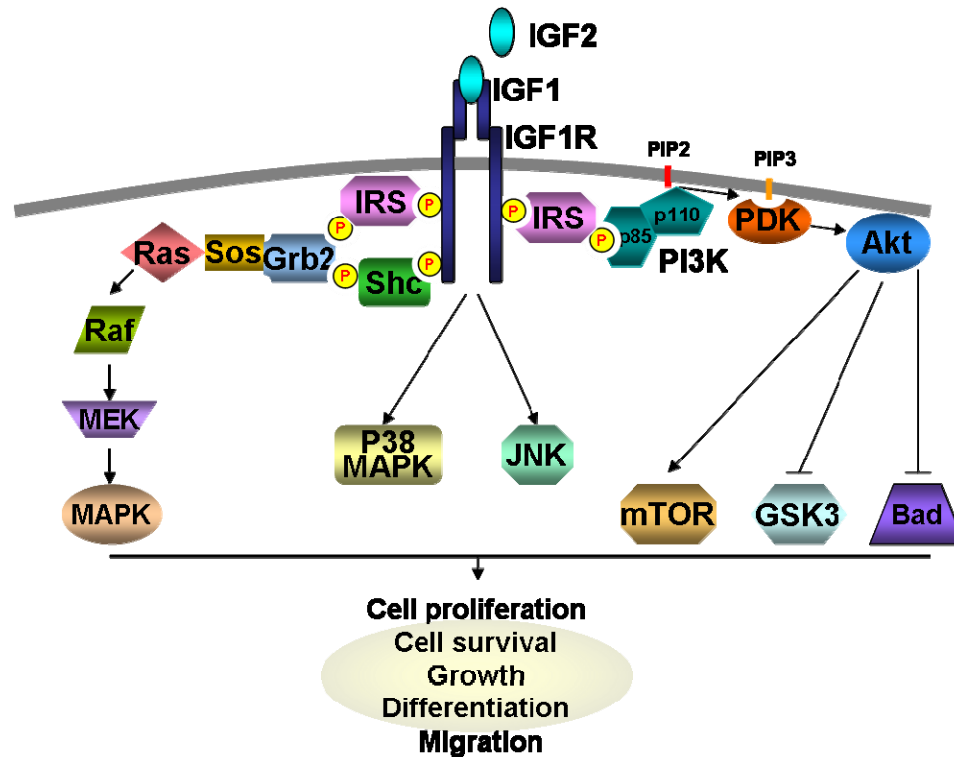


Figure 1.1 IGF1R signal transduction pathways

Ligand binding induces receptor autophosphorylation, which then activates several substrates including the insulin receptor substrates (IRS) 1-4 and the Src homology collagen (Shc). Once activated, IRS and Shc bind to growth factor receptor-bound protein 2 (Grb2), which then recruits the guanine-nucleotide-exchange factor (Sos). This leads to activation of the Ras/Raf/mitogen-activated protein kinase kinase (MEK)/mitogen-activated protein kinase (MAPK) pathway. Phosphorylated IRS also activates phosphatidylinositol 3-kinases (PI3K). PI3K activates phosphoinositol-dependent kinases (PDKs), which subsequently phosphorylate Akt. Akt activation can phosphorylate multiple downstream targets, including mTOR, GSK3, and Bad. IGF1R phosphorylation can also activate two other MAPK families, p38 and JNK. The activated IGF signaling leads to a series of responses depending on the cellular context.

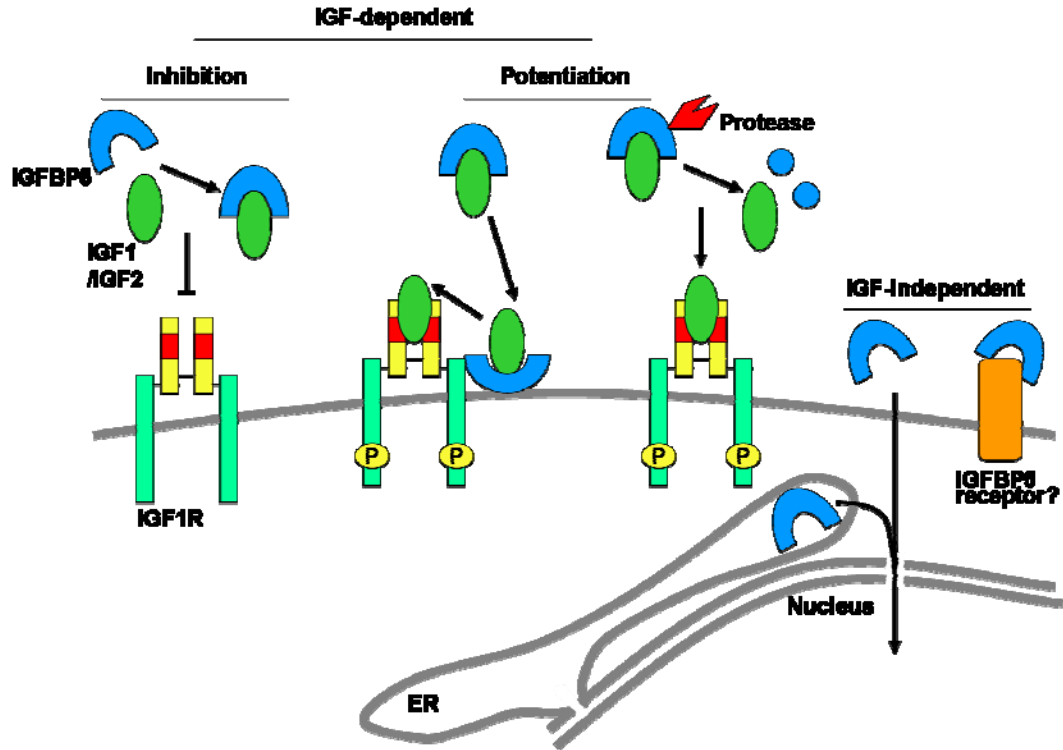


Figure 1.2 Proposed mechanisms of IGF-BP5 actions

In the inhibition model, IGF-BP5 sequesters IGFs from their receptors. There are two potentiation models, one proposes that IGF-BP5 transports IGFs to their site of action through cell surface binding. Another model states that IGF-BP5-specific proteases can cleave the high affinity binding protein into fragments with lower affinity for IGFs, thereby increasing free IGF bioavailability. Besides modulating IGF function, IGF-BP5 also has IGF- and IGF receptor-independent functions. One proposed mechanism is that IGF-BP5 can function as a transcriptional (co)activator. Two mechanisms have been proposed for the nuclear entry: Endocytosis from the secreted pool or retrograde trafficking from the ER. A putative IGF-BP5 receptor has been proposed.

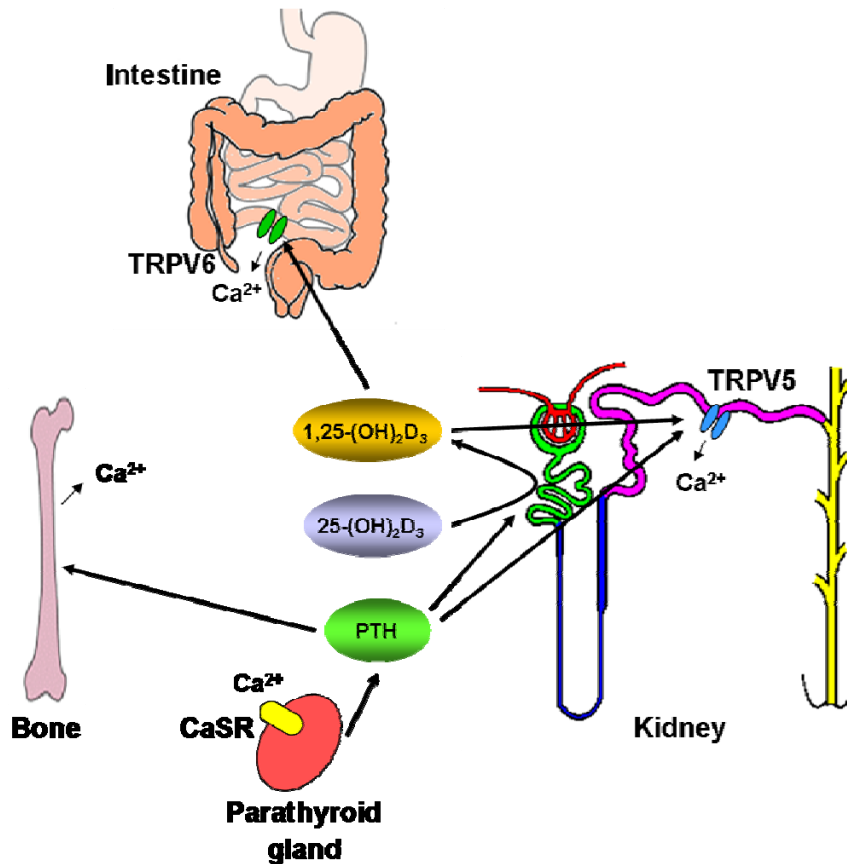


Figure 1.3 Mechanism of Ca^{2+} homeostasis

Ca^{2+} homeostasis is maintained by concerted actions in three organs: intestine absorption, kidney reabsorption, and bone turnover. When the chief cells in the parathyroid gland sense low serum Ca^{2+} concentration through the Ca^{2+} sensing receptor (CaSR), they secrete PTH, which stimulates $1,25\text{-(OH)}_2\text{D}_3$ production in the kidney. Increased $1,25\text{-(OH)}_2\text{D}_3$ works on both the intestine and kidney to increase Ca^{2+} absorption and reabsorption. PTH also acts on the bone to trigger Ca^{2+} release. Figure is adapted from (Suzuki et al., 2008b).

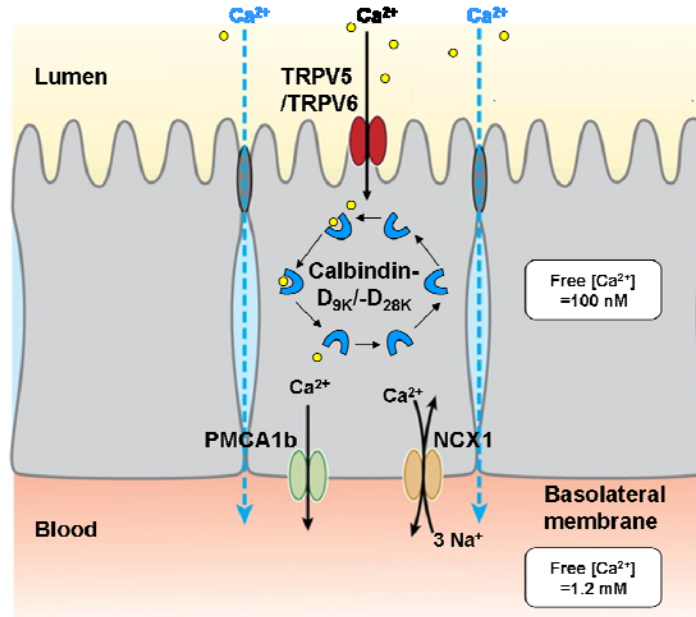


Figure 1.4 Mechanism of epithelial Ca^{2+} absorption

When Ca^{2+} concentration in the lumen is high enough, paracellular transport work through the tight junction following electrochemical gradient of Ca^{2+} . When the lumen Ca^{2+} level is low, transcellular transport plays a major role in active Ca^{2+} uptake. The transcellular transport pathway is composed of three steps: Ca^{2+} entry across the apical membrane through the epithelial Ca^{2+} channels TRPV5/TRPV6, Ca^{2+} transport inside of the cell mediated by the Ca^{2+} carrier proteins calbindin- $\text{D}_{9\text{K}}/\text{-D}_{28\text{K}}$, and Ca^{2+} extrusion across the basolateral membrane through the $\text{Na}^+/\text{Ca}^{2+}$ exchanger (NCX1) and the plasma membrane Ca^{2+} -ATPase (PMCA1b). Figure is modified from (Hoenderop et al., 2005; Suzuki et al., 2008b).

CHAPTER 2

Duplicated zebrafish insulin-like growth factor binding protein-5 genes with split functional domains: Evidence for evolutionarily conserved IGF binding, nuclear localization, and transactivation activity¹

2.1 Abstract

Insulin-like growth factor binding protein (IGFBP)-5 is a secreted protein that binds to IGF and modulates IGF actions. IGFBP-5 is also found in the nucleus of mammalian cells and has transactivation activity. The structural basis of this transactivation activity and its role in mediating IGF-independent actions are not clear. Here we report that there are two *igfbp-5* genes in zebrafish and other teleost fish. In zebrafish, *igfbp-5a* and *-5b* are expressed in spatially restricted, mostly non-overlapping domains during early development. The IGF binding site is conserved in both zebrafish IGFBP-5s, and they are both secreted and capable of IGF binding. Both proteins contain a consensus bipartite nuclear localization signal and were found in the nucleus when introduced into cultured cells. While zebrafish IGFBP-5b possesses transactivation activity, zebrafish IGFBP-5a lacks this activity. Mutational analysis demonstrated that two unique amino acids in positions 22 and 56 of IGFBP-5a are responsible for its lack of transactivation activity. These findings suggest that the duplicated zebrafish IGFBP-5s have evolved divergent regulatory mechanisms and distinct biological properties by

¹ This chapter is published in *FASEB J.* 2010 Jun; 24(6):2020-9.

partitioning of ancestral structural domains and provide new evidence for a conserved role of the IGF binding, nuclear localization, and transactivation domain of this multifunctional IGFBP.

2.2 Introduction

Regulation of peptide growth factor actions by secreted binding proteins has emerged as a common mechanism in cellular signaling. Among the most extensively studied examples are the insulin-like growth factor binding proteins (IGFBPs). Six distinct IGFBPs, designated as IGFBP-1 to -6, have been characterized in humans and other mammals (Duan and Xu, 2005; Firth and Baxter, 2002). These IGFBPs bind to IGFs with equal, or even greater, affinities than do the IGF-1 receptors (IGF-1R), and modulate the distribution, stability, and biological activities of IGFs.

IGFBP-5 is the most conserved member of the IGFBP family. Mammalian IGFBP-5 has a highly conserved N-domain where the primary ligand binding domain (LBD) is located (Kalus et al., 1998), and a conserved C-domain containing a nuclear localization signal (NLS) (Firth and Baxter, 2002; Schedlich et al., 2000). The central variable linker (L) domain contains several posttranslational modification sites. Studies have suggested that IGFBP-5 is a multi-functional protein. In the blood, IGFBP-5 can form a ternary complex with IGF and the acid labile subunit (ALS). This ternary complex controls the efflux of IGFs from the vascular space and prolongs the half-lives of IGFs (Firth and Baxter, 2002). In cultured cells, IGFBP-5 has been shown to inhibit IGF activities by binding to IGF and inhibiting IGF binding to the cell surface IGF-1 receptor (IGF-1R) (Rozen et al., 1997). IGFBP-5 has also been shown to potentiate IGF actions via its interactions with extracellular matrix (ECM) components (Mohan et al., 1995;

Parker et al., 1998; Ren et al., 2008). Recent studies suggest that IGFBP-5 itself can act as a growth factor with cellular effects that are not dependent on its IGF-binding ability (Abrass et al., 1997; Berfield et al., 2000; Hsieh et al., 2003; Miyakoshi et al., 2001). In addition to these findings based on studies in various mammalian cell culture systems, recent mouse genetic studies have begun to shed light on the IGF-dependent and -independent actions *in vivo* (Ning et al., 2007; Salih et al., 2004; Tripathi et al., 2009).

Despite this progress, the molecular and biochemical mechanisms underlying the IGF-independent actions of IGFBP-5 are still poorly understood. Recent studies suggest that mammalian IGFBP-5 is not only secreted but can also be found in the nucleus and has the ability to interact with nuclear proteins (Amaar et al., 2002; Jaques et al., 1997; Li et al., 1997; Schedlich et al., 2000; Schedlich et al., 1998; Xu et al., 2004). Furthermore, the IGFBP-5 N-domain has been shown to have a functional transactivation (TA) domain that is separable from its IGF binding site (Xu et al., 2004; Zhao et al., 2006). The *in vivo* roles of the nuclear IGFBP-5 and its transactivation domain in mediating the IGF-independent actions, however, are not clear. Addressing this issue using the mouse model is difficult due to the redundancy issues inherited with the mammalian systems and because of the multiple functionality nature of IGFBP-5.

Like in mammals, the IGF signaling systems in teleosts are composed of IGF ligands, receptors, and IGFBPs (Wood et al., 2005a). Recent studies have suggested that many teleost fish, including zebrafish, experienced an additional genome wide duplication event (Postlethwait et al., 2004; Taylor et al., 2003). For instance, there are two functional genes for IGF-1R, IGFBP-1, IGFBP-2, and IGFBP-6 in zebrafish (Kamei et al., 2008; Maures et al., 2002; Schlueter et al., 2006; Wang et al., 2009a; Zhou et al.,

2008). In this study, we present evidence that zebrafish and several other fishes possess two functional *igfbp-5* genes. Exploiting the availability of two zebrafish IGFBP-5s, we show that the duplicated zebrafish IGFBP-5s have evolved distinct biological properties by partitioning of ancestral structural domains such as the TA domain.

2.3 Result

2.3.1 Identification of two *igfbp-5* genes in zebrafish and other teleost fish species

By searching public databases, screening a cDNA library, and performing 5'- and 3'-RACE experiments, we identified and cloned two distinct zebrafish genes (GenBank accession number GQ892882 and AY100478). For reasons evident thereafter, we termed them as *igfbp-5a* and *-5b* and the encoded proteins as IGFBP-5a and -5b. As shown in Fig. 2.1A, zebrafish IGFBP-5a has a putative signal peptide of 19 amino acids (aa) and a mature protein of 249 aa. IGFBP-5b has a putative signal peptide of 17 aa and a mature protein of 248 aa. Comparison of the two zebrafish IGFBP-5 sequences with six human IGFBPs revealed that they share the highest sequence identities with that of human IGFBP-5 (47%-52%, see Table 2.4). Their sequence identities to human IGFBP-3 are 36% and 37%, and around 30% to other human IGFBPs. There is a typical IGFBP motif in the N-domain and a thyroglobulin type-1 repeat in the C-domain in both zebrafish IGFBP-5s. Both proteins contain a consensus LBD motif (Kalus et al., 1998) in their N-domain and a NLS motif (Schedlich et al., 2000) in the C-domain (Fig. 2.1A).

Phylogenetic analysis grouped both proteins into the IGFBP-5 subgroup (Fig. 2.1B). The two zebrafish *igfbp-5* genes also share similar exon/intron organization with the human *IGFBP-5* gene: they all contain 4 exons and 3 introns (Fig. 2.1C). While zebrafish *igfbp-5a* is located on LG6, *igfbp-5b* is on LG9. The two zebrafish *igfbp-5*

genes are adjacent to the two previously reported *igfbp-2* genes (Zhou et al., 2008), arranged in a tail to tail fashion (Fig.2.1D). This is very similar to the situations in the human and mouse genomes (Beattie et al., 2006).

To determine whether there are two *igfbp-5* genes in other teleost fish, we searched the fugu, stickleback, medaka, and tetraodon genome databases, and found that they all contain two *igfbp-5* genes. Again, the two *igfbp-5* genes are adjacent to two *igfbp-2* genes in a tail to tail fashion in all these teleost genomes (Fig. 2.1D). Likewise, there are several other syntenic genes (*TNS1*, *STK11IP*, *SLC4A3*) (Fig. 2.1D). Phylogenetic analysis indicated that the duplication of the *igfbp-5a/b* subfamily likely originated from a genome duplication event occurred early during ray-fin fish evolution (Fig. 2.1E).

2.3.2 The duplicated *igfbp-5* genes exhibit distinct expression patterns

As shown in Fig. 2.2A, in adult tissues, *igfbp-5a* mRNA was detected in brain and gill at high levels. It was also detected in eye, heart, gut, kidney and gonad, but not in liver and muscle (Fig. 2.2A). In comparison, *igfbp-5b* mRNA was expressed in all adult tissues examined. There were no obvious gender differences (Fig. 2.2A). During early development, *igfbp-5a* mRNA was not detectable until 14 hours post fertilization (hpf). It gradually increased from 14 to 72 hpf and was maintained at high levels thereafter (Fig. 2.2B). *igfbp-5b* mRNA was detected at low levels in 8 hpf embryos. Starting from 12 hpf, *igfbp-5b* mRNA levels maintained at high levels thereafter (Fig. 2.2B). The results of whole mount *in situ* hybridization analysis are shown in Fig. 2.2C and D. *igfbp-5a* mRNA was first detected at 20 hpf in a small number of cells on the surface of the yolk sac and yolk tube and this became more evident at 36 hpf (Fig. 2.2C, panel a). The

number of *igfbp-5a* mRNA expressing cells increased as the embryos grew (Fig. 2.2C, panel b). At 96 and 120 hpf, *igfbp-5a* mRNA was also highly expressed in cells spreading in the gill filament regions (Fig. 2.2C, panel c). *igfbp-5a* mRNA was also detected in a small number of cells located within the inner ear (Fig. 2.2C, panels d-f). In contrast, *igfbp-5b* mRNA was primarily detected in differentiating somites, gill arches, pectoral fin, and in some neural tissues (Fig. 2.2D). Its expression in the somites disappeared at 60 hpf (Fig. 2.2D, panel b). At 36 and 48 hpf, *igfbp-5b* mRNA was also highly expressed in the epithelial cells in the otic vesicles (panels c and d). In larvae (120 hpf), *igfbp-5b* mRNA was detected in the layers of cells surrounding the gill cartilage (Fig. 2.2D, panel e) and some cells in the brain (Fig. 2.2D, panel f). These results suggest that the two *igfb-5* genes are expressed in non-overlapping domains during development.

2.3.3 Both IGFBP-5a and -5b are secreted proteins and they both bind to IGF and modulate IGF actions

To test whether zebrafish *igfbp-5a* and/or *-5b* encode functional IGFbps, recombinant zebrafish IGFBP-5a, -5b, and human IGFBP-5 were produced in HEK 293 cells and purified from the culture media. Human and zebrafish IGFBP-5s had apparent sizes of ~36 kDa on SDS-PAGE (Fig. 2.3A) and they were all able to bind IGF-1, as shown by ligand blot (Fig. 2.3A).

We next determined the biological activities of zebrafish IGFBP-5a and -5b and compared them to that of human IGFBP-5. As shown in Fig. 2.3B, addition of IGF-1 to cultured U2OS cells caused a significant increase in cell growth. When human IGFBP-5, zebrafish IGFBP-5a, or zebrafish IGFBP-5b was added together with IGF-1 at a 1:1 molar ratio, they abolished the IGF-1-induced increase. Addition of any one of these

IGFBP-5s alone had little effect. Similar results were also obtained in HEK 293 cells (Fig. 2.3C). These results suggest that zebrafish *igfbp-5a* and *-5b* encode secreted proteins that bind IGF-1 and modulate IGF-1 actions.

2.3.4 Both IGFBP-5a and -5b are localized in the nucleus, but only IGFBP-5b has transactivation activity

Previous studies have shown that human IGFBP-5 is not only secreted but can also be found in the nucleus of cultured mammalian cells and mouse embryos (Amaar et al., 2002; Schedlich et al., 2000; Schedlich et al., 1998; Xu et al., 2004; Zhao et al., 2006). Furthermore, the IGFBP-5 N-domain has transactivation activity (Xu et al., 2004; Zhao et al., 2006). Since both zebrafish IGFBP-5s contain a consensus NLS in their C-domains (Fig. 2.1A, open box), we investigated the possible nuclear localization of zebrafish IGFBP-5a and -5b. U2OS cells were chosen for subcellular localization analysis because of their large and flat morphology. When cells were transfected with human IGFBP-4:EGFP, EGFP signal was only detected in the cytoplasm. But when cells were transfected with human IGFBP-5:EGFP, EGFP signal was seen in the nucleus. Like human IGFBP-5:EGFP, zebrafish IGFBP-5a:EGFP, and -5b:EGFP were also found in the nucleus (Fig. 2.4A). Similar results were also observed in HEK 293 cells (data not shown).

We next investigated whether zebrafish IGFBP-5a and/or -5b have any transactivation activity. The zebrafish IGFBP-5b N-domain caused a GAL4 dependent transactivation 4-fold greater than the pBIND control group when tested in HEK 293 cells (Fig. 2.4B). In contrast, the zebrafish IGFBP-5a N-domain did not cause any significant increase. As reported previously (Xu et al., 2004), the human IGFBP-5 N-

domain caused a 20-fold increase in activating the reporter gene expression. To rule out the possibility of species-specific effect, the transactivation activities of these fusion proteins were also tested in ZF4 cells, a cell line derived from zebrafish embryos. In these zebrafish cells, human IGFBP-5 still had the strongest activity (9-fold increase over the pBIND control, $P < 0.001$) and zebrafish IGFBP-5b N-domain had significant activity (3-fold increase, $P < 0.05$). Again, the zebrafish IGFBP-5a N-domain had no activity (Fig. 2.4C). Western immunoblot analysis revealed that expression levels of these fusion proteins were similar (Fig. 2.4D), thus excluding the possibility that the difference was due to different levels of protein expression and/or degradation.

2.3.5 Several unique residues in the IGFBP-5 N-domain are critical for the transactivation activity

The two zebrafish IGFBP-5s share the same domain arrangement, high sequence identity, nuclear localization, and the ability to bind IGFs, but only IGFBP-5b has transactivation activity. Taking advantage of this finding, we compared the amino acid sequences of these two highly homologous proteins with that of human IGFBP-5. Among the eight residues in the human IGFBP-5 N-domain that are known to be critical for its transactivation ability (Zhao et al., 2006), five are conserved in zebrafish IGFBP-5a and -5b (Fig. 2.5A indicated by *). When three of these conserved residues in zebrafish IGFBP-5b were substituted with their corresponding residues from human IGFBP-1 (E8A/D11S/E43L), the transactivation activity was abolished (Fig. 2.5B). Since zebrafish IGFBP-5b, but not IGFBP-5a, has transactivation activity, we focused on the 12 residues that differed between these two zebrafish IGFBP-5s in this region (Fig. 2.5A, indicated by ^). Among the four tested, we found that changing P22 or H56 in IGFBP-5b to the

corresponding residue in IGFBP-5a reduced the transactivation activity by more than 50% and the P22R/H56R double mutant had essentially no transactivation activity (Fig. 2.5B). In comparison, the L15M and N64I mutants had only moderate effects. These results suggest that R22 and R56 in the IGFBP-5a N-domain are largely responsible for its lack of transactivation activity. To further test whether these two positions are sufficient to establish the transactivation activity, we changed R22 and R56 in zebrafish IGFBP-5a N domain to the corresponding residues of IGFBP-5b in individual and double mutants. The R22P mutant had significant transactivation activity. The R22P/R56H double mutant had transactivation activity comparable to that of zebrafish IGFBP-5b (Fig. 2.5C). Taken together, our results suggest that the two different amino acids in positions 22 and 56 are responsible for the different transactivation activity observed in the two zebrafish IGFBP-5s.

We also investigated the structural determinants accounting for the different activities observed between human IGFBP-5 and zebrafish IGFBP-5b. Among the eight residues in the human IGFBP-5 N-domain that are known to be critical for its transactivation ability (Zhao et al., 2006), three of them differ between zebrafish IGFBP-5b and human IGFBP-5 (Fig. 2.5A indicated by *). Changing the zebrafish IGFBP-5 residue at position 56 into the corresponding residue from the human sequence resulted in a significant increase in its activity (R56Q and R22P/R56Q mutants in Fig. 2.5C and H56Q mutant in Fig. 2.5D). We further generated double and triple zebrafish IGFBP-5b mutants, H56Q/G52E and H56Q/G52E/Q12E, by changing residues from the zebrafish IGFBP-5b into the corresponding ones from the human IGFBP-5 sequence. The H56Q/G52E mutant had 80% activity compared to the human IGFBP-5 (Fig. 2.5D), and

the H56Q/G52E/Q12E mutant fully achieved the same high transactivation activity as human IGFBP-5. All mutants were expressed at comparable levels as shown by immunoblot (Fig. 2.5E). These results indicate that the difference in transactivation activities observed between human IGFBP-5 and zebrafish IGFBP-5b is due to their different amino acid residues in positions 12, 52 and 56.

2.4 Discussion

In this study, we identified two *igfbp-5* genes in zebrafish. Several lines of evidence indicated that they are co-orthologs of human *IGFBP-5*: (i) Sequence comparison at the protein level showed that they share the highest identity with human IGFBP-5, (ii) Phylogenetic analysis grouped the two zebrafish IGFBPs in the IGFBP-5 cluster, (iii) The gene structure and exon/intron size are most similar to human *IGFBP-5*, and (iv) The chromosome loci indicated conserved synteny with human *IGFBP-5*. We also found two *igfbp-5* genes in other teleost fish. Both the conserved synteny and phylogenetic analyses indicate that the duplication event that produced these two genes happened early in teleost evolution (Fig. 2.6).

In human and mouse, *IGFBP-5* mRNA has been detected in a wide range of tissues and cell types. Analyzing the expression patterns in zebrafish, we found that the two duplicate *igfbp-5* genes diverge in expression pattern both spatially and temporally. In adult tissues, while *igfbp-5b* is expressed in all the tissues examined at relatively high levels, *igfbp-5a* is most strongly expressed in brain and gill. During embryogenesis, *igfbp-5b* is expressed earlier than *igfbp-5a*. More interestingly, they are expressed in distinct tissues and cells. While *igfbp-5a* expression is restricted in the epidermal cells and in the inner ear, *igfbp-5b* is expressed in somites, branchial arches, pectoral fin, and

several domains in the brain. The divergent temporal and spatial expression patterns indicate that the *cis*-regulatory elements in these two genes may have diverged after the duplication event (Fig. 2.6). Studies of duplicated genes in zebrafish indicated that this may be a common mechanism for diversification (Kleinjan et al., 2008; McClintock et al., 2002). Further studies are needed to determine the conserved and divergent *cis*-regulatory elements in these 2 zebrafish *igfbp-5* genes.

Mammalian IGFBP-5 is a multifunctional protein that contains several structural modules/domains. We performed molecular, biochemical and cell biological approaches to identify structural components that have diversified in the duplicate zebrafish IGFBP-5s. We found that while some of the domains are preserved in both genes (LBD and NLS), others (TA) diverged during evolution (Fig. 2.6). Protein function usually requires intra- and inter-molecular domain interactions. Therefore, the related domains usually co-evolve (Chothia et al., 2003). It has been shown that transactivation activity and nuclear localization is well correlated in the six IGFbps, with IGFBP-3, and -5 showing nuclear localization and possessing the highest transactivation activity (Zhao et al., 2006). It is intriguing to ask why IGFBP-5a preserves the NLS while losing the TA domain. One possible explanation from the structural point of view is that the conserved stretch of basic residues in the C-domain has multiple functional roles. In addition to being a functional NLS (Schedlich et al., 2000; Xu et al., 2004), this region is also involved in IGFBP-5's interaction with ALS, heparin, and ECM components (Arai et al., 1996; Firth et al., 2001). Therefore, selection force may conserve these residues even if one of their functions become unnecessary. The LBD motif and the transactivation (TA) domain have been shown to be structurally separable and functionally independent (Xu et al., 2004). It

is possible that IGFBP-5a may have lost the transactivation activity while retaining its IGF-binding function.

The two zebrafish IGFBP-5s share the same domain arrangement, high sequence identity, and the ability to bind IGFs, but only zebrafish IGFBP-5b has transactivation activity. Taking advantage of this finding, we were able to identify the key residues critical for the transactivation activity. By swapping their different residues, we discovered that two residues at position 22 and 56 are both necessary and sufficient for the transactivation activity in zebrafish IGFBP-5s. These results indicate that IGFBP-5a lacks transactivation activity due to its unique residues in these critical positions. This conclusion is also consistent with our current understanding of gene evolution. After gene duplication, it is thought that the duplicated genes are likely to be retained if they acquire non-redundant functions (Force et al., 1999). The high divergence of the transactivation domains observed in the duplicated zebrafish *igfbp-5* paralogs may account for an adaptation or specialization of function of these two genes. We speculate that this may not be unique to zebrafish, as aligning the IGFBP-5 N-domain sequences of zebrafish, fugu, and stickleback together with that of human and mouse suggests that position 56 showed clear divergence in the two branches. Specifically, it is a R in all members of the IGFBP-5a group, while Q or H in the IGFBP-5b group (Fig.2.8). The other position, 22, identified in this study does not seem to be conserved in the two groups, suggesting that this residue change is a more recent event during evolution in zebrafish. When we tested the transactivation activity in ancestral IGFBPs in amphioxus (our unpublished observations), we found that they do exhibit high transactivation activity like the human IGFBP-5, suggesting that this activity has an ancient origin.

It has been shown that zebrafish contain two *igf-1* genes, two *igf-2* genes, and two *igf-1r* genes (Schlueter et al., 2006; Zou et al., 2009). In addition, zebrafish have two *igfbp-1* genes, two *igfbp-2* genes, and two *igfbp-6* genes (Kamei et al., 2008; Wang et al., 2009a; Zou et al., 2009). In this study, we provide evidence that there are two functional *igfbp-5* genes in zebrafish and other teleost fish, *igfbp-5a* and *igfbp-5b*. We show that the duplicated *igfbp-5s* exhibited non-overlapping expression patterns during zebrafish embryogenesis. We also determined the structural changes accounting for functional divergence by mapping critical amino acid changes in the TA domain. These findings provide insight into the evolution of the IGFBP gene family and lay the foundations for further elucidation of the physiological functions of the nuclear IGFBP-5 and its transactivation activity *in vivo*.

2.5 Materials and Methods

All chemicals and reagents were purchased from Fisher Scientific (Pittsburgh, PA, USA) unless stated otherwise. Restriction enzymes were purchased from Promega (Madison, WI, USA). Taq DNA polymerase and Vent DNA polymerase were purchased from New England Biolabs (Ipswich, MA, USA). Oligonucleotide primers and cell culture media were purchased from Invitrogen (Carlsbad, CA, USA).

Experimental animals: Wild type zebrafish (*Danio rerio*) were maintained on a 14 h light/10 h dark cycle at 28°C and fed twice daily. Fertilized eggs were raised in embryo medium at 28.5 °C and staged according to the standard method (Kimmel et al., 1995). To inhibit pigmentation, embryo medium was supplemented with 0.003% (w/v) *N*-phenylthiourea. All experiments were carried out in accordance with the guidelines

established by the University Committee on the Use and Care of Animals at the University of Michigan (<http://www.ucuca.umich.edu/>).

Molecular cloning and molecular evolutionary analyses: Two zebrafish cDNAs encoding IGFBP-5 like sequences were found by database search and by screening a cDNA library. Their full-length cDNA sequences were determined by 5'- and 3'- rapid amplification of cDNA ends (RACE) using the SMART RACE kit (Clontech, Mountain View, CA, USA). Amino acid sequences of IGFBP-5s were aligned by ClustalX (Larkin et al., 2007). Phylogenetic analyses were conducted using full-length amino acid sequences by the Minimum Evolution method in MEGA4 (Tamura et al., 2007). The GenBank accession numbers of various IGFBPs are listed in Supplemental Table 2.1. The structures of the two zebrafish *igfbp-5* genes were determined by comparing full-length cDNAs and the zebrafish genome sequence (<http://www.genome.ucsc.edu/cgi-bin/hgBlat>). Synteny analysis was carried out based on *Homo sapiens* Build 36.3, *Mus musculus* Build 37.1, *Danio rerio* Zv7, *Takifugu rubripes* FUGU 4.0 and *Gasterosteus aculeatus* BROAD S1. Genes used for this study are summarized in Table 2.2.

Reverse transcription (RT)-PCR and whole mount *in situ* hybridization:

Total RNA was isolated from embryos and adult zebrafish tissues using TRIzol reagent (Invitrogen). One µg total RNA was reverse-transcribed to single strand cDNA using M-MLV reverse transcriptase (Invitrogen) according to the manufacturer's instructions. RT-PCR was performed with three sets of primers (*igfbp-5a*: 5'-GGGTACATGTGGACGAGGA -3' and 5'-GAAAGAGCCATCACTCTGGAA -3', *igfbp-5b*: 5'-GGGAGTGTGTACGAACGAGAA -3' and 5'-

TCCTGTCACAGTTAGGCAGGTA -3', β -actin: 5'- GCCGGTTTTGCTGGAGATGAT -3' and 5'- ATGGCAGGGGTGTTGAAGGTC -3') using Taq DNA polymerase.

For whole mount *in situ* hybridization analysis, plasmids containing complete CDS (*igfbp-5a*: 807 bp, *igfbp-5b*: 798 bp) or partial 3'UTRs (*igfbp-5a*: 501 bp, *igfbp-5b*: 485 bp after stop codon) were linearized by restriction enzyme digestion, followed by *in vitro* transcription reactions with either T7 or SP6 RNA polymerase (Promega), to generate antisense or sense riboprobes using DIG RNA labeling mix (Roche, Indianapolis, IN, USA). The specificity of the riboprobes was verified by dot-blot assay and they did not cross-react with each other's target. Hybridization was carried out as described previously (Maures et al., 2002).

Construction of plasmids: To produce purified recombinant proteins for biochemical assays, the ORFs (with the stop codon deleted) of zebrafish IGFBP-5a, -5b, and human IGFBP-5 were amplified by PCR and subcloned into pcDNA3.1(-)/myc-His A expression vector (Invitrogen) at XhoI and HindIII sites. To determine the subcellular localization of the two zebrafish IGFBP-5s, their ORFs (with the stop codon deleted) were amplified by PCR and subcloned into pCS2+/EGFP expression vector as reported (Li et al., 2005). The construction of human IGFBP-4:EGFP and IGFBP-5:EGFP constructs was already reported (Xu et al., 2004). To produce the GAL4 DNA-binding domain (DBD) and IGFBP-5a N-domain fusion protein, DNA fragment corresponding to the N-domain of zebrafish IGFBP-5a was generated by PCR and subcloned into pBIND vector (Promega). The pBIND constructs containing human IGFBP-5 or zebrafish IGFBP-5b N-domain were already reported (Xu et al., 2004; Zhao et al., 2006). The IGFBP-5 N-domain mutants were generated by PCR using Pfu Turbo DNA polymerase

(Stratagene, La Jolla, CA, USA) as described previously (Zhao et al., 2006). Primers used for constructing these plasmids are listed in Table 2.3. All constructs were sequenced at the University of Michigan DNA Sequencing Core Facility.

Expression and purification of recombinant proteins: Myc- and 6xHistidine-tagged human and zebrafish IGFbps were produced and purified following previously reported procedures (Kamei et al., 2008). The purified proteins were quantified using a BCA protein assay kit (Pierce Biotechnology, Rockford, IL, USA). The purity was confirmed by silver staining and Western immunoblot using an anti-c-myc (9E10) antibody (Santa Cruz Biotechnology, Santa Cruz, CA, USA). Their IGF binding abilities were determined by ligand blot using DIG-labeled human IGF-1 following published procedure (Shimizu et al., 2000a).

Cell growth assay: The biological activities of various IGFBP-5s were studied using MTS assay (Promega) in cultured human embryonic kidney cells (HEK 293) and human osteosarcoma cells (U2OS). Cells were cultured in DMEM (HEK 293) or McCoy's 5A (U2OS) supplemented with 10% FBS, penicillin and streptomycin in a humidified-air atmosphere incubator containing 5% CO₂. After a 20 h serum starvation, 25 nM purified IGFBP was added in the presence or absence of 25 nM IGF-1 (Novozymes GroPep, Adelaide, SA, Australia). The assays were terminated after 48 h following the manufacturer's instructions.

Subcellular localization of zebrafish IGFBP-5a and -5b: U2OS cells were transiently transfected with an IGFBP:EGFP expression vector using Lipofectamine 2000 (Invitrogen) following the manufacturer's instructions. 24 h after transfection, cells were washed with 1 x PBS, fixed by 4% paraformaldehyde for 1h, and stained with 0.5 µg/ml

4',6-diamidino-2-phenylindole (DAPI) for 5 min. The cells were washed, mounted and examined under a fluorescence microscope (Nikon Eclipse E600). Images were acquired using Leica TCS SP5 confocal microscope with the Leica LAS AF software.

Transcription activation assay: Mammalian one-hybrid transcription activation assay was performed as described previously (Zhao et al., 2006). The transactivation activities of various IGFBPs were also examined in a zebrafish embryonic cell line (ZF4). ZF4 cells were cultured in DMEM/F12 supplemented with 10% FBS, penicillin and streptomycin in a humidified-air atmosphere incubator containing 5% CO₂ at 28°C. FuGENE 6 (Roche) was used for transfection in ZF4 cells. 24 h after transfection, cells were washed and lysed. Transcription activation activity was quantified using the Dual-Luciferase Reporter Assay System (Promega). To detect the expression level of GAL4 (DBD):IGFBP N-domain fusion proteins, equal amounts of cell lysates were separated by 12.5% SDS-PAGE and transferred to Immobilon P membranes (Millipore, Billerica, MA, USA) followed by western immunoblot using an anti-GAL4 (DBD) (RK5C1) antibody (Santa Cruz Biotechnology) and an anti-Tubulin antibody (Sigma-Aldrich, St. Louis, MO, USA).

Statistics: All values are represented as means ± standard deviation (S.D.). Statistical differences among experimental groups were analyzed by one-way analysis of variance (ANOVA), followed by Newman-Keuls multiple comparison test using GraphPad Prism 5 (GraphPad Software, Inc., La Jolla, CA, USA).

2.6 Acknowledgements

The authors thank Mr. John Allard for critical reading of this manuscript. This study was supported by NIH Grant 2RO1HL60679 and NSF Research Grant IOB

0110864 to CD. HK is supported in part by a postdoctoral fellowship from Japan Society for the Promotion of Science.

A

signal peptide, N domain
 IGFBP-5 MVLITAVILLLLAYASPACSLGSSFVHCPEPCDEKALSMCPFSRLGCELVKPEPGCGCCMTCA
 IGFBP-5a --MLLSLYALVAFWWGLTGISAFVFCPEPCDQKAMSMCPVVRNGCQVVKPEPGCGCCLTCA
 IGFBP-5b ----MALIVLGTGLTIVLSVSCSSFVFCPEPCDQKALSMCPVFEVGCQLVKPEPGCGCCYTCA
* * * * *

N domain L domain
 IGFBP-5 LAEGQSCGVYTERCAQGLRCLPRQDEEKPLHALLHGRGVLNERS--YR-EQVKTEEDDR
 IGFBP-5a LIIEGQACGVYTGTCGRGLRCLPRHIGEEKPLHALLYKGVQVOMNEKLSPIYSMMMPKQDQESD
 IGFBP-5b LAEGQACGVYTGCTHGLRCLPRNGEEKPLHALLHGRGVCTNERG--YRPPPPIDRESI
* * *

L domain C domain
 IGFBP-5 EHEEPTTSEMARETYS--PKIFRKHTRISELKAEEAVKKDRRKLTKQSKFVCGAENTAH
 IGFBP-5a E--IGMVSEVTEDLLQAKVPLPQR--DHINSKKAQAMRKDRRQCAKLRTRSHVDYSLFG
 IGFBP-5b EHDDTVKPDTEIQI--KIPLYRPPVINSKKAALFKDKKQCEKLRSSVSLDYSPLR

L domain C domain
 IGFBP-5 RIISAPEMRQESLQSPCRRHMEASLQELKASPRMVPRAVYLPNCDKRGFYKRRKQCKPSRG
 IGFBP-5a -----MEKHQSDIIGPCRRKLDGIVORMKDTSRVMALSLYLPNCDKKGFFKRRKQCKPSRG
 IGFBP-5b -----IDKHEPPEFGPCRRKLDGIIQSMKDTSRVMALSLYLPNCDKRGFFKRRKQCKPSRG

IGFBP-5 RKRIGICWCVDKYGKMLPGMENVVDGDFQCHTFDSSNVE--
 IGFBP-5a RKRIGICWCVDKHGVQMPGDFENGGNIQCKEVESSHNNNE
 IGFBP-5b RKRIGICWCVDKYGVLPGTDYSGNGIQCKDLNENNNNE

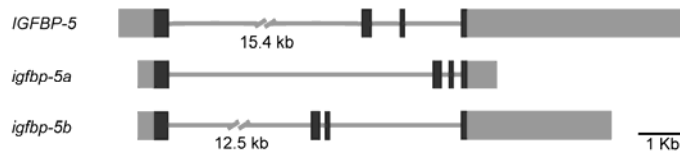
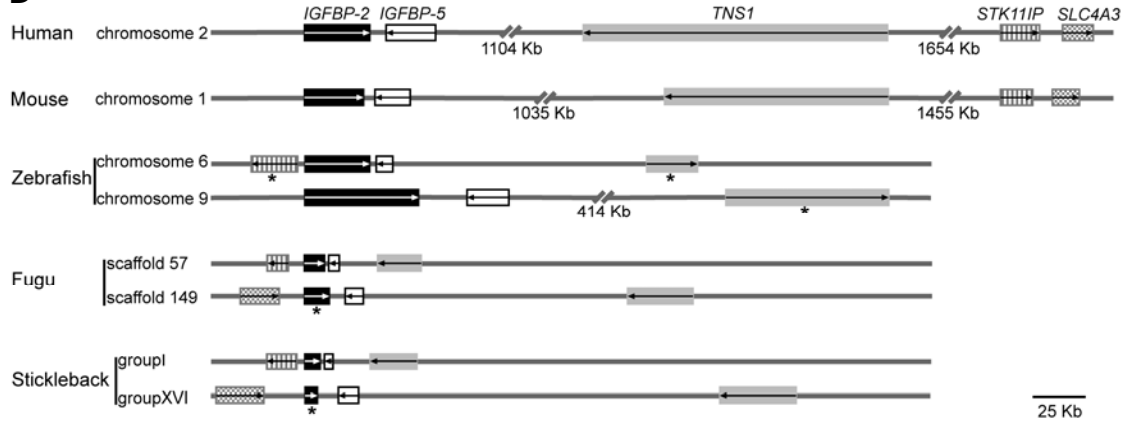
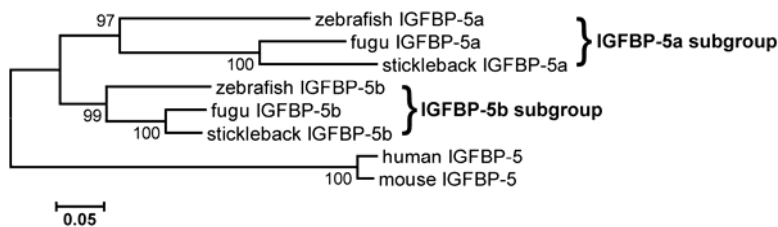
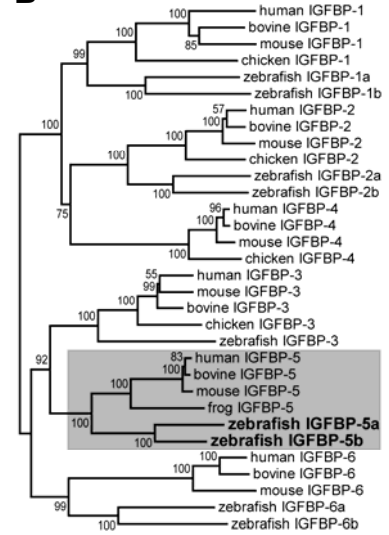
C**D****E****B**

Figure 2.1 There are two *igfbp-5* genes in zebrafish and other teleost fish

A) Sequence alignment of human IGFBP-5, zebrafish IGFBP-5a, and -5b. Identical and similar amino acid residues are darkly and lightly shaded, respectively. Vertical lines indicate the boundaries between signal peptide, N, L, and C domains. Residues in the N domain known to be critical for IGF binding (LBD) are underlined. NLS is shown in the box. Asterisks indicate residues that are critical for the TA activity of human IGFBP-5. B) Phylogenetic tree of the IGFBP family. Values on branches are percentages of replicate trees in which the genes clustered together in the bootstrap test (1000 replicates). Branch lengths are drawn in units of 0.1 aa substitutions/ site. C) Structure of human IGFBP-5 and zebrafish *igfbp-5a* and -5b. Exons are shown as boxes and introns as lines. Lightly and darkly shaded areas represent UTRs and ORF, respectively. D) Chromosomal loci of IGFBP-5 genes in various vertebrate genomes. Arrows indicate the transcript orientation. IGFBP-2, IGFBP-5, TNS1, STK11IP, and SLC4A3 are shown as black box, open box, grey box, vertical-line filled box, and wave-line filled box, respectively. Asterisk indicates partial transcript information from gene annotation. (Chromosomal locus of SLC4A3 in zebrafish is unknown.) E) Phylogenetic analysis of several teleost IGFBP-5a and -5b. Values on branches are the percentages of replicate trees in which genes clustered together in the bootstrap test (1000 replicates). Branch lengths are drawn in units of 0.05 aa substitutions/site.

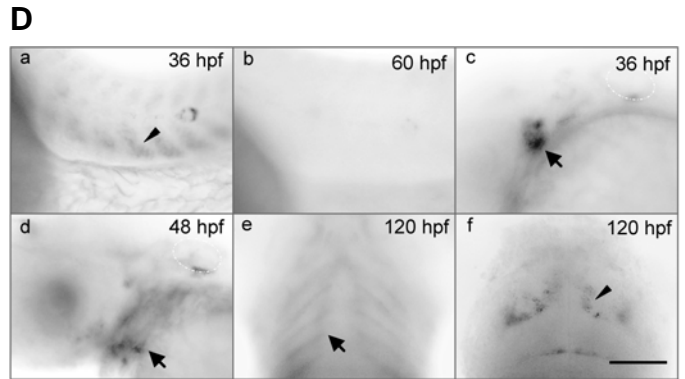
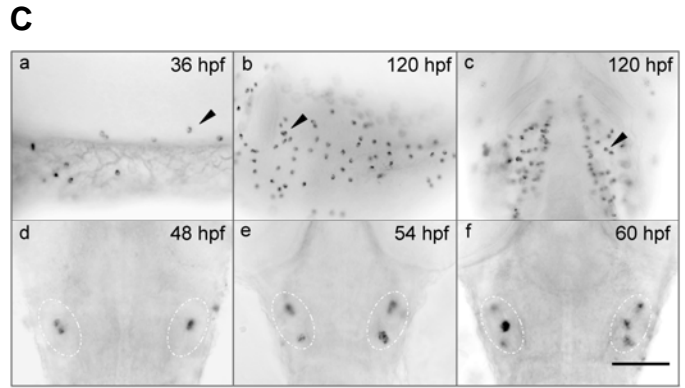
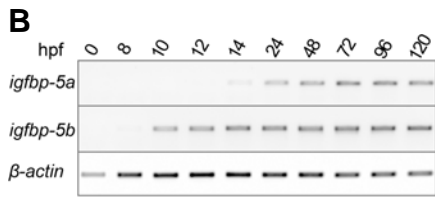
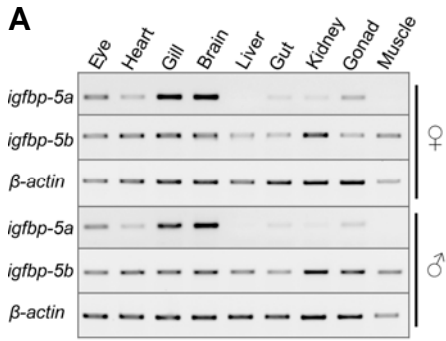


Figure 2.2 Zebrafish *igfbp-5a* and *-5b* exhibit distinct spatial and temporal expression pattern

A) RT-PCR analysis of *igfbp-5a* and *-5b* mRNAs in female and male adult zebrafish tissues. B) RT-PCR analysis of *igfbp-5a* and *-5b* mRNAs in zebrafish embryos at the indicated stages. Developmental stages are shown at top. hpf, hours postfertilization. C) *In situ* hybridization analysis of *igfbp-5a* mRNA in whole-mount zebrafish embryos. Developmental stage is at top right in each panel. a,b) Lateral view of yolk tube/sac region with anterior at left. c) Ventral view of gill arch region with anterior at top. Arrowheads indicate one representative epidermal cell. d-f) Dorsal view of head region with anterior at top. Dotted line indicates position of otic vesicles. D) *In situ* hybridization analysis of *igfbp-5b* mRNA. a,b) Lateral view of trunk region with anterior at left. Arrowhead indicates signals in somites. c,d) Lateral view of head region with anterior at left. Dotted line indicates position of otic vesicles. e) Ventral view of gill arch region with anterior at top. Arrows indicate signals in gill arch. f) Dorsal view of head region with anterior at top. Arrowhead indicates signal in midbrain. Scale bars = 100 μ m.

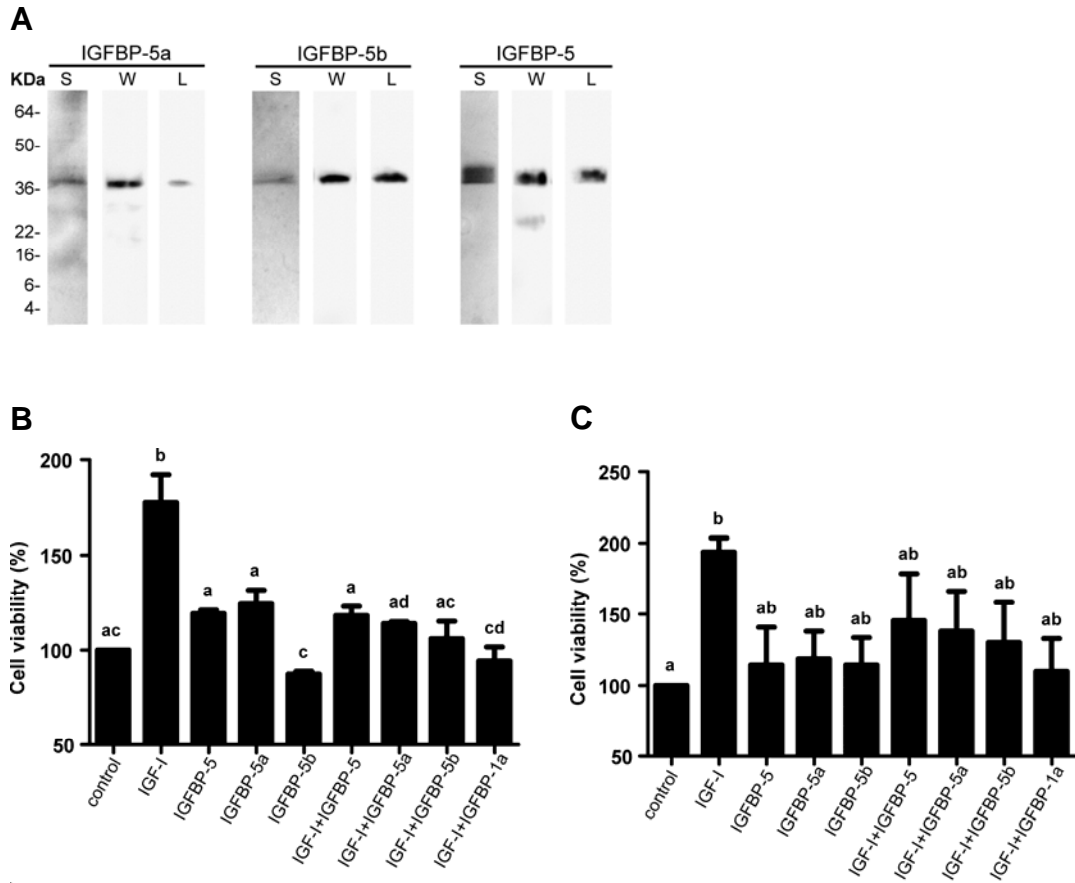


Figure 2.3 Both zebrafish IGFBP-5a and -5b can bind IGF-1 and regulate its biological activity

A) Western immunoblot and ligand blot analyses of purified zebrafish IGFBP-5a and -5b, and human IGFBP-5 proteins. L, ligand blot with DIG-labeled IGF-1; S, silver staining; W, Western immunoblot with an anti-myc antibody. B, C) Effects of various IGFBP-5s on IGF-1-stimulated cell growth in U2OS cells (B) and HEK 293 cells (C). Values are means \pm S.D. of 2 separate experiments, each performed in triplicate. Groups with different letters are significantly different from each other ($P < 0.05$).

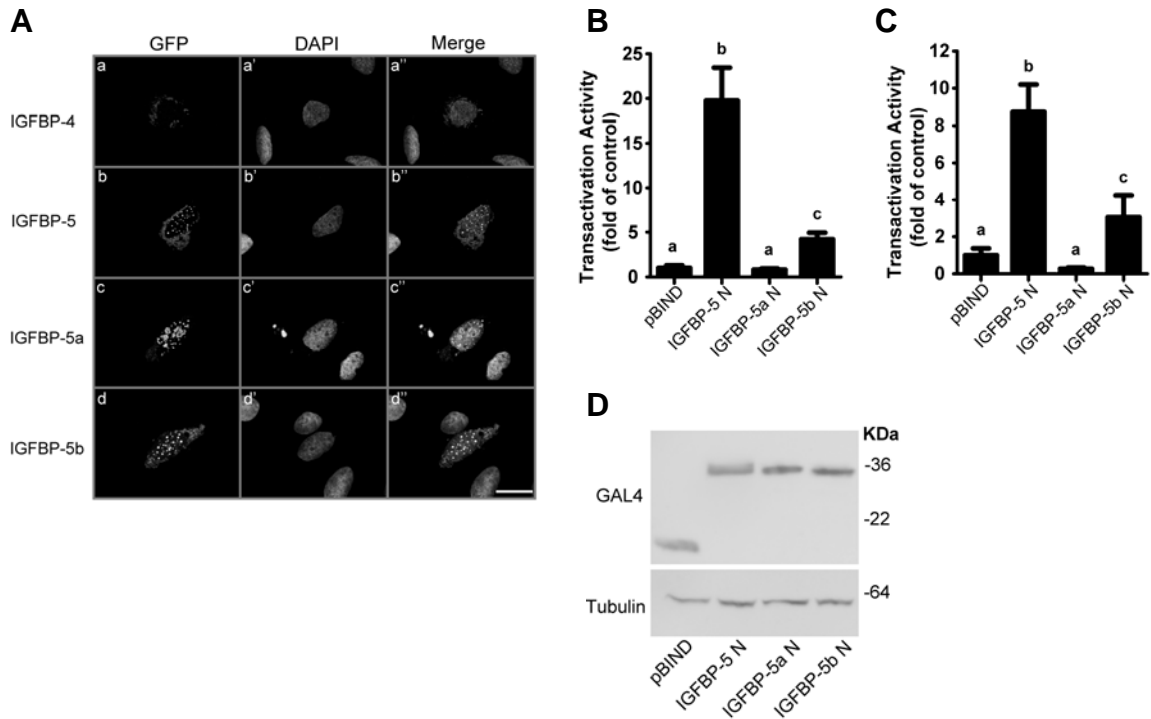


Figure 2.4 Nuclear localization and TA activities of zebrafish IGFBP-5a and -5b

A) Subcellular localization of IGFBP:EGFP. U2OS cells were transfected with human IGFBP-4:EGFP (IGFBP-4), human IGFBP-5:EGFP (IGFBP-5), zebrafish IGFBP-5a:EGFP (IGFBP-5a), and zebrafish IGFBP-5b:EGFP (IGFBP-5b) expression plasmid. EGFP signal was visualized (left panels) 24 h after transfection. Corresponding DAPI staining is shown in the middle panels and merged views in the right panels. Scale bar = 25 μ m. B, C) N domain of zebrafish IGFBP-5b but not that of IGFBP-5a has TA activity in HEK 293 cells (B) and ZF4 cells (C). TA activity is expressed as fold over the pBIND control group. Values are means \pm S.D. (n=3-5). Groups with different letters are significantly different from each other ($P < 0.05$). D) Expression levels of fusion proteins were analyzed by Western immunoblot using an anti-GAL4 (DBD) antibody and an anti-tubulin antibody.

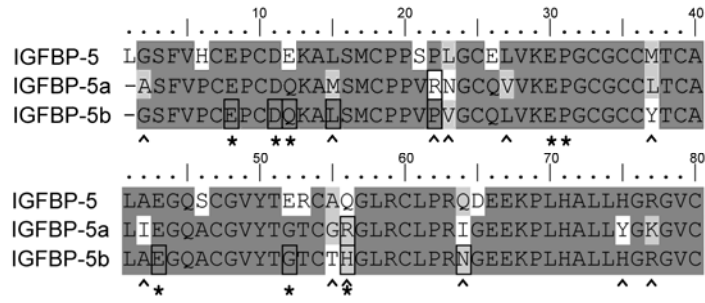
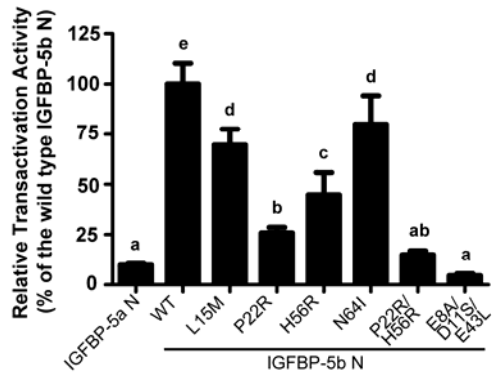
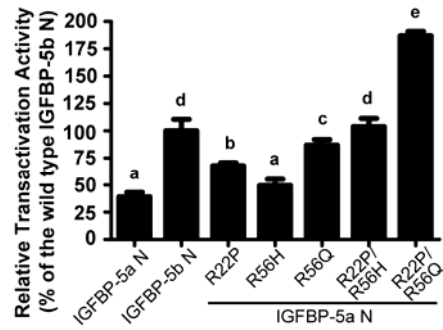
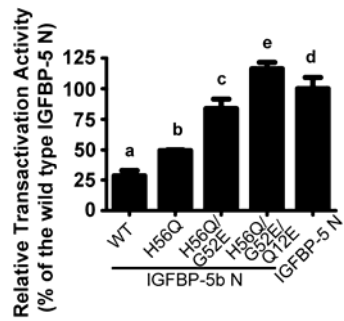
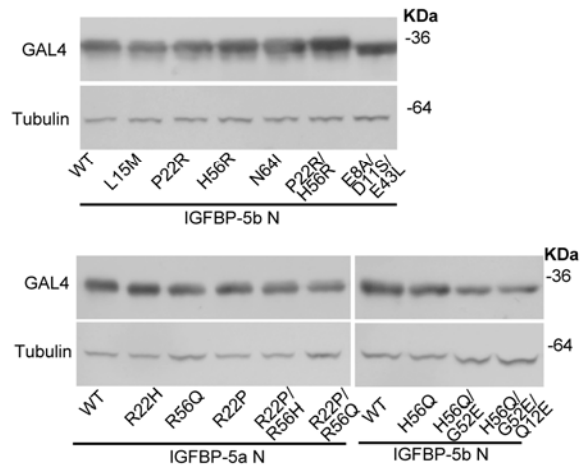
A**B****C****D****E**

Figure 2.5 Two unique amino acid changes in the IGFBP-5a N domain are responsible for its lack of TA activity

A) Sequence alignment of the N domain of human IGFBP-5 and zebrafish IGFBP-5a and -5b. Asterisks indicate residues known to be important for the TA activity of human IGFBP-5; carets indicate residues that differ between zebrafish IGFBP-5a and -5b; open squares indicate residues tested in this study. B -D) TA activities of wild-type and mutant zebrafish IGFBP-5b and -5a. Indicated constructs were introduced into HEK 293 cells together with a GAL4 reporter plasmid by transient transfection. Values are expressed as percentages of the wild-type zebrafish IGFBP-5b N-domain group (B, C) or the human IGFBP-5 N-domain group (D). Values are means \pm S.D. (n=3). Groups with the same letters are not significantly different from each other ($P < 0.05$). E) Expression levels of mutant fusion proteins were analyzed by Western immunoblot using an anti-GAL4 (DBD) antibody and an anti-tubulin antibody.

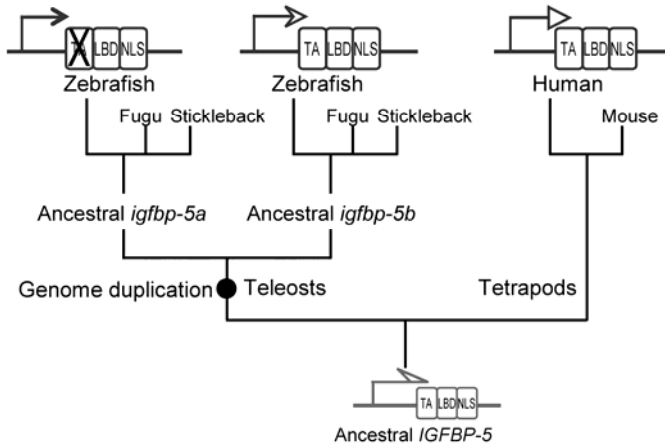


Figure 2.6 Proposed model for the gene expression and functional divergence of *igfbp-5* genes in teleost fish

The ancestral *IGFBP-5* gene was duplicated early in teleost evolution as the result of a genome duplication event. The duplicated *igfbp-5* genes may have undergone subfunctionalization at the levels of expression pattern, through divergent expression regulation (indicated by different arrows), and protein functionality, through the loss of critical structural motifs, such as the TA domain in the case of zebrafish *igfbp-5a*.

```

human IGFBP-5 SFVHCEPCDEKALSMCPPSPILGCRILVKEPGCGCCMTCALAEGQS CGVYTERCAQGLRCLP RQDEEKPLHALLHGRGVC
mouse IGFBP-5 SFVHCEPCDEKALSMCPPSPILGCRILVKEPGCGCCMTCALAEGQS CGVYTERCAQGLRCLP RQDEEKPLHALLHGRGVC
zebrafish IGFBP-5b SFVPCPCDQKALSMCPPVPVGCQLVKEPGCGCCYTCALAEQOACGVYTGCTEGLRCLP RNGEKPLHALLHGRGVC
fugu IGFBP-5b SYVPCPCDQKALSMCPPVPVGCQLVKEPGCGCCLTCALSEGOACGVYTGCTQGLRCLP RSGEEKPLHALLHGRGVC
stickleback IGFBP-5b SYVPCPCDQKALSMCPPVPVGCQLVKEPGCGCCLTCALSEGOACGVYTGCTQGLRCLP RSGEEKPLHALLHGRGVC
zebrafish IGFBP-5a SFVPCPCDQKALSMCPPVPVGCQLVKEPGCGCCLTCALIEGOACGVYTGCTGRGLRCLP RIGEEKPLHALLHGRGVC
fugu IGFBP-5a SFVPCPCDQKALSMCPPVPVGCQLVKEPGCGCCLTCALIEGOACGVYTGCTGRGLRCLP RINGEEKPLHALLHGRGVC
stickleback IGFBP-5a SYVPCPCDQKALSMCPPVPVGCQLVKEPGCGCCLTCALIEGOACGVYTGCTGRGLRCLP RINGEEKPLHALLHGRGVC

```

Figure 2.7 (supplementary to Figure 2.5.) Sequence alignment of several mammalian and teleost IGFBP-5 N-domains

Identical and similar amino acid residues are darkly and lightly shaded, respectively.

Asterisks (*) mark the residues that are critical for the different transactivation activities between zebrafish IGFBP-5a and -5b.

Protein †Species	IGFBP-1	IGFBP-2	IGFBP-3	IGFBP-4	IGFBP-5	IGFBP-6
human	NP_000587	NP_000588	NP_000589	NP_001543	NP_000590	NP_002169
bovine	NP_776979	NP_776980	NP_776981	NP_776982	NP_001098797	NP_001035585
mouse	NP_032367	NP_032368	NP_032369	NP_034647	NP_034648	NP_032370
chicken	NP_001001294	NP_990690	NP_001094504	NP_989684	-	-
frog	-	-	-	-	NP_001083938	-
zebrafish	NP_775390 NP_001091727	NP_571533 ABS30427	NP_991314	-	NP_001092224 NP_001119935	NP_001154873 NP_001154874
fugu	-	-	-	-	ENSTRUG00000013829 ENSTRUG00000004347	-
stickleback	-	-	-	-	ENSGACG00000014275 ENSGACG00000002508	-

Table 2.1 Accession numbers of the IGFBP sequences used for the phylogenetic analyses

†: human (*Homo sapiens*), bovine (*Bos taurus*), mouse (*Mus musculus*), chicken (*Gallus gallus*), frog (*Xenopus laevis*), zebrafish (*Danio rerio*), fugu (*Takifugu rubripes*), stickleback (*Gasterosteus aculeatus*).

Gene †Species	IGFBP-2	IGFBP-5	TNS1	STK11IP	SLC4A3
human	3485	3488	7145	114790	6508
mouse	16008	16011	21961	71728	20536
zebrafish a	794176	795084	565181	795019	
zebrafish b	798920	403039	572346		100151543
fugu a	ENSTRUG000 00013702	ENSTRUG000 00013829	ENSTRUG000 00013916	ENSTRUG000 00013564	
fugu b	ENSTRUG000 00003825	ENSTRUG000 00004347	ENSTRUG000 00004813		ENSTRUG000 00002078
sticklebac k a	ENSGACG00 000014280	ENSGACG00 000014275	ENSGACG00 000014268	ENSGACG00 000014289	
sticklebac k b	ENSGACG00 000002506	ENSGACG00 000002508	ENSGACG00 000002511		ENSGACG00 000002501

Table 2.2 NCBI or Ensembl Gene ID of the genes used for the conserved synteny analysis

†: human (*Homo sapiens*), mouse (*Mus musculus*), zebrafish (*Danio rerio*), fugu (*Takifugu rubripes*), stickleback (*Gasterosteus aculeatus*).

Vector	Target region	Primer name	Primer sequence
pcDNA3.1(-)/myc-His A	zebrafish IGFBP-5a ORF	IGFBP-5a XhoI F	5'-GTCTCGAGACCATGCTGCTAAGTTTGTATGCT-3'
		IGFBP-5a HindIII R	5'-CAAAGCTTTTCGTTGTTGTTGCTGTG-3'
pcDNA3.1(-)/myc-His A	zebrafish IGFBP-5b ORF	IGFBP-5b XhoI F	5'-GTCTCGAGACCATGGCTCTTCTGTGCTGGGTACA-3'
		IGFBP-5b HindIII R	5'-CAAAGCTTCTCGTTGTTGTTGTTGCTGTTCTCC-3'
pcDNA3.1(-)/myc-His A	human IGFBP-5 ORF	IGFBP-5 XhoI F	5'-GTCTCGATATGGTGTGCTCACCGCG-3'
		IGFBP-5 HindIII R	5'-GTAAGCTTCTCAACGTTGCTGCTGTC-3'
pCS2+/EGFP	zebrafish IGFBP-5a ORF	IGFBP-5a BamHI F	5'-GTGGATCCACCATGCTGCTAAGTTTGTATGCT-3'
		IGFBP-5a ClaI R	5'-CAATCGATGTTTCGTTGTTGTTGCTGTG-3'
pCS2+/EGFP	zebrafish IGFBP-5b ORF	IGFBP-5b BamHI F	5'-GTGGATCCACCATGGCTCTTCTGTGCTGGGTACA-3'
		IGFBP-5b ClaI R	5'-CAATCGATGCTCGTTGTTGTTGTTGCTGTTCTCC-3'
pBIND	zebrafish IGFBP-5a N-domain	IGFBP-5aN BamHI F	5'-CGGGATCCCAGCGTCTCGTGCCAT-3'
		IGFBP-5aN NotI R	5'-ATAAGAATGCGGCCGCTCAGCAAACCTCTTTGCCGTA-3'
pBIND	zebrafish IGFBP-5b N-domain L15M	IGFBP-5bN L15M F	5'-GCGATCAGAAGCGATGTCCATGTGCTCTCC-3'
		IGFBP-5bN L15M R	5'-GGAGGACACATGGACATCGCCTTCTGATCGC-3'
pBIND	zebrafish IGFBP-5b N-domain P22R	IGFBP-5bN P22R F	5'-GTCCTCCGGTCCGGGTGGGCTGTC-3'
		IGFBP-5bN P22R R	5'-GACAGCCACCCGGACCGGAGGAC-3'
pBIND	zebrafish IGFBP-5b N-domain H56R	IGFBP-5bN H56R F	5'-GTACATGCACACGCGGGCTGCGTG-3'
		IGFBP-5bN H56R R	5'-CAGCGCAGCCCGTGTGCATGTAC-3'
pBIND	zebrafish IGFBP-5b N-domain N64I	IGFBP-5bN N64I F	5'-CTGCCGCGCATCGGCGAGGAGAAG-3'
		IGFBP-5bN N64I R	5'-CTTCTCCTCGCCGATGCGCGGACAGG-3'
pBIND	zebrafish IGFBP-5b N-domain E8A/D11S/E43L	IGFBP-5bN E8A/D11S F	5'-GTACCGTGCGCGCCGTGCAGTCAGAAGGCGC-3'
		IGFBP-5bN E8A/D11S R	5'-GCGCCTTCTGACTGCACGGCGCGCACGGTAC-3'
		IGFBP-5bN E43L F	5'-GCGCTCTGGCGCTGGGGCAGGCGTG-3'
		IGFBP-5bN E43L R	5'-CACGCTGCCCCAGCGCCAGAGCGC-3'
pBIND	zebrafish IGFBP-5a N-domain R22P	IGFBP-5aN R22P F	5'-GTCTCCGGTGCCGAACGGGTGTCAG-3'
		IGFBP-5aN R22P R	5'-CTGACACCCGTTCCGGACCCGAGGAC-3'
pBIND	zebrafish IGFBP-5a N-domain R56H	IGFBP-5aN R56H F	5'-CCGGTACATGTGGACACGGACTGCGATGCC-3'
		IGFBP-5aN R56H R	5'-GGCATCGCAGTCCGTGTCCACATGTACCGG-3'
pBIND	zebrafish IGFBP-5a N-domain R56Q	IGFBP-5aN R56Q F	5'-CGGTACATGTGGACAAGGACTGCGATGCC-3'
		IGFBP-5aN R56Q R	5'-GGCATCGCAGTCCCTGTCCACATGTACCG-3'
pBIND	zebrafish IGFBP-5b N-domain H56Q	IGFBP-5bN H56Q F	5'-GTACATGCACACAGGGGCTGCGCTGC3-3'
		IGFBP-5bN H56Q R	5'-GCAGCGCAGCCCTGTGTGCATGTAC-3'
pBIND	zebrafish IGFBP-5b N-domain H56Q/G52E	IGFBP-5bN H56Q/G52E F	5'-GGTGTACACCGAGACATGCACACAGGGGCTGCGCTG-3'
		IGFBP-5bN H56Q/G52E R	5'-CAGCGCAGCCCTGTGTGCATGTCTCGGTGTACACC-3'
pBIND	zebrafish IGFBP-5b N-domain H56Q/G52E/Q12E	IGFBP-5bN Q12E F	5'-GCCGTGCGATGAGAAGGCGCTCTCC-3'
		IGFBP-5bN Q12E R	5'-GGAGAGCGCCTTCTCATCGCACGGC-3'

Table 2.3 Oligonucleotide primers used for plasmid construction in Chapter 2

Protein †Species	IGFBP-1	IGFBP-2	IGFBP-3	IGFBP-4	IGFBP-5	IGFBP-6
human	28/29	26/24	36/37	30/32	47/52	28/29
mouse	29/28	27/27	36/41	30/31	48/53	27/29

Table 2.4 Sequence identities between zebrafish IGFBP-5a/-5b and IGFBPs in human and mouse.

†: human (*Homo sapiens*), mouse (*Mus musculus*).

CHAPTER 3

Expression and functional characterization of *Igfbp5a* in the *trpv6*-expressing ionocytes in zebrafish embryos

3.1 Abstract

Insulin-like growth factor-binding protein (IGFBP)-5 is an evolutionarily conserved modulator of the IGF signaling pathway. It binds IGF *in vitro* with high affinity, suggesting an *in vivo* role in regulating IGF bioavailability. Nevertheless, the *in vivo* function of IGFBP5 is not well understood. In zebrafish, two *igfbp5a* genes have been identified. One of them, *igfbp5a*, is uniquely expressed in the embryonic skin. In this study, we identified the specific cell type that expresses *igfbp5a* to be the *trpv6*-expressing ionocytes, which mediates epithelial Ca^{2+} absorption. Morpholino knockdown of *igfbp5a* increased the number of *trpv6*-expression ionocytes and elevated Ca^{2+} content and Ca^{2+} influx in the embryos. These findings suggest that *Igfbp5a* functions as a regulator of Ca^{2+} homeostasis by negatively modulating the population of *trpv6*-expressing ionocytes.

3.2 Introduction

Hormones and growth factors are essential physiological regulators of animal development and homeostasis. Insulin-like growth factor (IGF) can function not only globally as an endocrine hormone to affect animal development, but also tissue specifically as a local growth factor (Le Roith et al., 2001). How the activity of IGF in

local tissue is fine-tuned is not well understood. One mechanism for such modulation may be attributed to the high affinity IGF-binding proteins (IGFBPs) that display different expression patterns and biochemical properties (Duan and Xu, 2005; Firth and Baxter, 2002).

IGFBP5 is the most conserved member within the IGFBP family. Similar to IGFBP3, IGFBP5 can form a tertiary complex with IGF and acid-labile subunit (ALS) in blood circulation (Twigg and Baxter, 1998). Such complex formation functions to restrict IGF in circulation (Binoux and Hossenlopp, 1988) and prolong half-life of IGF (Ueki et al., 2000). Locally produced IGFBP5 can function in an autocrine/paracrine manner to modulate IGF activities. In some tissues and cell types, it can inhibit IGF activity by sequestering the ligand from the receptors (Rozen et al., 1997). In others, it potentiates IGF activity via binding to extracellular matrix (ECM) components (Jones et al., 1993; Ren et al., 2008). IGFBP5 has also been shown to exhibit IGF-independent activities (Hsieh et al., 2003; Miyakoshi et al., 2001).

Although the functions of IGFBP5 are well studied *in vitro*, its *in vivo* roles are still poorly understood. In mice, minor overall growth deficiency was observed in single IGFBP5 knockouts, which can be partly explained by upregulation of IGFBP3 expression, its close homolog (Ning et al., 2007). IGFBP-3, -4, -5 triple knockouts showed more severe growth deficiency (Ning et al., 2006). Therefore, redundancy and complementation may explain the lack of global growth phenotype. On the other hand, detailed analysis of the local IGFBP5 producing tissues is starting to reveal the *in vivo* functions of IGFBP5 (Ning et al., 2007).

Zebrafish serves as an appealing model to study the role of IGFBP5 *in vivo* due to its rapid external embryonic development. Another feature of the zebrafish model is that duplication of the IGFBP5 gene results in diverged expression patterns during embryogenesis. Interestingly, one of them, *igfbp5a*, is specifically expressed in some skin cells in a salt and pepper pattern (Dai et al., 2010). However, the specific cell type that expresses *igfbp5a* in the skin was not known.

The architecture of the zebrafish embryonic skin differs from the mammalian one. It is composed of the external enveloping layer (EVL) and the basal deep layer (DEL) (Kimmel et al., 1990; Le Guellec et al., 2004). Living in an aquatic environment, fish meet more challenge to maintain ion-water balance compared with terrestrial animals. Therefore, fish skin not only serves as a protective barrier, it also functions as an osmoregulatory organ during the embryonic stage before the gill is fully functional (Hirose et al., 2003; Hwang, 2009). In addition to the skin stem cells and keratinocytes (Bakkers et al., 2002; Lee and Kimelman, 2002), the zebrafish skin contains ionocytes (chloride cells, mitochondria-rich cells) which are functionally equivalent to the cells involved in transepithelial transport in mammalian transport epithelia. At least three types of skin ionocytes have been identified using molecular markers in zebrafish: H⁺-ATPase-rich (HR) cells, Na⁺-K⁺-ATPase-rich (NaR) cells, and Na⁺-Cl⁻-cotransporter (NCC) cells (Hwang, 2009). HR cells express the H⁺-ATPase subunit *atp6v1a1* and are involved in acid secretion (Lin et al., 2006). The epithelial Ca²⁺ channel *trpv6* is expressed in a subset of NaR cells and mediates Ca²⁺ uptake (Pan et al., 2005). NCC cells express the Na⁺-Cl⁻-cotransporter *slc12a10.2* responsible for chloride uptake (Wang et al., 2009b).

In this study, we aim to examine the *in vivo* role of *igfbp5a* in its target tissue. We found that *Igfbp5a* is specifically expressed in the *trpv6*-expressing ionocytes. We performed a loss-of-function study and revealed that *Igfbp5a* functions as a negative regulator of the *trpv6*-expressing ionocytes and Ca^{2+} uptake.

3.3 Result

3.3.1 Overlapping spatial and temporal expression patterns of *igfbp5a* and *trpv6*

We previously found that zebrafish *igfbp5a* is expressed in a unique salt-and-pepper pattern on the skin covering the yolk and gill, and the mRNA is first detected at 14 hour post fertilization (hpf) (Dai et al., 2010). This pattern is similar to that of *trpv6* marking the epithelial Ca^{2+} channel-expressing ionocytes (Pan et al., 2005), or *atp6v1al* marking the H^+ -ATPase-expressing ionocytes (Horng et al., 2007), which are detected starting from 24 hpf. To compare the expression onset of those three genes during embryogenesis, we sampled zebrafish embryos from 6-somite stage (12 hpf) to prim-5 stage (24 hpf) in close intervals (2-4 hr). *igfbp5a* and *trpv6* showed concurrent expression patterns initiated at 14 hpf, while *atp6v1al* started to express at an earlier time point (Fig. 3.1A). We also quantified the mRNA levels of *igfbp5a* and *trpv6*. Similar patterns were observed for both *igfbp5a* (Fig. 3.1B) and *trpv6* (Fig. 3.1C). They show a significant increase from 48 hpf to 72 hpf (*igfbp5a*, 3.45 ± 0.18 fold; *trpv6*, 4.00 ± 1.22 fold), and remain relatively constant thereafter.

We also compared the spatial expression pattern of *igfbp5a*, *trpv6*, and *atp6v1al*. All three genes are expressed in a salt-and-pepper pattern on the skin covering yolk sac, yolk tube, and yolk/trunk boundary areas in the zebrafish embryos (Fig. 3.2). Later than 72 hpf, their expression in the gill increases (Fig. 3.2C, F, I). While *igfbp5a* and *trpv6*

show similar number of cells on the skin, more *atp6v1al* cells are detected. *atp6v1al* is also strongly expressed in the brain throughout development (Fig. 3.2G-I, arrows), while *igfbp5a* is transiently expressed in the inner ear at 48 hpf (Fig. 3.2A, arrowhead).

3.3.2 *igfbp5a* mRNA colocalizes with *trpv6* but not *atp6v1al*

To identify the cell type that expresses *igfbp5a*, we co-stained *igfbp5a* with *trpv6* or *atp6v1al*. From 36 hpf to 96 hpf, *igfbp5a* mRNA colocalized with *trpv6* mRNA both in the yolk tube (Fig. 3.3 A-A''') and in the gill (Fig. 3.3 C-C'''), whereas it did not colocalize with *atp6v1al* mRNA (Fig. 3.3 B-B''' and D-D'''). Within three groups of fish aged 36 hpf, 72 hpf, and 96 hpf, we found 222 *igfbp5a* and *trpv6* colocalized cells out of 225 cells that express either *igfbp5a* or *trpv6*. In contrast, no *igfbp5a* and *atp6v1al* co-expression was found in a total of 192 cells examined. Therefore, *igfbp5a* is specifically expressed in the *trpv6*-expressing ionocytes, but not in the *atp6v1al*-expressing ionocytes.

3.3.3 The number of *trpv6*-expressing ionocytes increases in *Igfbp5a* morphants

To test whether *Igfbp5a* is involved in the formation and/or maintenance of the *trpv6*-expressing ionocytes, we took a loss-of-function approach using morpholino-modified antisense oligonucleotides (MOs). Three MOs, designated translation-blocking MO (TB)-1~3, target nonoverlapping sequences within the 5' untranslated region (UTR) toward the start codon region of *igfbp5a*. To determine the efficiency of these MOs for blocking the translation initiation complex, we constructed a GFP reporter containing partial 5'UTR and coding sequence of *igfbp5a*. Capped mRNA encoding the reporter was injected into zebrafish embryos together with control MO (CT) or TBs. All three TBs, but not CT, blocked GFP reporter translation at 1.5 ng / embryo (Fig. 3.4A, top panel). When their doses were reduced to 0.5 ng /embryo, TB1 could not block as effectively as TB2

and TB3 (Fig. 3.4A, lower panel). To test whether knocking down *Igfbp5a* lead to developmental defects, the morphology of the morphants were examined. When injected at 4 ng / embryo, both TB2 and TB3 injected morphants were normal, whereas TB1 resulted in smaller head and eyes (Fig. 3.4B, arrow). The body length was not affected by either of the MOs (Fig. 3.4C). The inconsistent morphological abnormalities resulting from different TBs suggested off-target effect on TB1. Therefore, we adopted a combination of TB2 and TB3 at 4 ng / embryo each, in order to achieve high efficacy and minimum nonspecific effect. Interestingly, we found that the expression level of *igfbp5a* mRNA was significantly reduced in the morphants (Fig. 3.4D), suggesting an *in vivo* targeting effect of TB for *igfbp5a*. After verifying the TBs, we tested the effect of knocking down *igfbp5a* on *trpv6*-expressing ionocytes. Unexpectedly, TB injected embryos showed more cells compared with the control group (Fig. 3.4E, $P < 0.0001$). Expression level of *trpv6* did not increase significantly in individual cells (data not shown).

To validate that loss of *Igfbp5a* lead to increased number of *trpv6*-expressing ionocytes, another independent knockdown approach by inhibiting the splicing of the pre-RNA was used. The splice-inhibiting MO (SI) targets the exon 2-intron 2 boundary (Fig. 3.5A, underline). The knockdown effect was verified by RT-PCR using a pair of primers flanking the target site (Fig. 3.5A, arrows). The RT-PCR product for the correctly spliced mRNA should be 414 bp, while the aberrant product resulting from inclusion of intron 2 is larger (Fig. 3.5B). SI works in a concentration-dependent manner (Fig. 3.5B, left panel), and the effect is optimal at 2 dpf than later stages (Fig. 3.5B, right panel). Incorrectly spliced pre-RNA often cannot be transported out of the nucleus (Eisen and

Smith, 2008). Indeed nuclear localization appeared to be predominant in the SI injected morphants (Fig. 3.5C, right panel), whereas in the control group, *igfbp5a* mRNA was mostly detected in the cytoplasm (Fig. 3.5C, left panel). After validating the *in vivo* targeting efficacy of SI, we assessed the effect of SI on the embryos. No obvious morphological defect was observed in the SI injected morphants (Fig. 3.5D and E). Importantly, consistent with TB, SI injected embryos also showed more *trpv6*-expressing ionocytes compared with the control group (Fig. 3.5F, P=0.0014).

3.3.4 Igfbp5a affects development rather than function of the *trpv6*-expressing ionocytes.

Increase in cell number of *trpv6*-expressing ionocytes were found in larvae acclimated to low-Ca²⁺ water (Pan et al., 2005), suggesting the adjustment of cell number as a mechanism to adapt to insufficient Ca²⁺ uptake. The increased number of *trpv6*-expressing ionocytes in Igfbp5a morphants could be due to potentiated development of those cells, or due to a feedback to insufficient Ca²⁺ uptake resulting from loss-of-function of the *trpv6*-expressing ionocytes. To differentiate between these two possibilities, we tested whether the increased *trpv6*-expressing ionocytes in Igfbp5a morphants were functional. The speed of Ca²⁺ uptake was significantly higher in the Igfbp5a morphants (Fig. 3.6A, P<0.0001). The whole body Ca²⁺ content was also significantly elevated in the Igfbp5a knockdown group compared with the control (Fig. 3.6B, P=0.0001). The fold of increase in Ca²⁺ content (1.23 ± 0.07 fold over control) and Ca²⁺ influx (1.35 ± 0.11 fold over control) is comparable to that of cell number (Fig. 3.4E, 1.38 ± 0.27 fold over control), supporting that the increased *trpv6*-expressing ionocytes in the Igfbp5a morphants are functional.

3.4 Discussion

In this study, we discovered a unique co-expression of *igfbp5a* with *trpv6*. This specific expression is supported by tight correlation of spatial and temporal patterns, and confirmed by an almost complete colocalization. Knockdown of *Igfbp5a* resulted in an increase in the number of *trpv6*-expressing ionocytes and a comparable increase in Ca^{2+} influx and Ca^{2+} content, suggesting a negative regulatory role of *Igfbp5a* in these cells.

Our discovery may provide molecular cues to how IGF signaling regulates Ca^{2+} homeostasis. In fish, growth hormone (GH) and IGF have long been recognized to play a role in seawater adaptation (Evans, 2002). Injecting GH or IGF1 into fish potentiated the seawater tolerance and increased the size and density of chloride cells (McCormick, 2001). Bone is an important organ for maintaining Ca^{2+} balance, and in mammals, IGF signaling regulates bone growth and turnover (Sims et al., 2000; Wang et al., 2006; Zhang et al., 2002). Also, IGF signaling regulates Ca^{2+} uptake in the placenta (Dilworth et al., 2010), which is critical for fetal development. The specificity of such regulation is not well understood, considering the global expression of IGFs and IGF1R. *Igfbp5a* may serve as the local modulator of the IGF signaling in Ca^{2+} homeostasis. Loss of IGF1R results in global growth retardation (Liu et al., 1993; Schlueter et al., 2006). Similar to the IGFBP5 knockout mice (Ning et al., 2007), loss of *Igfbp5a* in zebrafish did not affect the overall growth and development. Since the development of the *trpv6*-expressing ionocytes are dependent on the developmental stage (Pan et al., 2005), further tissue specific downregulation of IGF1R will be needed to reveal whether *Igfbp5a* action is IGF-dependent.

IGFBP5 also has IGF-independent functions, which may be attributed to its interaction with transcription factors in the nucleus (Amaar et al., 2002; Schedlich et al., 2007). The nuclear activity of IGFBP5 may be due to its transcriptional activation activity residing in the N-terminus, which is conserved from humans to zebrafish (Xu et al., 2004; Zhao et al., 2006). However, *Igfbp5a* does not possess this activity due to mutations in two amino acids in the N-terminus (Dai et al., 2010). In this study, we tested whether *igfbp5a* may be involved in regulating *trpv6* gene expression. *igfbp5a* expression does not precede that of the *trpv6*, and knockdown of *Igfbp5a* did not affect *trpv6* expression levels per cell significantly. Therefore, it is not very likely that *igfbp5a* functions as a transcriptional co activator to regulate *trpv6* expression. It is not clear whether *Igfbp5a* may exert other IGF-independent role *in vivo*.

Our study also contributes to the knowledge of the tissue specific role of IGFBP *in vivo*. Although overexpression studies suggest a growth inhibitory role of IGFBPs (Salih et al., 2004), loss-of-function studies used to test the global growth inhibitory/promoting function of IGFBPs *in vivo* show normal growth (Leu et al., 2003; Ning et al., 2007; Wood et al., 2000). Interestingly, studies of the tissue specific expression of the IGFBPs *in vivo* are starting to give insight into how local IGF signaling is regulated by the IGFBPs (Leu et al., 2003; Ning et al., 2007; Wood et al., 2000). The zebrafish model has several advantages in studying different tissues during embryogenesis. Due to the transparency of the embryos, the gene expression pattern can be readily explored in great detail. The external embryogenesis process also facilitates the manipulation of the embryos at different stages. Indeed, studies of the expression tissues

have yielded valuable knowledge into how locally expressed IGFbps function to regulate growth and development of specific tissues and cells (Li et al., 2005; Wood et al., 2005b).

In summary, our findings provide a close molecular link between the IGF axis and Ca^{2+} homeostasis. Such knowledge may have broader implications in other tissues to explain how IGFbp may serve as a local modulator of the IGF signaling *in vivo*.

3.5 Materials and Methods

Experimental animals: Wild-type zebrafish (*Danio rerio*) were maintained on a 14 hr light/10 hr dark cycle at 28°C and fed twice daily. Fertilized eggs were raised in fish medium at 28.5°C and staged according to the standard method (Kimmel et al., 1995). To inhibit pigmentation, fish medium was supplemented with 0.003% (w/v) N-phenylthiourea. All experiments were conducted in accordance with the guidelines established by the University Committee on the Use and Care of Animals at the University of Michigan.

Whole-mount *in situ* hybridization and double fluorescent *in situ*

hybridization: For single-color *in situ* hybridization, digoxigenin-labeled antisense riboprobes for *igfbp5a* (Dai et al., 2010), *trpv6* (Pan et al., 2005), and *atp6v1al* (Lin et al., 2006) were generated by *in vitro* transcription, and whole-mount *in situ* hybridization was performed as previously described (Maures et al., 2002). Images were captured with a compound microscope (Nikon Eclipse E600) equipped with a Nikon DC50NN camera, and a stereomicroscope (Leica MZ16F) equipped with a QImaging QICAM camera.

For double fluorescent *in situ* hybridization, *igfbp5a*, *trpv6*, and *atp6v1al* riboprobes were labeled with either digoxigenin or dinitrophenol following the published

protocol (Hsiao et al., 2007). Images were acquired using Leica TCS SP5 confocal microscope with the Leica LAS AF software.

Reverse transcription (RT)-PCR and quantitative real-time PCR (qPCR):

Total RNA was isolated from embryos using TRIzol reagent (Invitrogen). One μ g total RNA was reverse-transcribed to single strand cDNA using M-MLV reverse transcriptase (Invitrogen). Semi-quantitative RT-PCR was performed using Taq DNA polymerase (New England Biolabs). Four sets of primers were used (*igfbp5a*: 5'-GGGTACATGTGGACGAGGA-3' and 5'-GAAAGAGCCATCACTCTGGAA-3'; *trpv6*: 5'-GCTGCGAGTCACTGGAATA-3' and 5'-ACCGACGCTCACCTCAAAC-3'; *atp6v1a1*: 5'-CCTGGAGGTGGCTAAACTCA-3' and 5'-GCTTCACCCTCTTTCCTGG-3'; β -*actin*: 5'-GCCGGTTTTGCTGGAGATGAT-3' and 5'-ATGGCAGGGGTGTTGAAGGTC-3').

qPCR was carried out using iQ SYBR Green Supermix (Bio-Rad) with an iCycler iQ Multicolor real-time PCR detection system (Bio-Rad). The efficiency and specificity of the qPCR were verified by standard curve and denaturing curve analyses. The expression level of a particular gene transcript was calculated based on the standard curve and normalized to β -*actin* mRNA level. Three sets of primers were used (*igfbp5a*: 5'-GCTGCACGCTCTGCTTAC-3' and 5'-AATGGAACCTTGGCCTGAG-3'; *trpv6*: 5'-GGACCCTACGTCATTGTGATAC-3' and 5'-GGTACTGCGGAAGTGCTAAG-3'; β -*actin*: 5'-GATCTGGCATCACACCTTCTAC-3' and 5'-CCTGGATGGCCACATACAT-3').

MO microinjection: MOs were obtained from Gene Tools (Philomath, OR, USA) and injected into 1~2 cell stage embryos as reported (Li et al., 2005). Three translation-

blocking MOs were designed to target against *igfbp5a* start codon (TB1, 5'-CAGCTTTGAAATGGCAAACCGAAG-3' targets nucleotides -52 to -28; TB2, 5'-CAAACCTTAGCAGCATCGTCCTACTG-3' targets nucleotides -10 to 15; and TB3, 5'-TTTGTATCGTTTAAGGTTCCCGAGT-3' targets nucleotides -78 to -54). One splice-inhibiting MO (5'-AGAAACCTACAATGTCAGACTGATG-3') was designed to target against *igfbp5a* exon 2-intron 2 boundary. A standard control MO (5'-CCTCTTACCTCAGTTACAATTTATA-3') was used as control.

To determine the efficiency of the translation-blocking MO, a 180-bp DNA fragment corresponding to partial 5'UTR (81 bp) and coding sequence (99 bp, which encodes the signal peptide and the first 14 residues of the predicted mature protein) of the zebrafish *igfbp5a* gene was generated by PCR (5'-gtgatccGGTACTCGGGAACCTTAAACG-3' and 5'-caatcgatGCATTGCTTTCTGGTCACACG-3'; the linker sequences are in lowercase). The amplified DNA was subcloned in frame into pCS2/EGFP expression vector (Li et al., 2005) to fuse the *Igfbp5a* partial sequence N-terminally of EGFP. The construct was sequenced at the University of Michigan DNA Sequencing Core Facility.

To validate the efficacy of the splice-inhibiting MO, total RNA was extracted from the injected embryos at various time points and RT-PCR was conducted as described above. The resulting higher molecular weight PCR product was sequenced at the University of Michigan DNA Sequencing Core Facility.

To measure the number of *trpv6*-expressing ionocytes, the injected embryos were raised in a 0.02 mM low-Ca²⁺ media in order to increase the intensity of *trpv6* whole-mount *in situ* hybridization signal. The other ion concentrations of the media were the

same as the normal medium ($[\text{Mg}^{2+}]$, 0.16 mM; $[\text{Na}^+]$, 0.5 mM; $[\text{K}^+]$, 0.165 mM; $[\text{Cl}^-]$, 0.5 mM; and $[\text{PO}_4^{3-}]$, 0.085 mM). Artificial freshwater was prepared with double-deionized water (Milli-Q Academic System, Millipore, Billerica, MA, USA) supplemented with adequate $\text{CaCl}_2 \cdot 2\text{H}_2\text{O}$, $\text{MgSO}_4 \cdot 7\text{H}_2\text{O}$, NaCl , Na_2SO_4 , K_2HPO_4 , and KH_2PO_4 , according to the method reported (Chen et al., 2003) with some modifications.

Measurement of whole body Ca^{2+} influx and Ca^{2+} content: Whole body Ca^{2+} influx was measured following previously described methods (Chen et al., 2003) with some modifications. Embryos were dechorionated, rinsed briefly in deionized water, and transferred to a 4-ml $^{45}\text{Ca}^{2+}$ (Amersham, Piscataway, NJ; final working specific activity, 1–2 mCi/mmol)-containing medium for a subsequent 4-hr incubation. After incubation, embryos were washed several times in isotope-free water medium. Then embryos were anesthetized with MS-222 and digested with tissue solubilizer (Solvable; Packard, Meriden, CT) at 50°C for 8 hr. The digested solutions were supplemented with counting solution (Ultima Gold; Packard), and the radioactivities of the solutions were counted with a liquid scintillation beta counter (LS6500; Beckman, Fullerton, CA).

To measure whole body Ca^{2+} content, embryos were anesthetized with MS-222, dechorionated, and briefly rinsed in deionized water. HNO_3 (13.1 N) was added to samples for digestion at 60°C overnight. Digested solutions were diluted with double-deionized water, and the total Ca^{2+} content was measured with an atomic absorption spectrophotometer (Z-8000; Hitachi). Standard solutions from Merck (Darmstadt, Germany) were used to make the standard curves.

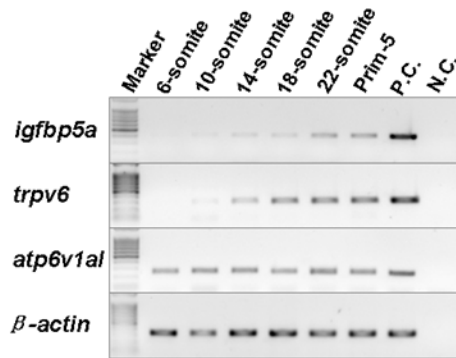
Statistics: Statistical differences among experimental groups were analyzed by unpaired t test or one-way analysis of variance (ANOVA) followed by Tukey's multiple

comparison test using GraphPad Prism 5 (GraphPad Software, Inc., La Jolla, CA, USA).
Significance was accepted at $P < 0.05$ or better.

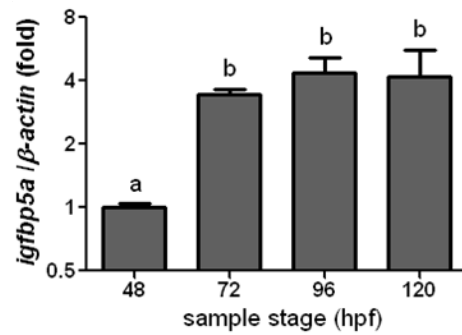
3.6 Acknowledgements

We thank Ms. Lisa Hebda and Ms. Catherine Nosal for critical reading this manuscript. This study was supported by NIH Grant 2RO1HL60679 and NSF Research Grant IOB 0110864 to CD.

A



B



C

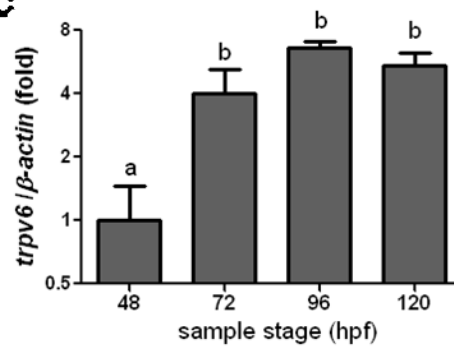


Figure 3.1 Overlapping temporal expression pattern of *igfbp5a* and *trpv6*

A) RT-PCR of *igfbp5a*, *trpv6*, and *atp6v1a1* mRNA in embryos at the indicated stages.

P.C., positive control of PCR using cDNA from 7 dpf larvae; N.C., negative control of

PCR using H₂O. B-C) Quantitative real-time PCR measurement of relative *igfbp5a* (C)

and *trpv6* (D) mRNA levels in embryos at the indicated stages.

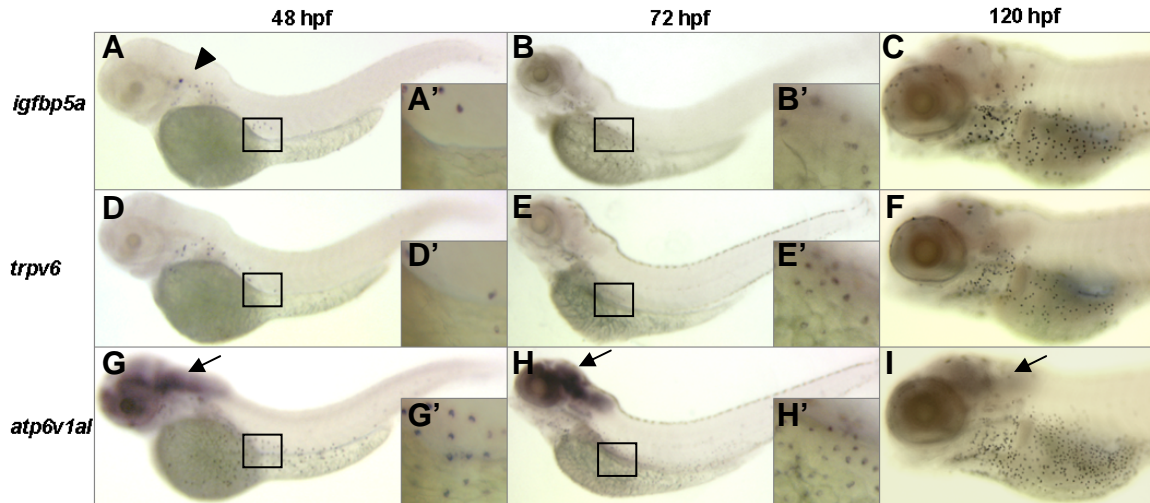


Figure 3.2 Similar spatial expression patterns of *igfbp5a* and *trpv6*

Whole-mount in situ hybridization of *igfbp5a* (A-C), *trpv6* (D-F), and *atp6v1a1* (G-I) mRNA in embryos at the indicated stages. Insets depict higher magnifications of areas boxed. All images are lateral views, anterior to the left.

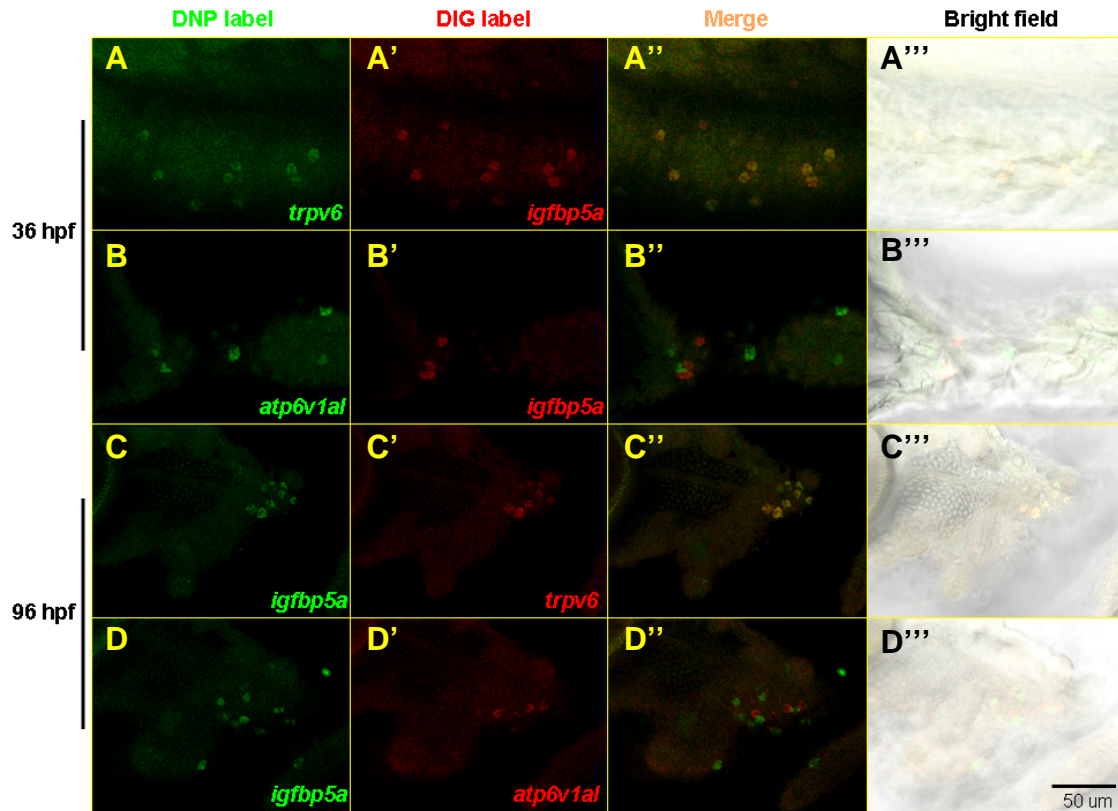


Figure 3.3 *igfbp5a* mRNA colocalizes with *trpv6* but not *atp6v1al*

Double fluorescent in situ hybridization of *igfbp5a* with *trpv6* (A-A''' and C-C'''), and *igfbp5a* with *atp6v1al* (B-B''' and D-D'''). Images shown are confocal micrographs of the yolk tube (A-A'' and B-B'') and gill (C-C'' and D-D'') areas. The riboprobe used is shown at the bottom right corner in the panel. The scale bar represents 50 μm .

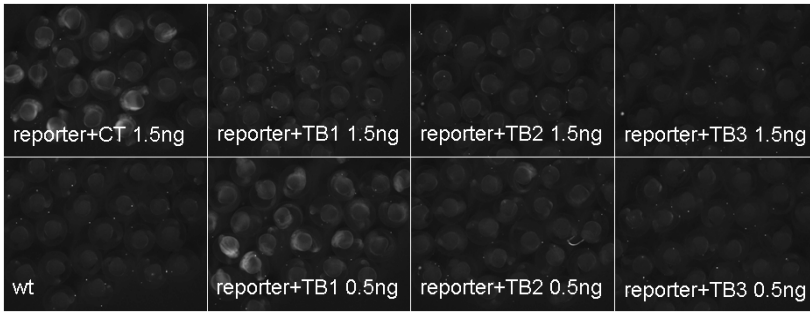
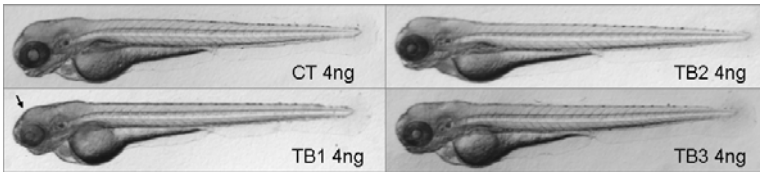
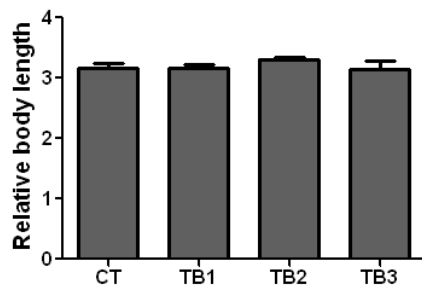
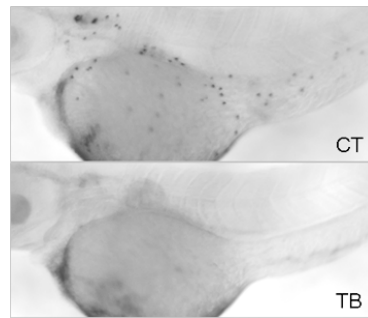
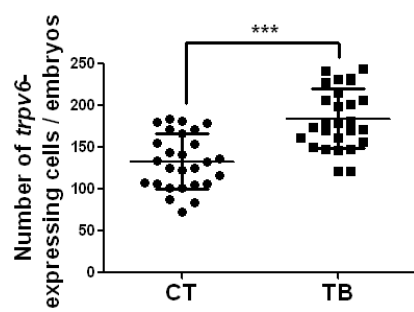
A**B****C****D****E**

Figure 3.4 Translation-blocking of *Igfbp5a* results in an increase in the number of *trpv6*-expressing ionocytes

A) Fluorescent microscopy images of GFP expression in 25 hpf embryos co-injected with MO and 250 pg *igfbp5a*-5'UTR:GFP reporter at 1~2 cell stage. B) Representative light microscopy images of MO injected embryos at 3 dpf. The arrow points to the region showing abnormality. C) Body length of MO injected embryos as shown in (B), mean \pm SD, n=3. D) Whole-mount in situ hybridization of *igfbp5a* mRNA in MO injected embryos at 2 dpf. CT, 8 ng; TB, 4 ng TB2 + 4 ng TB3. E) Number of *trpv6*-expressing ionocytes in MO injected embryos at 2 dpf (mean \pm SD, n=27). CT, 8 ng; TB, 4 ng TB2 + 4 ng TB3. CT, control MO; TB, translation-blocking MO. All images are lateral views, anterior to the left.

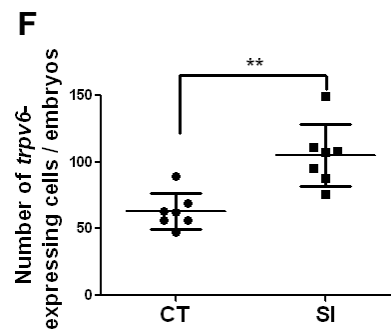
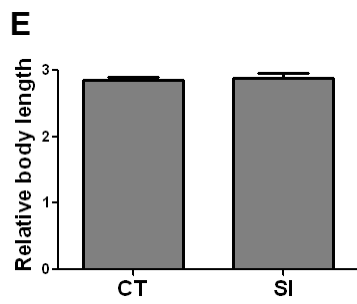
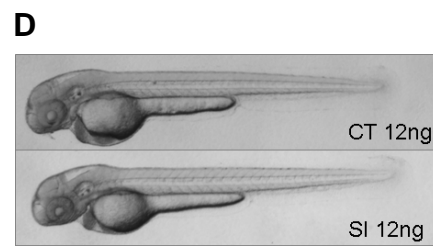
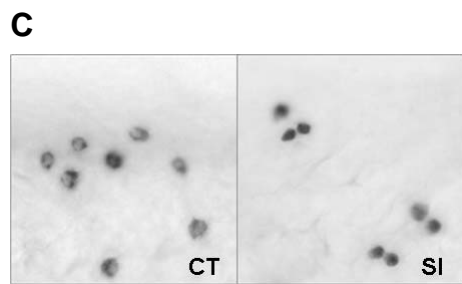
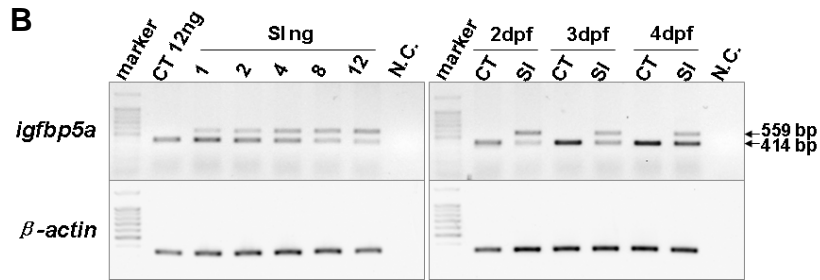


Figure 3.5 Splice-inhibiting of *Igfbp5a* results in an increase in the number of *trpv6*-expressing ionocytes

A) Structure of the zebrafish *igfbp5a* gene. Exons are shown as boxes, and introns are shown as lines. Light and dark shaded areas represent UTRs and ORF, respectively. The splice donor site targeted by the *Igfbp5a* MO is underlined. The primer set used for RT-PCR is shown as arrows. B) RT-PCR analyses of the dose-dependent effect of the *Igfbp5a* MO at 2 dpf, and the time-course effect of the *Igfbp5a* MO at 12 ng. C) Whole-mount in situ hybridization of *igfbp5a* mRNA in MO injected embryos at 2 dpf. CT, 12 ng; SI, 12 ng. Images shown are the yolk sac area of the zebrafish skin. D) Representative light microscopy images of MO injected embryos at 2 dpf. E) Body length of MO injected embryos as shown in (D), mean \pm SD, n=7. F) Number of *trpv6*-expressing ionocytes in MO injected embryos at 2 dpf (mean \pm SD, n=7). CT, 12 ng; SI, 12 ng. CT, control MO; SI, splice inhibiting MO. All images are lateral views, anterior to the left.

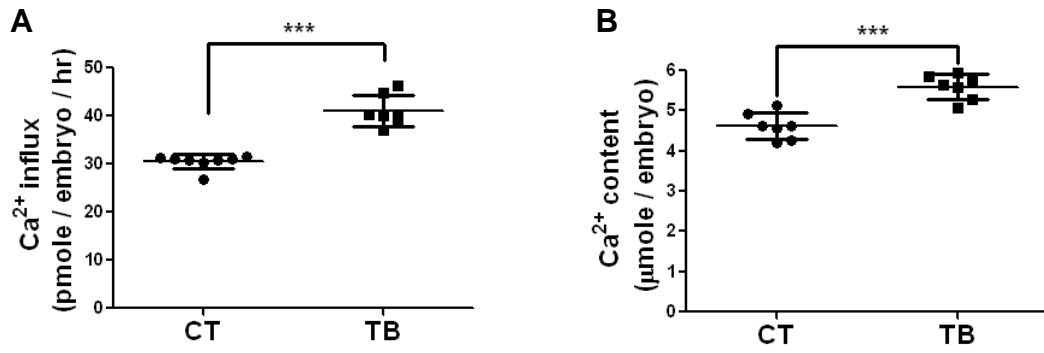


Figure 3.6 Knockdown of Igfbp5a results in an increase in Ca²⁺ influx and content

A) Ca²⁺ influx in MO injected embryos at 2 dpf (mean ± SD, n=7~8). B) Ca²⁺ content in MO injected embryos at 2 dpf (mean ± SD, n=7). CT, control MO, 8 ng; TB, translation-blocking MO, 4 ng TB2 + 4 ng TB3.

CHAPTER 4

Insulin-like growth factor (IGF) signaling is required for proliferation of the *trpv6*-expressing Na⁺-K⁺-ATPase-rich (NaR) cells in response to insufficient calcium supply in zebrafish

4.1 Abstract

Vertebrate transport epithelium is a highly adaptive tissue for nutrient uptake. In zebrafish, *igfbp5a* and *trpv6* co-expressing Na⁺-K⁺-ATPase-rich (NaR) cells involved in epithelial Ca²⁺ absorption increase their number in low-Ca²⁺ water. However, the underlying molecular mechanism was not clear. Here, we provide evidence that insulin-like growth factor (IGF) signaling pathway is required for the increase of the NaR cells during low-Ca²⁺ acclimation. First, IGF1R downstream Akt signaling is specifically activated upon low-Ca²⁺ treatment. Second, inhibition of IGF1R or PI3K abolishes the low-Ca²⁺ induced cell proliferation. Furthermore, low-Ca²⁺ acclimation increases the mRNA levels of one of the IGF1R ligands, *igf2a*. In summary, our study revealed a role of IGF/PI3K/Akt signaling in Ca²⁺ homeostasis by regulating the proliferation of the NaR cells in the transport epithelia.

4.2 Introduction

How animals adapt their physiological status to acclimate to the changing environment is a fundamental question in biology. One such environmental factor is nutrient availability. Ca²⁺ is an essential ion required for many different cellular processes, and it is also a major component in the bone. Animals need to uptake Ca²⁺ from

environmental resources to compensate for the daily loss in renal excretion and bone turnover. The demand for Ca^{2+} uptake becomes greater during skeletal growth in fetus and juveniles, as well as during pregnancy in females (Hoenderop et al., 2005; Suzuki et al., 2008b).

Mammalian Ca^{2+} uptake occurs in the transepithelial tissues, including the intestine, kidney, placenta, and mammary glands. Transcellular Ca^{2+} transport works through the apical Ca^{2+} channels TRPV5/TRPV6, the intracellular Ca^{2+} transporter calbindin- $\text{D}_{9\text{K}}/\text{D}_{28\text{K}}$, and the basolateral $\text{Na}^+/\text{Ca}^{2+}$ exchanger (NCX1)/plasma membrane Ca^{2+} ATPase (PMCA1b) (Hoenderop et al., 2005; Suzuki et al., 2008b). The activity of transcellular Ca^{2+} transport is regulated by dietary Ca^{2+} . When there is low Ca^{2+} supplementation in the diet, TRPV5/TRPV6 and calbindin gene expression becomes elevated (Song et al., 2003b).

Compared with terrestrial animals, fish absorb Ca^{2+} from their living aquatic environment. They have a specialized organ, the gill, for transepithelial Ca^{2+} transport. The transcellular Ca^{2+} uptake pathways are conserved between mammals and fish (Flik et al., 1995). The ionocytes (chloride cells or mitochondria-rich cells) in the gill are functionally equivalent to the epithelial cells in the mammalian transport epithelia. In the model organism zebrafish, a single *trpv6* gene has been identified (Pan et al., 2005). Similar to its mammalian counterparts, *trpv6* expression also increases in low- Ca^{2+} water (Liao et al., 2007). The *trpv6*-expressing cells are also named Na^+/K^+ -ATPase-rich (NaR) cells due to their strong and specific immunoreactivity with a heterologous Na^+/K^+ -ATPase antibody (Hwang, 2009). In zebrafish embryos and early larvae, these cells scatter on the yolk sac skin. The skin of zebrafish during early development provides an

appealing model to study the vertebrate transepithelial transport because it is readily accessible for experimental observation and manipulation (Hwang, 2009).

An interesting phenomenon of low-Ca²⁺ water adaptation in fish is that the number of chloride cells/mitochondria-rich cells/ NaR cells increases (McCormick et al., 1992; Pan et al., 2005; Perry and Wood, 1985). However, the underlying mechanism was poorly understood. It was not clear whether the increased cells come from transdifferentiation, migration, or proliferation. More importantly, although it is known that calcitropic hormones such as vitamin D₃ can upregulate Trpv6 (Song et al., 2003b), which hormone or growth factor stimulates the increase in cell number was elusive.

Recently, we discovered co-expression of *igfbp5a* in the NaR cells in zebrafish (Chapter 3). IGFBP5a belongs to a family of high-affinity IGF binding proteins that can regulate the bioavailability of IGF (Dai et al., 2010). The signal of IGF ligands, IGF1 and IGF2, are transduced into the cells through a plasma membrane receptor tyrosine kinase IGF1R. Major downstream cascades include the PI3K/Akt and MAPK pathway (Samani et al., 2007). IGF signaling plays critical roles in cell proliferation, differential, survival, and cell migration. Furthermore, GH and IGF1 can stimulate the number of chloride cells in fish gills during seawater adaption (McCormick, 2001). Therefore, IGF signaling appears to be a strong candidate for low-Ca²⁺ water adaptation.

In this study we aim to use zebrafish as a model to characterize the low-Ca²⁺ acclimation. We found that in addition to upregulation of *trpv6*, cell number gradually increases due to elevated cell proliferation during the larval stage. Importantly, IGF1R and Akt signaling is activated in the cells, and inhibition of them abolished the increase in cell number but not the *trpv6* expression. Furthermore, locally expressed *Igfbp5a* and

Igf2a may also be involved during the acclimation. These findings provide molecular cues to how growth factor signaling regulates cell population during environmental adaptation.

4.3 Result

4.3.1 Low-Ca²⁺ acclimation results in a dramatic increase in the NaR cells and a correlated increase in *igfbp5a* mRNA expression

We previously found that zebrafish *igfbp5a* is specifically expressed in the NaR cells, but not the *atp6v1al*-expressing cells (Chapter 3). It has been shown that the number of the NaR cells significantly increases when Ca²⁺ is reduced in the water (Pan et al., 2005). To test if *igfbp5a* is also regulated by Ca²⁺, we characterized the expression of *igfbp5a* in 5 dpf zebrafish larvae raised in artificial freshwater with different Ca²⁺ levels. Similar to *trpv6* (Fig. 4.1A, middle panel), the number of the NaR cells increased dramatically when Ca²⁺ was reduced from 2 to 0.001 mM (Fig. 4.1A, top panel and Fig. 4.1B). In comparison, the number of *atp6v1al*-expressing cells was not significantly different among the groups (Fig. 4.1A, bottom panel). The mRNA level of *igfbp5a* (Fig. 4.1C) correlates with its cell number (Fig. 4.1D), indicating that the expression level of *igfbp5a* per cell is similar in different Ca²⁺ conditions. In contrast, *trpv6* expression level per cell increases when Ca²⁺ level decreases (Fig. 4.1A, middle panel and Fig. 4.3). Therefore, *igfbp5a* expression level serves better than that of *trpv6* to estimate the number of the NaR cells. To further test the specificity of the regulation, other ion concentrations were altered in similar experiments. We found that *igfbp5a* expression is only regulated by Ca²⁺, but not other ions (Fig. 4.1E).

4.3.2 The increased NaR cells in low-Ca²⁺ water is due to elevated cell proliferation during the larval stage

To understand how the number of the NaR cells was elevated in low-Ca²⁺ water, we first investigated the critical time window for the cell number increase in response to low Ca²⁺. The number of the NaR cells did not change in water with different Ca²⁺ levels at 60 hpf (Fig. 4.2A). By switching embryos from normal- to low-Ca²⁺ water, or vice versa, at different time points (Fig. 4.2B and 2C), we found that low-Ca²⁺ treatment from 72 to 120 hpf increased *igfbp5a* expression to a similar extent compared with the 5-day treatment (Fig. 4.2B). However, low-Ca²⁺ treatment during 0 to 72 hpf did not cause a significant change in 120 hpf larvae (Fig. 4.2C). We adopted low-Ca²⁺ treatment from 72 hpf in our following experiments for two reasons: 1) the time period for treatment is shortened; 2) the early embryonic development is left intact, which helps us to focus on physiological response rather than embryonic developmental defect.

To test if the cell number increase is due to elevated cell proliferation, BrdU labeling was performed. For larvae incubated in BrdU from 96 to 120 hpf, few BrdU positive cells were detected on the skin covering the yolk sac, in normal-Ca²⁺ water. In contrast, a large population of cells incorporated BrdU in low-Ca²⁺ water (Fig. 4.2D). When larvae were pulse labeled with BrdU during 84-96 hpf and sampled at 5 dpf, we also found more BrdU positive cells in the low-Ca²⁺ group than the normal-Ca²⁺ group. More importantly, most BrdU positive cells in low-Ca²⁺ water co-expressed *igfbp5a*, whereas colocalization of BrdU and *igfbp5a* was hardly detected in normal-Ca²⁺ water (Fig. 4.2E), suggesting that the increased the NaR cells result from elevated cell proliferation. Furthermore, for as short as a 30 min incubation in BrdU, we observed that

the majority of BrdU incorporating cells in the low-Ca²⁺ group are *igfbp5a* positive (Fig. 4.2F), suggesting that the NaR cells are proliferating. Taken together, low-Ca²⁺ treatment induces NaR cell proliferation.

4.3.3 Low Ca²⁺ acclimation increases *trpv6* gene expression in addition to the NaR cell number change

In addition to the cell number increase, *trpv6* expression level per cell also increases in low-Ca²⁺ water (Fig. 4.1A, middle panel) (Pan et al., 2005). To further characterize the regulation of *trpv6* expression, we performed more detailed analyses during different acclimation time points. First, when embryos were raised in normal- or low-Ca²⁺ water and sampled before 72 hpf (Fig. 4.2A and 3A), we found no significant change in *igfbp5a* expression level or cell number. In contrast, *trpv6* expression level was 5.58 ± 2.58 fold higher in low-Ca²⁺ than normal-Ca²⁺ water at 48 hpf, and 4.35 ± 1.40 fold higher at 72 hpf (Fig. 4.3B). Second, when we switched larvae to normal- or low-Ca²⁺ water at 72 hpf and sampled them every 12 hr thereafter (Fig. 4.3C), we found that there was no significant change of *igfbp5a* expression until after 24 hr (Fig. 4.3D) when a 2.08 ± 0.08 fold increase was observed at 108 hpf, and a 3.76 ± 0.69 fold increase was observed at 120 hpf. However, *trpv6* expression becomes 4.05 ± 0.69 fold higher in as short as 12 hr and continues to increase thereafter (Fig. 4.3E). When normalized by *igfbp5a*, *trpv6* expression remains 4.14-6.77 fold higher in low-Ca²⁺ than in normal-Ca²⁺ water (Fig. 4.3F). Third, during 24 hr acclimation to high- or low- Ca²⁺ water (Fig. 4.3G), *igfbp5a* expression level stays relatively constant, whereas *trpv6* expression can be up- or down-regulated significantly (Fig. 4.3H). Such change is mostly due to the change of *trpv6* expression level in individual cells, as revealed by in situ hybridization analysis

(Fig. 4.3I, lower panels). Therefore, these experiments further demonstrate that the increase in *trpv6* gene expression is due to an increase in cell number as well as expression level per cell, and the latter change occurs faster than the former one.

4.3.4 Low Ca^{2+} acclimation activates Akt but not MAPK signaling in the NaR cells through an IGF1R-dependent mechanism

Cell proliferation is one major cellular outcome of activated IGF signaling. Major intracellular signaling cascades downstream of IGF1R include PI3K-Akt and MAPK pathways (Samani et al., 2007). To test if IGF and downstream signaling activities change during low- Ca^{2+} treatment, we examined the phosphorylation status of the IGF1R, Akt, and MAPK. First, we validated whether the heterogeneous antibodies work for the zebrafish proteins. Although all of the antibodies detected proteins of the correct size in western blot, only pAkt and pMAPK antibodies worked in immunohistochemistry in cultured zebrafish cells (data not shown). When used in zebrafish, pIGF1R staining also failed to yield specific signals (data not shown).

Interestingly, when we examined the phosphorylation status of Akt and MAPK in 5 dpf larvae that were acclimated to normal- or low- Ca^{2+} water, we found that the number of cells showing pAkt signal and the intensity of signal in the cells increase when Ca^{2+} level in the water decreases (Fig. 4.4A), and the pattern mimics that of the NaR cells (Fig. 4.1C). In contrast, pMAPK signal was detected in some different types of cells on the yolk skin, and its pattern did not appear to be significantly different between normal- and low- Ca^{2+} groups (Fig. 4.4B). To examine the time course of Akt phosphorylation induced by low- Ca^{2+} water, we collected samples at different time points following low- Ca^{2+} treatment. pAkt signal starts to appear in the yolk skin cells in 30 min. The intensity of

the pAkt signal and the number of cells increase at later time points (Fig. 4.4C). To confirm that Akt is indeed activated in the NaR cells, we co-stained pAkt with *trpv6*. In a total of 62 pAkt positive cells examined, we found that *trpv6* was co-expressed in all of them (Fig. 4.4D).

To test whether IGF signaling acts upstream of Akt in the NaR cells, we assayed if inhibition of IGF1R would affect pAkt induction during low-Ca²⁺ treatment. Two selective pharmacological inhibitors against IGF1R, BMS-754807 (Carboni et al., 2009) and NVP-AEW541 (Garcia-Echeverria et al., 2004), were used. Importantly, similar to PI3K inhibitors wortmannin and LY294002, inhibition of IGF1R using BMS-754807 and NVP-AEW541 significantly reduced pAkt signal in low-Ca²⁺ water (Fig. 4.4E). Meanwhile, although MEK inhibitors U0126 and PD98059 significantly reduced pMAPK signal on the yolk sac skin, neither IGF1R inhibitors showed any inhibitory effect on the pMAPK signal (Fig. 4.4F). These results suggest that IGF1R acts upstream of Akt in the NaR cells, whereas the MAPK signals observed are not activated by the IGF signaling.

4.3.5 IGF1R and Akt signaling is required for the low-Ca²⁺ induced increase in NaR cell proliferation

The rapid activation of pAkt upon low-Ca²⁺ treatment and the following increase of the NaR cells prompted us to ask whether IGF signaling may play a role in the low-Ca²⁺ induced cell proliferation. We titrated the dose so that the inhibitors could significantly reduce pAkt or pMAPK, but they did not affect survival of the larvae. Both BMS-754807 (14 out of 14 larvae) or NVP-AEW541 (9 out of 11 larvae) inhibited the cell number increase in low-Ca²⁺ water, albeit they had little effect in normal-Ca²⁺ water

(Figures 5A and 5B, left panels). In comparison, Notch inhibitor DAPT (Geling et al., 2002) did not affect the cell number in either normal- or low-Ca²⁺ water (Figures 5A and 5B, middle panels). We further tested whether the PI3K-Akt or MAPK pathway is required for the low-Ca²⁺ induced increase of the NaR cells. Both PI3K inhibitors, wortmannin (11 out of 11 larvae) and LY294002 (9 out of 12 larvae), abolished the cell number increase in low-Ca²⁺ water, whereas MEK inhibitors, U0126 and PD98059, had little effect (Figures 5A and 5B, right panels).

The cell number change is further corroborated by quantifying the expression level of *igfbp5a* (Fig. 4.5C). In the DMSO control group, low-Ca²⁺ water induced a 3.22 ± 0.82 fold increase in *igfbp5a* mRNA. A similar increase is observed in the DAPT, U0126, and PD98059 treatment groups. Such an increase is significantly abolished in the BMS-754807 (0.76 ± 0.15 fold over normal-Ca²⁺ water) and NVP-AEW541 (1.55 ± 0.11 fold over normal-Ca²⁺ water) treatment groups, as well as wortmannin (0.89 ± 0.03 fold over normal-Ca²⁺ water) and LY294002 (1.18 ± 0.35 fold over normal-Ca²⁺ water) treatment groups.

4.3.6 Igfbp5a modulates local Igf actions in the NaR cells in low-Ca²⁺ water

IGF1R is activated by its ligands IGF1 or IGF2, and the availability of the ligand is further regulated by extracellular IGFbps. To test if the expression levels of four different *igf* ligands (Zou et al., 2009) change between normal- and low-Ca²⁺ treatment groups, we performed whole-mount *in situ* hybridization. Interestingly, one of the four ligands, *igf2a* (Fig. 4.6A, middle panel), is expressed in many cells on the yolk skin in low-Ca²⁺ water, whereas its expression is barely detected in normal-Ca²⁺ water.

Expression of the other three ligands, *igf1a*, *igf1b*, and *igf2b*, was not detected on the yolk skin (Fig. 4.6A, right panel and data not shown),

The fact that *igfbp5a* is distinctly expressed in the NaR cells prompted us to ask whether Igfbp5a plays a role in modulating IGF signaling in these cells. Since *igf2a* is the local *igf* that increases its expression level in low-Ca²⁺ water, we first tested whether Igfbp5a binds IGF2. Previously, we have shown that Igfbp5a can bind human IGF1 (Dai et al., 2010). Similarly, we confirmed that both GFP tagged and myc tagged Igfbp5a can bind human IGF2 *in vitro* (Fig. 4.6B). We next used antisense morpholinos (MOs) to knockdown Igfbp5a. The specificity and efficiency of the Igfbp5a targeting MOs were verified using 5' untranslated region:GFP reporters (data not shown). No apparent morphological abnormality was observed in the Igfbp5a morphants (data not shown). Interestingly, compared with the control MO injected group, Igfbp5a morphants showed significantly reduced pAkt signal following 2 hr low-Ca²⁺ treatment. The signal level in the Igfbp5a morphants after 8 hr low- Ca²⁺ treatment was not significantly different from the control (Fig. 4.6C). Therefore, Igfbp5a appears to be a local modulator of IGF signaling by facilitating the rapid signal activation. However, the number of the NaR cells still increases in response to low-Ca²⁺ in the Igfbp5a morphants at 5 dpf (Fig. 4.6D).

4.3.7 IGF signaling is also required for the low-Ca²⁺ induced increase of the NaR cells in adult zebrafish gills

Our data suggested a new role of IGF signaling in Ca²⁺ homeostasis regulation by adjusting the population of the NaR cells in zebrafish larva (Fig. 4.7A). To test if this is conserved in adult Ca²⁺ homeostasis regulation, adult zebrafish gill, the main organ involved in ionoregulation, was assayed in Ca²⁺ acclimation conditions. Similar to what

happens at the larval stage (Fig. 4.3C-F), a rapid increase in *trpv6* and a gradual increase in *igfbp5a* expression levels are also observed in gills when the adult fish were acclimated to low-Ca²⁺ water (Fig. 4.7B-E). Upregulation of *igf2a* expression (Fig. 4.7B, 2.56 ± 0.66 fold over normal-Ca²⁺ water, $P < 0.02$), but not other *igf* ligands or receptors (Fig. 4.8), was also found in adult zebrafish gills in low-Ca²⁺ water. Furthermore, IGF1R inhibitor BMS-754807 (Fig. 4.7G, 0.38 ± 0.17 fold over normal-Ca²⁺ water) also abolished the increase of *igfbp5a* expression in response to low-Ca²⁺ water in the control group (9.86 ± 5.08 fold over normal-Ca²⁺ water).

4.4 Discussion

We show that IGF signaling is required for regulating Ca²⁺ uptake capacity in the vertebrate transport epithelia. We discovered an increased proliferation rate as a cellular mechanism to expand the population of the NaR cells during low-Ca²⁺ water acclimation in zebrafish. We identified IGF1R/PI3K/Akt signaling as a key player during this physiological adaptation.

We found that IGF signaling is necessary for low-Ca²⁺ adaptation in both zebrafish larvae and adults. However, low-Ca²⁺ treatment prior to 72 hpf did not increase the number of the NaR cells. This may be explained by the negligible demand for Ca²⁺ absorption during embryogenesis, when internal Ca²⁺ preserved in the yolk ball is sufficient for early developmental events (Pan et al., 2005). In fish gills, it has been shown that injecting GH or IGF increases the number of chloride cells (McCormick, 2001). It would be interesting to test whether IGF signaling is sufficient to induce the NaR cells in the larvae.

Our study also reveals that the environmental Ca^{2+} level can rapidly induce intracellular signaling for cell proliferation. Interestingly, low Ca^{2+} also induces cell proliferation in colon cells both *in vitro* and *in vivo* (Buset et al., 1986; Kallay et al., 1997). A model involving Ca^{2+} -sensing receptor (CaSR) signaling has been proposed (Lamprecht and Lipkin, 2003; Whitfield, 2009). TRP channels are well known in sensing environmental stimuli (Clapham, 2003), and TRPV6 channel activity can be regulated by the extracellular Ca^{2+} level (Bodding and Flockerzi, 2004). In keratinocytes, TRPV3 activity can induce TGF- α release to activate the EGF receptor (Cheng et al., 2010). Moreover, in breast cancer cells, calmodulin mediated Ca^{2+} signaling has been shown to activate Akt (Coticchia et al., 2009). Further studies are needed to clarify how Ca^{2+} signaling and IGF signaling may crosstalk to accelerate cell cycles during low- Ca^{2+} acclimation.

Our findings may have implications in mammalian systems. We found that the onset of the *igfbp5a* expression level increase was slower compared with *trpv6*, and the magnitude was smaller. Similarly, in mammalian intestinal tissues or cell lines, induced expression level of *Calbindin*, the intracellular Ca^{2+} -binding protein, was also found to be lower than that of *Trpv6*, and the upregulation also initiated later (Song et al., 2003b; Wood et al., 2001). It will be interesting to examine whether the number of cells that mediates Ca^{2+} uptake in mammalian transport epithelia also increase when the demand for transcellular Ca^{2+} transport elevates. We found that *igf2a* expression levels increase during low- Ca^{2+} acclimation. IGF2 has also been shown to act as a local hormone to trigger the tissue specific response of PRL in the mammary gland (Briskin et al., 2002). Placental-specific expression of IGF2 is important for fetal Ca^{2+} supply in mice (Dilworth

et al., 2010). Meanwhile, TRPV6 is also expressed in the mammary gland (Zhuang et al., 2002) and required for maternal-fetal Ca^{2+} transport (Suzuki et al., 2008a). A potential role of IGF in regulating the mammalian TRPV6-expressing epithelial cells may be explored.

This study may also provide broader insights into our understanding of how physiological adaptation occurs at the cellular and molecular level. Change in cell proliferation rate in response to altered physiological conditions has been demonstrated in other systems, such as increased proliferation of β -cells in the pancreas during pregnancy (Parsons et al., 1992). Furthermore, both IGF signaling and TRPV6 expression level correlate with human malignancy (Peng et al., 2001b; Pollak et al., 2004; Samani et al., 2007). Studying the mechanism of the crosstalk will aid in developing therapeutic strategies.

4.5 Materials and Methods

Experimental animals and acclimation conditions: Wild-type zebrafish (*Danio rerio*) were maintained on a 14 hr light/10 hr dark cycle at 28°C and fed twice daily. Fertilized eggs were raised in fish medium at 28.5 °C and staged according to the standard method (Kimmel et al., 1995). To inhibit pigmentation, fish medium was supplemented with 0.003% (w/v) N-phenylthiourea. All experiments were conducted in accordance with the guidelines established by the University Committee on the Use and Care of Animals at the University of Michigan.

Acclimation conditions were made according to the method reported (Chen et al., 2003) with minor modifications: artificial freshwater was prepared with double-deionized water (Milli-Q Academic System, Millipore, Billerica, MA, USA) supplemented with

adequate $\text{CaSO}_4 \cdot 2\text{H}_2\text{O}$, $\text{CaCl}_2 \cdot 2\text{H}_2\text{O}$, $\text{MgSO}_4 \cdot 7\text{H}_2\text{O}$, $\text{MgCl}_2 \cdot 6\text{H}_2\text{O}$, NaCl , Na_2SO_4 , K_2HPO_4 , KH_2PO_4 , KCl , $\text{Na}_2\text{HPO}_4 \cdot 7\text{H}_2\text{O}$, and $\text{NaH}_2\text{PO}_4 \cdot \text{H}_2\text{O}$. Nominal ion concentrations and osmolarity of the media are summarized in Table S1. Fish medium was refreshed every day.

Whole-mount *in situ* hybridization: Digoxigenin-labeled antisense riboprobes for *igfbp5a* (Dai et al., 2010), *trpv6* (Pan et al., 2005), *atp6v1al* (Lin et al., 2006), *igf2a*, and *igf2b* (Zou et al., 2009) were generated by *in vitro* transcription, and whole-mount *in situ* hybridization was performed as previously described (Maures et al., 2002). Images were captured with a compound microscope (Nikon Eclipse E600) equipped with a Nikon DC50NN camera or a Photometric CoolSNAP EZ camera, and a stereomicroscope (Leica MZ16F) equipped with a QImaging QICAM camera.

Reverse transcription (RT)-PCR and quantitative real-time PCR (qPCR): Total RNA was isolated from 12~15 embryos/larvae or 1~2 adult zebrafish gills per sample using TRIzol reagent (Invitrogen). One μg total RNA was reverse-transcribed to single strand cDNA using M-MLV reverse transcriptase (Invitrogen). Semi-quantitative RT-PCR was performed using Taq DNA polymerase (New England Biolabs). qPCR was carried out using iQ SYBR Green Supermix (Bio-Rad) with an iCycler iQ Multicolor real-time PCR detection system (Bio-Rad). The efficiency and specificity of the qPCR were verified by standard curve and denaturing curve analyses. The expression level of a particular gene transcript was calculated based on the standard curve and normalized to *β -actin* mRNA level. Primers used are listed in Table S2.

BrdU labeling and co-staining with *in situ* hybridization: BrdU labeling was performed by incubating the larvae in 10 mM BrdU (Sigma) dissolved in fish medium

(Mueller and Wullimann, 2002). BrdU staining was performed using a mouse anti-BrdU antibody (Sigma) at 1:100 followed by anti-mouse-HRP (Jackson ImmunoResearch) and Nickel-diaminobenzidine staining according to the published protocol (Shepard et al., 2005). *In situ* hybridization and BrdU co-staining was performed by fluorescent *in situ* hybridization using DIG-labeled *igfbp5a* riboprobe followed by BrdU staining. Images were captured with a compound microscope (Nikon Eclipse E600) equipped with a Photometric CoolSNAP EZ camera.

Whole-mount immunohistochemistry and co-staining with *in situ*

hybridization: Zebrafish larvae were fixed in 4% paraformaldehyde, permeabilized in ethanol, and subsequently subjected to blocking with 5% serum. Samples were then incubated with primary antibody overnight at 4°C. Samples were washed and then incubated with anti-rabbit-HRP (Jackson ImmunoResearch) followed by Nickel-diaminobenzidine staining. We used the following antibodies: rabbit anti-pAkt (Cell Signaling) at 1:200, rabbit anti-pMAPK (Cell Signaling) at 1:400. Images were captured with a stereomicroscope (Leica MZ16F) equipped with a QImaging QICAM camera, or a compound microscope (Nikon Eclipse E600) equipped with a Photometric CoolSNAP EZ camera. For *in situ* hybridization and immunofluorescence co-staining, samples were subjected to *trpv6 in situ* hybridization (omit proteinase K treatment) and then to pAkt immunofluorescence. Images were acquired using Leica TCS SP5 confocal microscope with the Leica LAS AF software.

Chemical inhibitor treatment and MO microinjection: Zebrafish were treated with pIGF1R inhibitor BMS-754807 (JiHe Pharma) and NVP-AEW541 (Novartis); PI3K inhibitor wortmannin and LY294002 (Cell Signaling); MAPK inhibitor U0126 and

PD98059 (Cell Signaling); and Notch inhibitor DAPT (Sigma). The same concentration of DMSO was used for the control.

MOs were obtained from Gene Tools (Philomath, OR, USA) and injected into 1~2 cell stage embryos as reported (Li et al., 2005). Two translation-blocking MOs were designed to target against the *igfbp5a* start codon (5'-CAAACCTTAGCAGCATCGTCCTACTG-3' targets nucleotides -10 to 15, and 5'-TTTGTATCGTTTAAGGTTCCCGAGT-3' targets nucleotides -78 to -54) and injected at 4 + 4 ng/embryo. A standard control MO (5'-CCTCTTACCTCAGTTACAATTTATA-3') was injected at 8 ng/embryo.

Ligand blot and western blot: IGFBP::GFP and IGFBP::myc expression vectors were described previously (Dai et al., 2010). Human IGFBP5 ligand binding domain (LBD) mutant (K68N/P69Q/L70Q/L73Q/L74Q) (Imai et al., 2000) was used as a negative control in the GFP fusion protein group. A non-tagged GFP expressing vector was used as a negative control in the myc fusion protein group. The IGFBP fusion proteins were produced by transfecting cultured human embryonic kidney cells (HEK 293) with an expression vector using Lipofectamine 2000 (Invitrogen). One day post-transfection, cells were switched to serum-free medium containing 300 ng/ml heparin for another two days. Conditioned media were collected, and the expression levels of the IGFBP fusion proteins were measured by western blot using an anti-GFP antibody (Torrey Pines Biolabs, Houston, TX) or an anti-myc antibody (Santa Cruz Biotechnology, Santa Cruz, CA, USA). Their IGF binding abilities were determined by ligand blot using DIG-labeled human IGF1 and IGF2 following published procedure (Shimizu et al., 2000b).

Statistics: Statistical differences among experimental groups were analyzed by one-way analysis of variance (ANOVA), followed by Tukey's multiple comparison test using GraphPad Prism 5 (GraphPad Software, Inc., La Jolla, CA, USA). Correlation was analyzed by fitting the data to the equation $Y=X$ to calculate r^2 using GraphPad Prism 5. Significance was accepted at $P < 0.05$ or better.

4.6 Acknowledgements

We are grateful to Drs. Pung-Pung Hwang and Shenghui He for reagents and technical assistance. We also thank Ms. Lisa Hebda and Ms. Catherine Nosal for critical reading of this manuscript. This study was supported by NIH Grant 2RO1HL60679 and NSF Research Grant IOB 0110864 to CD and by a Rackham Graduate Student Research Grant to WD.

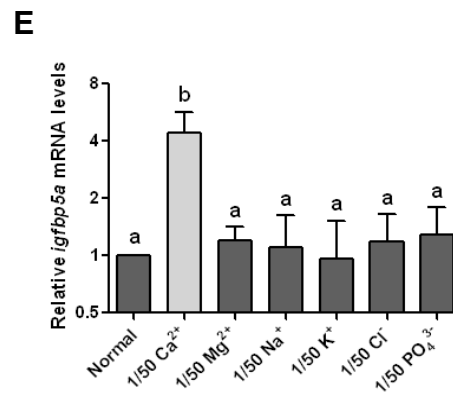
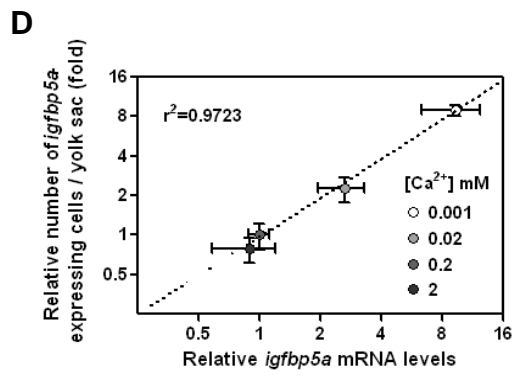
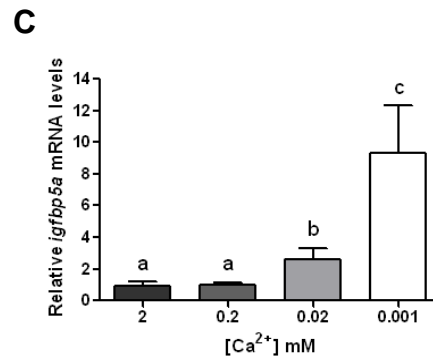
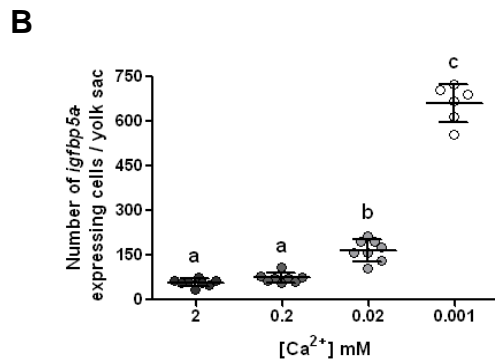
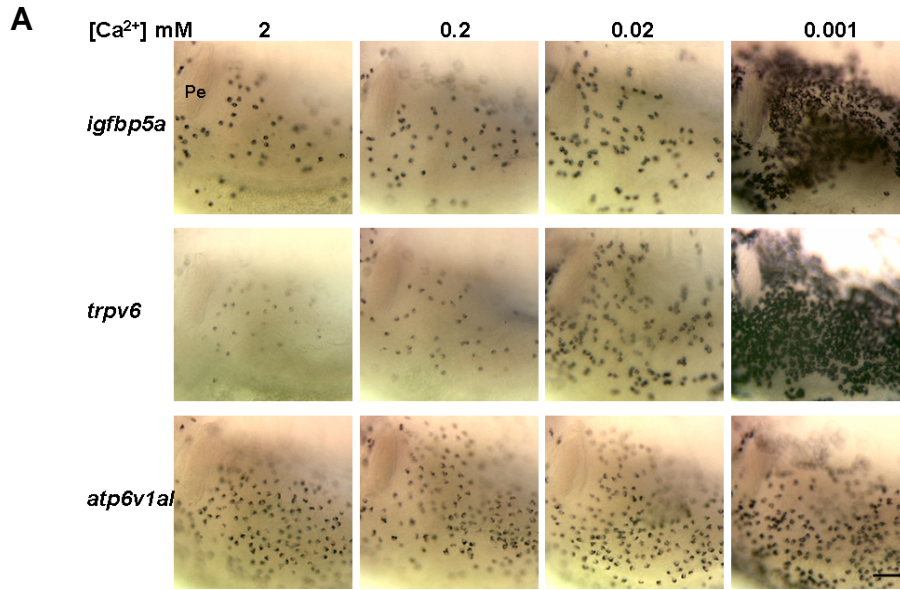


Figure 4.1 Low Ca^{2+} acclimation results in a dramatic increase in the NaR cells and a correlated increase in *igfbp5a* mRNA expression

A-B) Whole-mount *in situ* hybridization of 5 dpf larvae raised in artificial freshwater with different $[\text{Ca}^{2+}]$ for 5 days. Images shown are the yolk sac area of the zebrafish skin (A). All images are lateral views, anterior to the left. Pe, pectoral fin. The scale bar represents 50 μm . Number of *igfbp5a*-expressing cells was obtained by counting whole-mount *in situ* hybridization signals in one side of the yolk sac (B, mean \pm SD, n=6-8). C) Quantitative real-time PCR measurement of relative *igfbp5a* mRNA levels in 5 dpf larvae raised in artificial freshwater with different $[\text{Ca}^{2+}]$ for 5 days (mean \pm SD, n=3). D) Relationship between relative number of *igfbp5a*-expressing cells (B) and relative *igfbp5a* mRNA levels (C). E) Quantitative real-time PCR measurement of relative *igfbp5a* mRNA levels in 5 dpf larvae raised in artificial freshwater with altered ion concentrations for 5 days (mean \pm SD, n=3). Normal, 0.2 mM Ca^{2+} , 0.16 mM Mg^{2+} , 0.5 mM Na^+ , 0.165 mM K^+ , 0.5 mM Cl^- , and 0.085 mM PO_4^{3-} . Groups with no common letters are significantly different from each other ($p < 0.05$). dpf, day post fertilization.

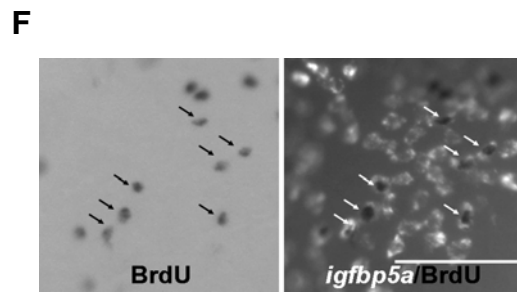
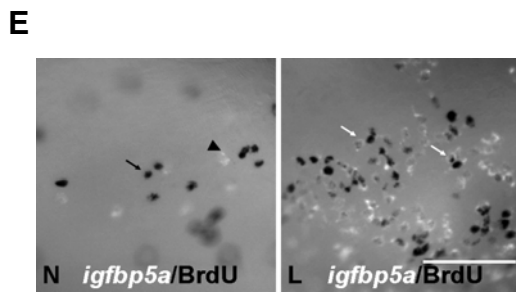
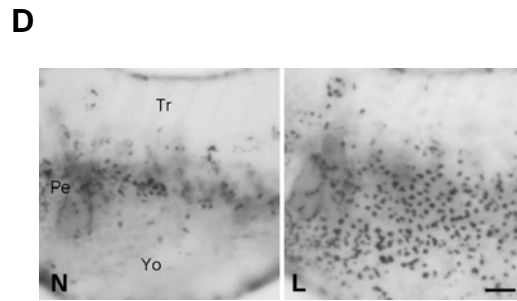
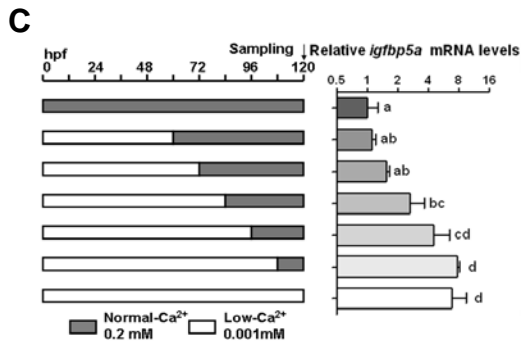
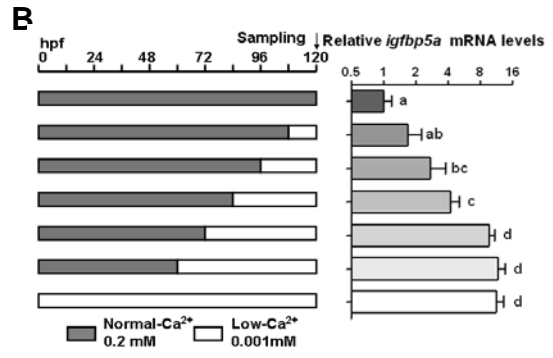
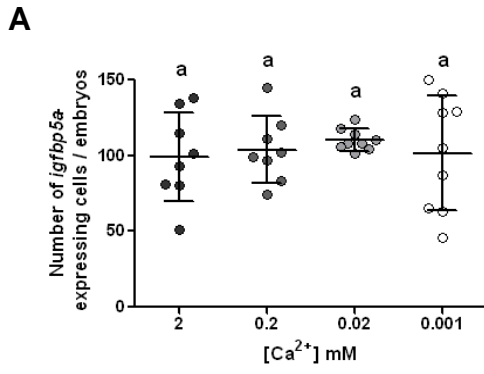


Figure 4.2 The increase in the NaR cells in low-Ca²⁺ water is due to elevated cell proliferation during the larval stage

A) Number of *igfbp5a*-expressing cells in 60 hpf embryos raised in artificial freshwater with different [Ca²⁺] by counting whole mount *in situ* hybridization signals (mean ± SD, n=8-9). B-C) Quantitative real-time PCR measurement of relative *igfbp5a* mRNA levels of 120 hpf larvae acclimated to normal- or low-Ca²⁺ water (mean ± SD, n=3). The schemes illustrate the fish raising procedures. D) BrdU staining of 120 hpf larvae acclimated to normal- or low-Ca²⁺ water starting from 72 hpf. Larvae were incubated in medium containing BrdU from 96 to 120 hpf. Tr, trunk; Pe, pectoral fin; Yo, yolk sac. E) *in situ* hybridization and BrdU co-staining of 120 hpf larvae acclimated to normal- or low-Ca²⁺ water starting from 72 hpf. Larvae were incubated in medium containing BrdU during 84-96 hpf. F) *in situ* hybridization and BrdU co-staining of 120 hpf larvae acclimated to low-Ca²⁺ water starting from 72 hpf. Larvae were incubated in medium containing BrdU for 30 min before sampling. Images shown are the yolk sac area of the zebrafish skin. All images are lateral views, anterior to the left. N, normal-Ca²⁺, 0.2 mM; L, low-Ca²⁺, 0.001 mM. hpf, hour post fertilization. The scale bar represents 50 μm.

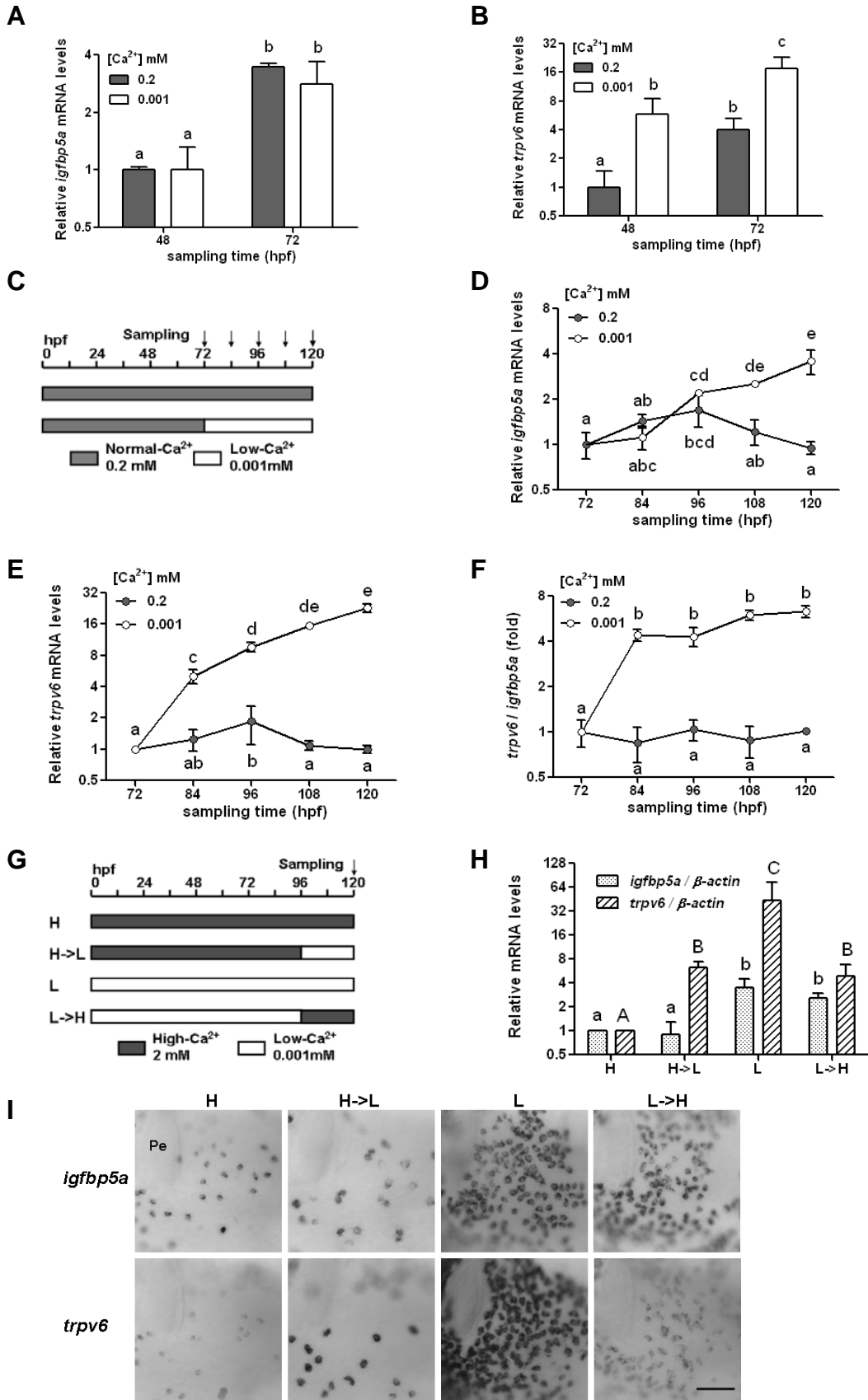


Figure 4.3 Low Ca^{2+} acclimation increases *trpv6* gene expression in addition to the NaR cell number change

A-B) Quantitative real-time PCR measurement of relative *igfbp5a* (A) and *trpv6* (B) mRNA levels in 48 and 72 hpf embryos raised in normal- or low- Ca^{2+} water (mean \pm SD, n=3). C-F) Quantitative real-time PCR measurement of relative *igfbp5a* (D) and *trpv6* (E) mRNA levels and the ratio of *trpv6/igfbp5a* (F) in larvae acclimated to normal- or low- Ca^{2+} water starting from 72 hpf and collected at different time points indicated (mean \pm SD, n=3). The scheme illustrates the fish raising procedures (C). G-I) 5dpf larvae acclimated to high- or low- Ca^{2+} water. The scheme illustrates the fish raising procedures (G). Relative *igfbp5a* and *trpv6* mRNA levels were measured by quantitative real-time PCR (mean \pm SD, n=3). *in situ* hybridization images are shown for the yolk sac area of the zebrafish skin (I). All images are lateral views, anterior to the left. H, high- Ca^{2+} , 2 mM; L, low- Ca^{2+} , 0.001 mM. The scale bar represents 50 μm . hpf, hour post fertilization.

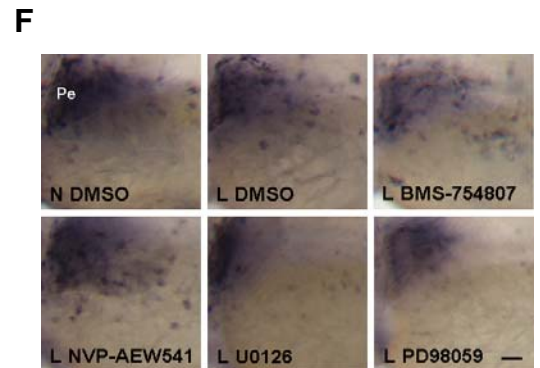
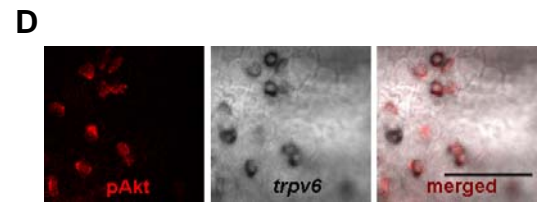
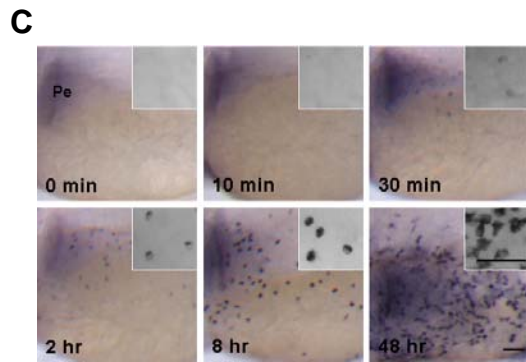
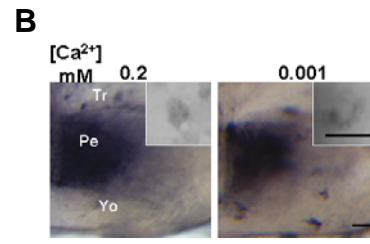
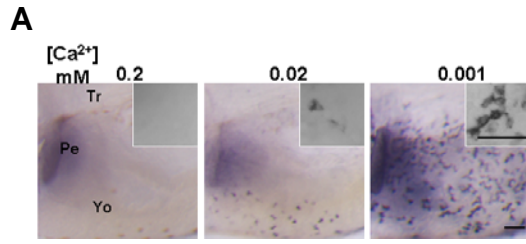
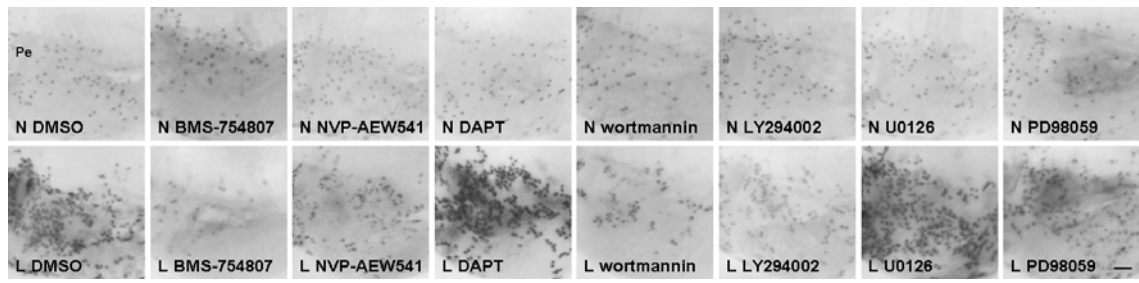


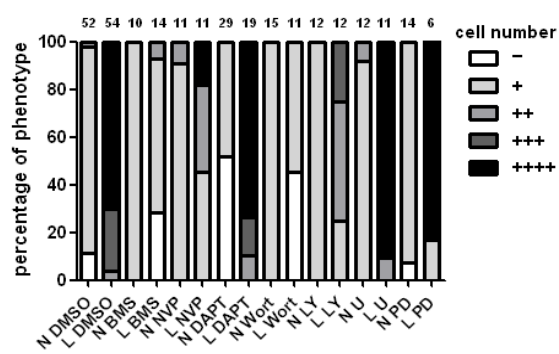
Figure 4.4 Low Ca^{2+} acclimation activates Akt but not MAPK signaling in NaR cells through an IGF1R-dependent mechanism

A-B) pAkt (A) and pMAPK (B) staining of 5 dpf larvae acclimated to artificial freshwater with different $[\text{Ca}^{2+}]$ starting from 72 hpf. C) pAkt staining of larvae switched from normal- to low- Ca^{2+} water at 72 hpf for the period of time indicated. D) *trpv6*/pAkt co-staining of 3 dpf larvae switched from normal- to low- Ca^{2+} water for 8 hr. E-F) pAkt (E) and pMAPK (F) staining of 3 dpf larvae acclimated to low- Ca^{2+} water for 8 hr. BMS-754807 0.6 μM , NVP-AEW541 6 μM , Wortmannin 0.06 μM , LY294002 5 μM , U0126 10 μM , PD98059 10 μM . Images shown are the yolk sac area of the zebrafish skin. Insets depict higher magnifications of signals in the panels. All images are lateral views, anterior to the left. N, normal- Ca^{2+} , 0.2 mM; L, low- Ca^{2+} , 0.001 mM. Tr, trunk; Pe, pectoral fin; Yo, yolk sac. hpf, hour post fertilization; dpf, day post fertilization. The scale bar represents 50 μm .

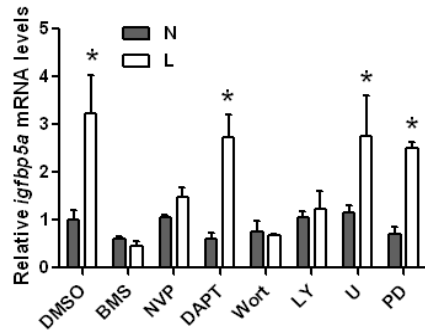
A



B



C



D

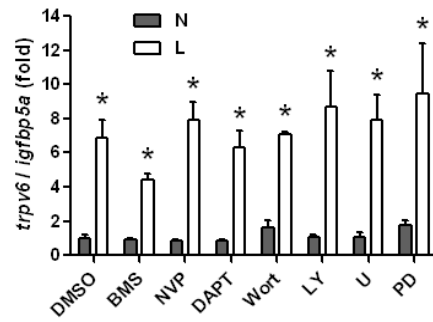


Figure 4.5 IGF1R and Akt signaling are required for the low-Ca²⁺ induced increase in NaR cell proliferation

A-B) Whole-mount in situ hybridization of *igfbp5a* in 5 dpf larvae acclimated to normal- or low-Ca²⁺ water starting from 72 hpf. BMS-754807 0.3 uM, NVP-AEW541 2 uM, DAPT 30 uM, Wortmannin 0.06 uM, LY294002 5 uM, U0126 10 uM, PD98059 10 uM.

Representative images are in (A), and proportions of the phenotype are summarized in (B). Images shown are the yolk sac area of the zebrafish skin. All images are lateral views, anterior to the left. Pe, pectoral fin. The scale bar represents 50 μm. C-D)

Quantitative real-time PCR measurement of relative *igfbp5a* (C) mRNA levels and the ratio of *trpv6/igfbp5a* (D) in 5 dpf larvae acclimated to normal- or low-Ca²⁺ water starting from 72 hpf (mean + SD, n=3). BMS-754807 0.6 uM, NVP-AEW541 2 uM, DAPT 30 uM, Wortmannin 0.06 uM, LY294002 5 uM, U0126 10 uM, PD98059 10 uM.

* p < 0.05 compared with the DMSO group in normal-Ca²⁺ water. N, normal-Ca²⁺, 0.2 mM; L, low-Ca²⁺, 0.001 mM. hpf, hour post fertilization; dpf, day post fertilization.

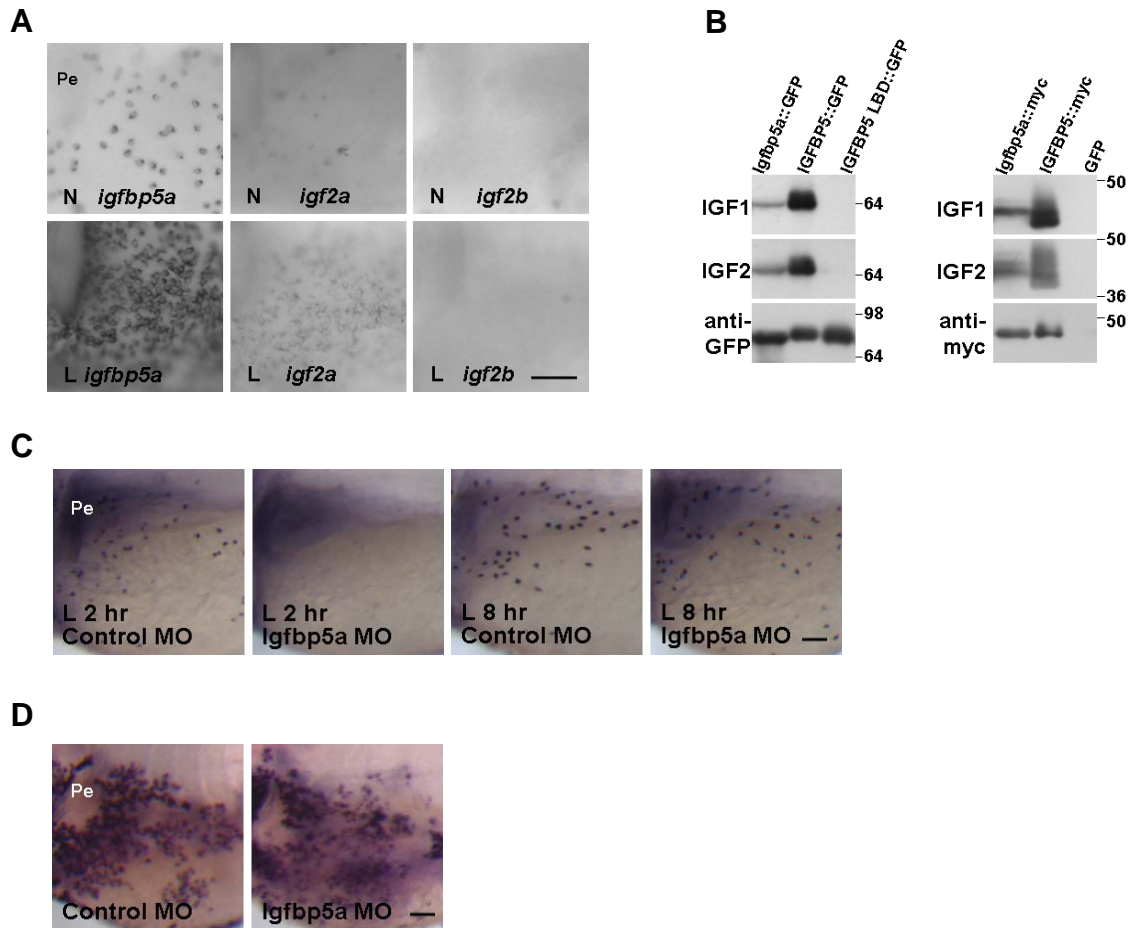


Figure 4.6 Igfbp5a modulates local Igf actions in the NaR cells in low- Ca^{2+} water

A) Whole-mount *in situ* hybridization of 5 dpf larvae acclimated to normal- or low- Ca^{2+} water for 5 days. B) Zebrafish Igfbp5a and human IGFBP5 proteins for ligand blot with DIG-labeled IGF1 or IGF2, and western blot with an anti-GFP or an anti-myc antibody. LBD, ligand binding domain mutant. C) pAkt staining of 3 dpf morphants acclimated to low- Ca^{2+} water for 2 hr or 8 hr. D) Whole-mount *in situ* hybridization of *trpv6* in 5 dpf larvae acclimated to low- Ca^{2+} water starting from 72 hpf. Images shown are the yolk sac area of the zebrafish skin. All images are lateral views, anterior to the left. N, normal- Ca^{2+} , 0.2 mM; L, low- Ca^{2+} , 0.001 mM. Pe, pectoral fin. hpf, hour post fertilization; dpf, day post fertilization. The scale bar represents 50 μm .

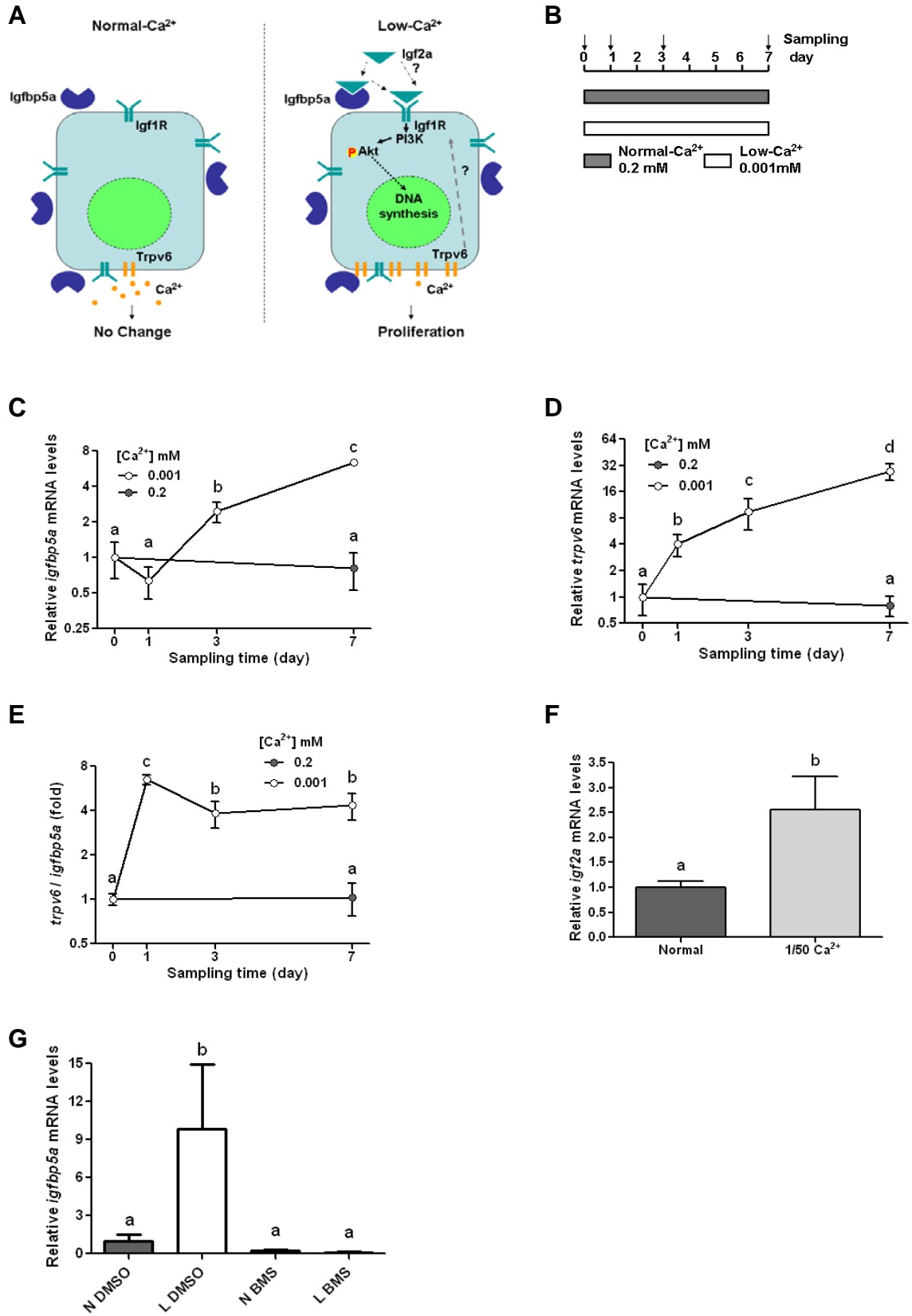


Figure 4.7 IGF signaling is also required for the low-Ca²⁺ induced increase of the NaR cells in adult zebrafish gills

A) Model for the role of IGF signaling in regulating the population of *trpv6*-expressing cells in adaptation to altered environmental Ca²⁺ concentration. B-E) Quantitative real-time PCR measurement of relative *igfbp5a* (C) and *trpv6* (D) mRNA levels and the ratio of *trpv6/igfbp5a* (E) in gills of adult zebrafish acclimated to normal- or low-Ca²⁺ water for the period of time indicated (mean \pm SD, n=4). The scheme illustrates the fish raising procedures (C). F) Quantitative real-time PCR measurement of relative *igf2a* mRNA levels in gills of adult zebrafish acclimated to normal- or 1/50 Ca²⁺ water for 2 weeks (mean \pm SD, n=4). G) Quantitative real-time PCR measurement of relative *igfbp5a* mRNA levels in gills of adult zebrafish acclimated to normal- or low-Ca²⁺ water for 4 days (mean \pm SD, n=4). BMS-754807 0.3 μ M. N, normal-Ca²⁺, 0.2 mM; L, low-Ca²⁺, 0.001 mM.

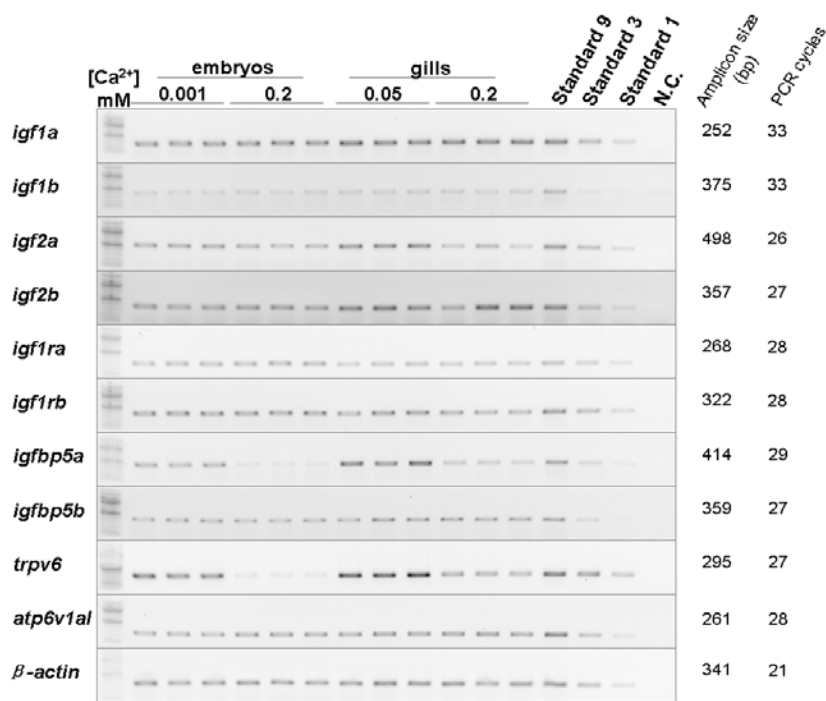


Figure 4.8 (supplementary to Figure 4.7.) Expression analysis of components in the IGF system in zebrafish larvae and adult gill

Semi-quantitative RT-PCR of the genes indicated. cDNA samples were from 5 dpf larvae acclimated to normal- or low-Ca²⁺ water for 5 days, and gills of adult zebrafish acclimated to normal- or 1/50 Ca²⁺ water for 2 weeks. 3 biological replicates were used for each group.

Medium	Ion concentration, mM							Osmolarity mOsmol/L
	[Ca ²⁺]	[Mg ²⁺]	[Na ⁺]	[K ⁺]	[Cl ⁻]	[PO ₄ ³⁻]	[SO ₄ ²⁻]	
0.001 mM [Ca ²⁺]	0.001	0.16	0.5	0.165	0.5	0.085	0.161	1.572
0.02 mM [Ca ²⁺]	0.02	0.16	0.5	0.165	0.5	0.085	0.18	1.610
0.2 mM [Ca ²⁺]	0.2	0.16	0.5	0.165	0.5	0.085	0.360	1.970
2 mM [Ca ²⁺]	2	0.16	0.5	0.165	0.5	0.085	2.16	5.570
Normal	0.200	0.160	0.500	0.165	0.500	0.085	0.360	1.970
1/50 Ca ²⁺	0.004	0.160	0.500	0.165	0.500	0.085	0.164	1.578
1/50 Mg ²⁺	0.200	0.003	0.500	0.165	0.500	0.085	0.203	1.656
1/50 Na ⁺	0.200	0.160	0.010	0.165	0.500	0.085	0.115	1.235
1/5 K ⁺	0.200	0.160	0.500	0.003	0.500	0.085	0.279	1.727
1/50 Cl ⁻	0.200	0.160	0.500	0.165	0.010	0.085	0.605	1.725
1/50 PO ₄ ³⁻	0.200	0.160	0.500	0.165	0.500	0.002	0.441	1.968

Table 4.1 Nominal ion concentrations and osmolarity of the fish media

Purpose	Target gene	Accession number	Primer sequence
Quantitative real-time PCR	<i>β-actin</i>	NM_131031	5'-GATCTGGCATCACACCTTCTAC-3'
			5'-CCTGGATGGCCACATACAT-3'
	<i>igfbp5a</i>	NM_001098754	5'-GCTGCACGCTCTGCTTTAC-3'
			5'-AATGGAACCTTGGCCTGAG-3'
	<i>trpv6</i>	NM_001001849	5'-GGACCCTACGTCATTGTGATAC-3'
			5'-GGTACTGCGGAAGTGCTAAG-3'
	<i>igf2a</i>	NM_001001815	5'-TAACCCTGTCTGCCTTCG-3'
			5'-CTGTGGGAAGAAGGATGG-3'
Semi-quantitative RT-PCR	<i>igf1a</i>	NM_131825	5'-CACGCTGCAGTTTGTGTGT-3'
			5'-GAAGAGTGGCTATGCCAGAT-3'
	<i>igf1b</i>	NM_001115050	5'-CTCTGTGCTGCGTTCTCATC-3'
			5'-GCGTTCGCTCTCTGATTCTC-3'
	<i>igf2a</i>	NM_001001815	5'-TAACCCTGTCTGCCTTCG-3'
			5'-CTGTGGGAAGAAGGATGG-3'
	<i>igf2b</i>	NM_131433	5'-TCAAACAGCCCGCCTCCTC-3'
			5'-TGGGACGATGGCAGGTTG-3'
	<i>igf1ra</i>	NM_152968	5'-CGTACCTCAATGCCAACAAG-3'
			5'-TAGGGCTGTTCGGCTAATGT-3'
	<i>igf1rb</i>	NM_152969	5'-AGACAAGGACAGACTGCATC-3'
			5'-GTCTCGTCCTCCTGTTTCAT-3'
	<i>igfbp5a</i>	NM_001098754	5'-GGGTACATGTGGACGAGGA-3'
			5'-GAAAGAGCCATCACTCTGGAA-3'
	<i>igfbp5b</i>	NM_001126463	5'-GGGAGTGTGTACGAACGAGAA-3'
			5'-TCCTGTACAGTTAGGCAGGTA-3'
	<i>trpv6</i>	NM_001001849	5'-GCTGCGAGTCACTGGAATA-3'
			5'-ACCGACGCTCACCTCAAAC-3'
	<i>atp6v1al</i>	NM_201135	5'-CCTGGAGGTGGCTAAACTCA-3'
			5'-GCTTCACCCTCTTCACTGG-3'
<i>β-actin</i>	NM_131031	5'-GCCGGTTTTGCTGGAGATGAT-3'	
		5'-ATGGCAGGGGTGTTGAAGGTC-3'	

Table 4.2 Oligonucleotide primers used Chapter 4

CHAPTER 5

Conclusions and future directions

5.1 Summary of contributions

5.1.1 Two zebrafish *igfbp5*s: gene duplication and functional diversification

The diversity of protein repertoire is largely achieved by domain recombination and gene duplication (Chothia et al., 2003). A multi-domain protein often possesses several biochemical properties and exerts pleiotropic functions in a spatial- and temporal-specific manner. Following gene duplication, sub-functionalization or neo-functionalization happens to prevent the redundant gene from becoming a pseudogene (Prince and Pickett, 2002). One of the well-characterized molecular mechanisms is through partitioning of cis-regulatory elements, resulting in a divergent expression pattern (Kleinjan et al., 2008). However, divergence in biochemical properties of the conserved domains is not well understood. My study of the duplicated zebrafish *igfbp5* genes extends the understanding of functional diversification after duplication. In this study, I found that the two *igfbp5* genes diverge in both expression patterns and biochemical properties. Specifically, *igfbp5a* and *-5b* are expressed in spatially restricted, mostly non-overlapping domains during early development. While zebrafish Igfbp5b possesses transactivation activity, zebrafish Igfbp5a lacks this activity. I further deciphered the molecular basis underlying such diversification using mutational analysis, and I revealed that two unique amino acids in positions 22 and 56 of Igfbp5a are responsible for its lack of transactivation activity.

The question remains whether the denoted divergence in biochemical properties have functional significance *in vivo*.

5.1.2 Igfbp5a in the *trpv6*-expressing NaR cells: a new regulator of calcium homeostasis

The *trpv6*-expressing NaR cells in zebrafish mediate epithelial Ca²⁺ absorption. However, it is not clear how their cell fate is controlled. In this study, I found that *igfbp5a* is specifically expressed in the NaR cells. I mapped the expression onset of *igfbp5a* and *trpv6* and found that they start to express at the same developmental stage. A loss-of-function approach was used to test the role of Igfbp5a in the NaR cells. An increase in the number of the NaR cells was found in the Igfbp5a morphants, together with elevated Ca²⁺ content and Ca²⁺ influx. These findings suggest that Igfbp5a negatively modulates the population of the NaR cells. This is the first study that links IGFBP5 with Ca²⁺ homeostasis by controlling the number of the NaR cells. The cellular and molecular mechanism underlying the function of Igfbp5a, however, awaits further testing.

5.1.3 The IGF system in low-calcium acclimation: growth factor signaling in environmental adaptation

Hormones and growth factors are important regulators of homeostasis, and they function in physiological adaptation to the changing environment. In zebrafish, the *trpv6*-expressing NaR cells increase their number in low-Ca²⁺ water. However, the underlying mechanism was not known. In this study, I provide evidence that IGF signaling plays a role in low-Ca²⁺ acclimation by inducing the proliferation of the NaR cells. First, Akt phosphorylation is elevated in the NaR cells in low-Ca²⁺ water, and it is dependent on IGF1R activity. Second, DNA synthesis follows rapid pAkt induction in the NaR cells.

Third, the increase of the NaR cells in low-Ca²⁺ water is inhibited by blocking IGF1R and PI3K. In addition, I found that knockdown of IGFBP5a attenuated rapid pAkt induction in low-Ca²⁺ water. *igf2a* is locally produced in the skin and its expression is upregulated in low Ca²⁺ water. Based on these findings, I propose a model that in low-Ca²⁺ water, IGFBP5a promotes IGF2a to activate the IGF1R/PI3K/Akt pathway, which leads to proliferation of the NaR cells. Further experiments on how low-Ca²⁺ water triggers IGF signaling activation will be needed to answer how the environmental stimuli are sensed and relayed to the intracellular signaling pathways (Fig. 5.1).

5.2 Future directions

5.2.1 Understand how low-calcium water activates IGF signaling.

When switched to low-Ca²⁺ water, Akt in the *trpv6*-expressing NaR cells in zebrafish larvae becomes phosphorylated. Weak pAkt signal can be detected in 30 min, and the signal becomes strong after 8 hrs. It is not clear how external Ca²⁺ level is sensed, and how IGF signaling is activated. In mammalian colon cells, low extracellular Ca²⁺ has been shown to induce cell proliferation in colon cells both *in vitro* and *in vivo* (Buset et al., 1986; Kallay et al., 1997), and a model involving CaSR signaling has been proposed (Lamprecht and Lipkin, 2003; Whitfield, 2009). CaSR is activated by high extracellular Ca²⁺ levels. Zebrafish also express CaSR (Okabe and Graham, 2004), although its mRNA level is low in the larvae and did not change in low-Ca²⁺ water (Fig. 5.3). CaSR expression in the NaR cells can be examined by in situ hybridization. CaSR agonists (Nemeth et al., 1998) and antagonists (De Santis et al., 2009) can be used to test if activating CaSR will inhibit pAkt elevation in low-Ca²⁺ water, and if inhibiting CaSR will induce pAkt in normal-Ca²⁺ water.

TRPV6 activity is also regulated by extracellular and intracellular Ca^{2+} levels (Hoenderop et al., 2005). TRPV6 is highly expressed in prostate cancer cells (Fixemer et al., 2003; Peng et al., 2001). In LNCaP human prostate cancer cells, siRNA knockdown of TRPV6 decreased cell proliferation and increased apoptosis (Lehen'kyi et al., 2007). To test if increased Trpv6 channel activity is required for activating IGF signaling in the NaR cells, TRPV6 blockers such as ruthenium red (Nilius et al., 2001) and lanthanum (Yue et al., 2001) can be used. In a pilot experiment, I found that both ruthenium red and lanthanum inhibits pAkt in low- Ca^{2+} water (Fig. 5.2). Since these blockers are not specific to the TRPV6 channels, antisense MOs (Tseng et al., 2009) can be used to target Trpv6 to confirm the specificity.

Besides the possible local change of Ca^{2+} signaling in the NaR cells, a systematic endocrine regulation may also be involved. I found that *igf2a* is locally produced in the skin and its expression is upregulated in low Ca^{2+} water. Studies show that IGF expression can be upregulated by prolactin (PRL) (Briskin et al., 2002; Hovey et al., 2003), growth hormone (GH), and parathyroid hormone (PTH) (Linkhart and Mohan, 1989; McCarthy et al., 1989). In fish, GH and IGF1 are well known for their role in seawater acclimation, and PRL is thought to be involved in freshwater adaptation (Sakamoto and McCormick, 2006). Somatolactin (SL) belongs to the GH/prolactin (PRL) family of pituitary hormones, but so far it has only been found in fish (Fukada et al., 2005). SL may play a role in regulating Ca^{2+} balance in fish: changes in SL plasma levels and sl pituitary gland mRNA expression at low ambient Ca^{2+} were observed, albeit only after several days (Kakizawa et al., 1993). From a preliminary screening of the expression of these hormones potentially involved in low- Ca^{2+} acclimation, I found that

pth1a, *prl*, and *smt11b* mRNA levels are upregulated in low-Ca²⁺ water, but not *pth1b*, *gh*, and *smt11a* (Fig. 5.3). Interestingly, knockdown of Prl and Sl, but not Gh, in zebrafish inhibits swimming bladder inflation (Zhu et al., 2007), a phenotype also observed in the low-Ca²⁺ treated larvae. However, in *pit1* mutants that lack lactotropes (expresses PRL) and somatotropes (expresses GH), swimming bladder inflation was normal (Nica et al., 2004). It will be interesting to test if the Prl/Sl morphants, or the *pit1* mutants, can still increase the number of the NaR cells in low-Ca²⁺ water. In addition, Pth1a MO can be designed and tested.

5.2.2 Explore how IGF signaling functions in low-calcium acclimation

During low-Ca²⁺ acclimation, pAkt in the *trpv6*-expressing NaR cells is induced through an IGF1R-dependent mechanism. Pharmacological inhibition of IGF1R and PI3K abolished the increase of the NaR cells. The IGF1R/PI3K/Akt pathway has been shown to induce cell proliferation by upregulating cyclin and downregulating cyclin-dependent kinase inhibitor (CDKN) (Dupont et al., 2003). It may increase cyclin D1 levels by increasing its translation through mTOR (Muisse-Helmericks et al., 1998), or by enhancing its stability and translocation into the nucleus through inhibition of GSK3B (Diehl et al., 1998; Hamelers et al., 2002). It may also downregulate CDKN1B through FOXO1 (Medema et al., 2000). Further studies of the downstream targets will help to elucidate whether the IGF1R/PI3K/Akt signaling pathway directly or indirectly leads to cell proliferation. Meanwhile, IGF1R/PI3K/Akt signaling has anti-apoptotic effects (Samani et al., 2007). Whether blocking IGF1R/PI3K/Akt signaling increases apoptosis, which leads to reduced cell number in low-Ca²⁺ water, also needs to be tested.

It is not known whether activation of the IGF1R/PI3K/Akt signaling pathway affects Trpv6 channel activity directly. IGF1 has been shown to affect TRPV1 and TRPV2 channel activity by regulating their translocation to the plasma membrane (Kanzaki et al., 1999; Van Buren et al., 2005). We found that IGF signaling does not regulate Trpv6 at the transcriptional level, since pharmacological blockage of IGF1R and PI3K did not affect *trpv6* mRNA level per cell. It remains to be tested whether inhibiting IGF signaling affects Trpv6 channel activity.

5.3 Conclusions and perspectives

Taken together, the study of the duplicated *igfbp5s* in zebrafish uncovers an unexpected role of the IGF system in Ca²⁺ homeostasis. It also contributes to our understanding of how growth factor signaling works in physiological adaptation. Furthermore, the findings made in this study raise new research questions such as how signaling pathways that lead to cell proliferation can be activated by environmental changes.

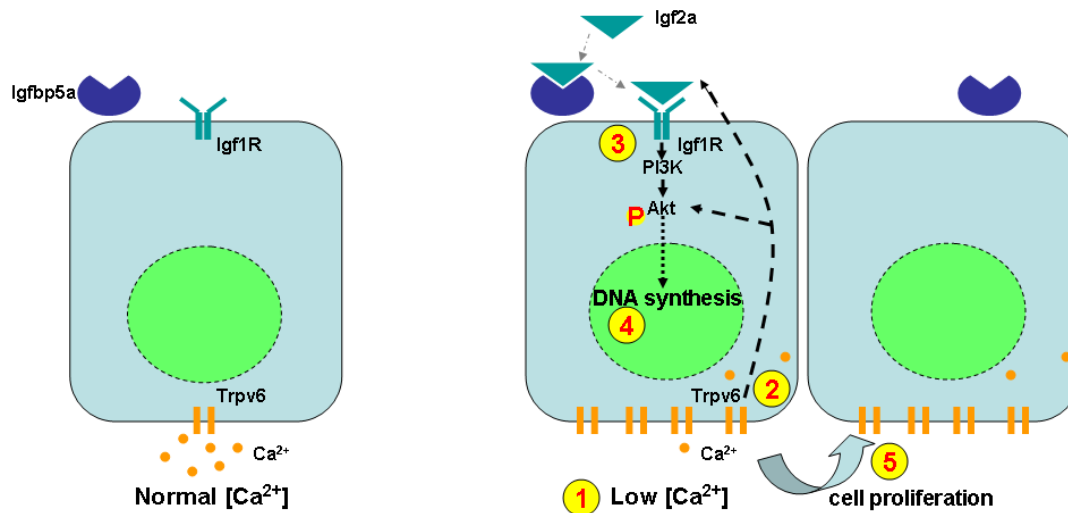


Figure 5.1 A proposed model on how epithelial Ca^{2+} absorption is increased in acclimation to low environmental Ca^{2+} supply:

1) Environmental trigger: Decrease in environmental Ca^{2+} level. 2) Ca^{2+} signaling: Trpv6 channel activity induces IGF1R-Akt signaling and stimulates Igf2a expression and possibly secretion. 3) IGF signaling: the increased Igf2a increases Akt phosphorylation via its binding to the Igf1r; this effect of Igf2a is potentiated by Igfbp5a specifically expressed in NaR cells. 4) Cell cycle: activation of PI3 kinase-Akt increases the proliferation rate of NaR cells. 5) Acclimation: Increased Trpv6 expression per cell and number of NaR cells increase Ca^{2+} absorption rate (Pan et al., 2005).

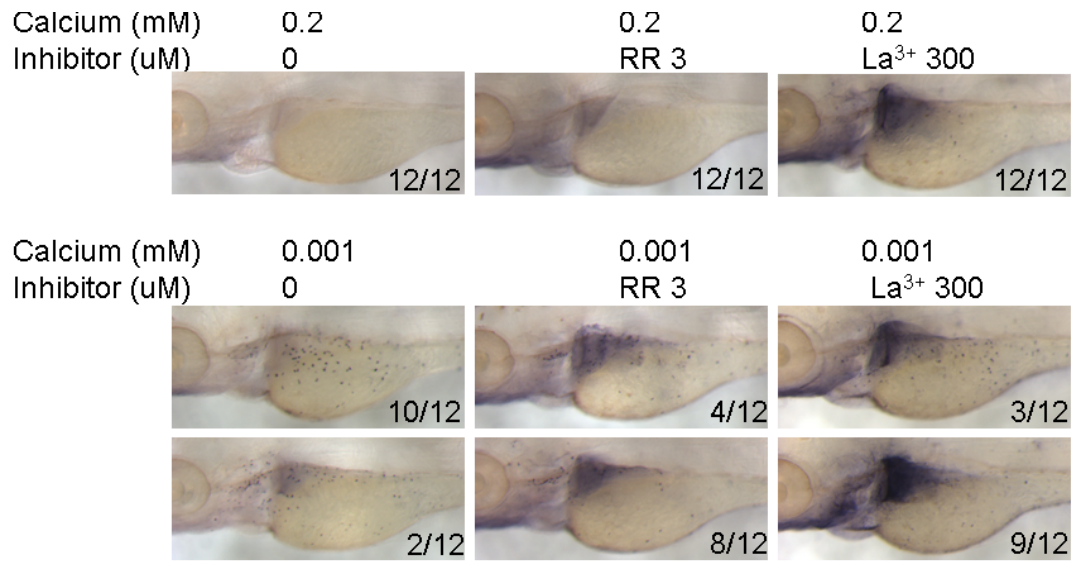


Figure 5.2 The TRPV6 inhibitors, ruthenium red or lanthanum, abolish low-Ca²⁺ water-induced Akt phosphorylation.

pAkt staining of 3 dpf larvae acclimated to water with different Ca²⁺ levels and inhibitors for 8 hr. The concentration of Ca²⁺ and inhibitor used is at the top. 12 larvae were analyzed in each treatment group. The number of larvae showing the representative pAkt staining versus the total number in each treatment group is at the bottom right in each panel. All images are lateral views, anterior to the left. RR, Ruthenium red. La³⁺, lanthanum.

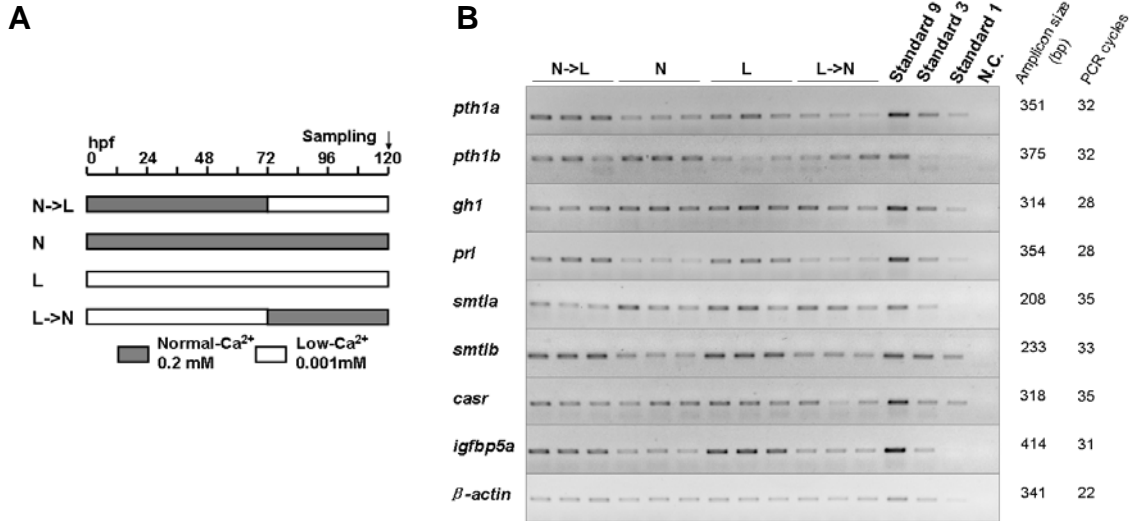


Figure 5.3 Expression analysis of several endocrine hormones in zebrafish larvae in response to change in Ca^{2+} levels in the water.

The left panel illustrates the fish raising procedures. The right panel shows semi-quantitative RT-PCR of the genes indicated. 3 biological replicates were used for each group. N, normal- Ca^{2+} , 0.2 mM; L, low- Ca^{2+} , 0.001 mM.

REFERENCES

(1996). Zebrafish Issue. *Development* 123.

Abrass, C.K., Berfield, A.K., and Andress, D.L. (1997). Heparin binding domain of insulin-like growth factor binding protein-5 stimulates mesangial cell migration. *Am J Physiol* 273, F899-906.

Abuzzahab, M.J., Schneider, A., Goddard, A., Grigorescu, F., Lautier, C., Keller, E., Kiess, W., Klammt, J., Kratzsch, J., Osgood, D., *et al.* (2003). IGF-I receptor mutations resulting in intrauterine and postnatal growth retardation. *N Engl J Med* 349, 2211-2222.

Al-Ansary, D., Bogeski, I., Disteldorf, B.M., Becherer, U., and Niemeyer, B.A. (2010). ATP modulates Ca²⁺ uptake by TRPV6 and is counteracted by isoform-specific phosphorylation. *FASEB J* 24, 425-435.

Aleman, A., Verhaar, H.J., De Haan, E.H., De Vries, W.R., Samson, M.M., Drent, M.L., Van der Veen, E.A., and Koppeschaar, H.P. (1999). Insulin-like growth factor-I and cognitive function in healthy older men. *J Clin Endocrinol Metab* 84, 471-475.

Allan, G.J., Tonner, E., Szymanowska, M., Shand, J.H., Kelly, S.M., Phillips, K., Clegg, R.A., Gow, I.F., Beattie, J., and Flint, D.J. (2006). Cumulative mutagenesis of the basic residues in the 201-218 region of insulin-like growth factor (IGF)-binding protein-5 results in progressive loss of both IGF-I binding and inhibition of IGF-I biological action. *Endocrinology* 147, 338-349.

Amaar, Y.G., Thompson, G.R., Linkhart, T.A., Chen, S.T., Baylink, D.J., and Mohan, S. (2002). Insulin-like growth factor-binding protein 5 (IGFBP-5) interacts with a four and a half LIM protein 2 (FHL2). *J Biol Chem* 277, 12053-12060.

Arai, T., Clarke, J., Parker, A., Busby, W., Jr., Nam, T., and Clemmons, D.R. (1996). Substitution of specific amino acids in insulin-like growth factor (IGF) binding protein 5 alters heparin binding and its change in affinity for IGF-I response to heparin. *J Biol Chem* 271, 6099-6106.

Bahner, M., Frechter, S., Da Silva, N., Minke, B., Paulsen, R., and Huber, A. (2002). Light-regulated subcellular translocation of *Drosophila* TRPL channels induces long-term adaptation and modifies the light-induced current. *Neuron* 34, 83-93.

- Baker, J., Liu, J.P., Robertson, E.J., and Efstratiadis, A. (1993). Role of insulin-like growth factors in embryonic and postnatal growth. *Cell* 75, 73-82.
- Bakkers, J., Hild, M., Kramer, C., Furutani-Seiki, M., and Hammerschmidt, M. (2002). Zebrafish DeltaNp63 is a direct target of Bmp signaling and encodes a transcriptional repressor blocking neural specification in the ventral ectoderm. *Dev Cell* 2, 617-627.
- Bartholdi, D., Krajewska-Walasek, M., Ounap, K., Gaspar, H., Chrzanowska, K.H., Ilyana, H., Kayserili, H., Lurie, I.W., Schinzel, A., and Baumer, A. (2009). Epigenetic mutations of the imprinted IGF2-H19 domain in Silver-Russell syndrome (SRS): results from a large cohort of patients with SRS and SRS-like phenotypes. *J Med Genet* 46, 192-197.
- Barton, E.R., Morris, L., Musaro, A., Rosenthal, N., and Sweeney, H.L. (2002). Muscle-specific expression of insulin-like growth factor I counters muscle decline in mdx mice. *J Cell Biol* 157, 137-148.
- Bauss, F., Lang, K., Dony, C., and Kling, L. (2001). The complex of recombinant human insulin-like growth factor-I (rhIGF-I) and its binding protein-5 (IGFBP-5) induces local bone formation in murine calvariae and in rat cortical bone after local or systemic administration. *Growth Horm IGF Res* 11, 1-9.
- Baxter, R.C., and Martin, J.L. (1989). Structure of the Mr 140,000 growth hormone-dependent insulin-like growth factor binding protein complex: determination by reconstitution and affinity-labeling. *Proc Natl Acad Sci U S A* 86, 6898-6902.
- Beattie, J., Allan, G.J., Lochrie, J.D., and Flint, D.J. (2006). Insulin-like growth factor-binding protein-5 (IGFBP-5): a critical member of the IGF axis. *Biochem J* 395, 1-19.
- Bendall, S.C., Stewart, M.H., Menendez, P., George, D., Vijayaragavan, K., Werbowetski-Ogilvie, T., Ramos-Mejia, V., Rouleau, A., Yang, J., Bosse, M., *et al.* (2007). IGF and FGF cooperatively establish the regulatory stem cell niche of pluripotent human cells in vitro. *Nature* 448, 1015-1021.
- Benn, B.S., Ajibade, D., Porta, A., Dhawan, P., Hediger, M., Peng, J.B., Jiang, Y., Oh, G.T., Jeung, E.B., Lieben, L., *et al.* (2008). Active intestinal calcium transport in the absence of transient receptor potential vanilloid type 6 and calbindin-D9k. *Endocrinology* 149, 3196-3205.
- Berfield, A.K., Andress, D.L., and Abrass, C.K. (2000). IGFBP-5(201-218) stimulates Cdc42GAP aggregation and filopodia formation in migrating mesangial cells. *Kidney Int* 57, 1991-2003.

- Berridge, M.J., Bootman, M.D., and Roderick, H.L. (2003). Calcium signalling: dynamics, homeostasis and remodelling. *Nat Rev Mol Cell Biol* 4, 517-529.
- Bezzerrides, V.J., Ramsey, I.S., Kotecha, S., Greka, A., and Clapham, D.E. (2004). Rapid vesicular translocation and insertion of TRP channels. *Nat Cell Biol* 6, 709-720.
- Bianco, S.D., Peng, J.B., Takanaga, H., Suzuki, Y., Crescenzi, A., Kos, C.H., Zhuang, L., Freeman, M.R., Gouveia, C.H., Wu, J., *et al.* (2007). Marked disturbance of calcium homeostasis in mice with targeted disruption of the *Trpv6* calcium channel gene. *J Bone Miner Res* 22, 274-285.
- Bilezikian, J.P., Brandi, M.L., Rubin, M., and Silverberg, S.J. (2005). Primary hyperparathyroidism: new concepts in clinical, densitometric and biochemical features. *J Intern Med* 257, 6-17.
- Binkert, C., Landwehr, J., Mary, J.L., Schwander, J., and Heinrich, G. (1989). Cloning, sequence analysis and expression of a cDNA encoding a novel insulin-like growth factor binding protein (IGFBP-2). *EMBO J* 8, 2497-2502.
- Binoux, M., and Hossenlopp, P. (1988). Insulin-like growth factor (IGF) and IGF-binding proteins: comparison of human serum and lymph. *J Clin Endocrinol Metab* 67, 509-514.
- Blakesley, V.A., Koval, A.P., Stannard, B.S., Scrimgeour, A., and LeRoith, D. (1998). Replacement of tyrosine 1251 in the carboxyl terminus of the insulin-like growth factor-I receptor disrupts the actin cytoskeleton and inhibits proliferation and anchorage-independent growth. *J Biol Chem* 273, 18411-18422.
- Blaustein, M.P., and Lederer, W.J. (1999). Sodium/calcium exchange: its physiological implications. *Physiol Rev* 79, 763-854.
- Bodding, M., and Flockerzi, V. (2004). Ca²⁺ dependence of the Ca²⁺-selective TRPV6 channel. *J Biol Chem* 279, 36546-36552.
- Bolanz, K.A., Hediger, M.A., and Landowski, C.P. (2008). The role of TRPV6 in breast carcinogenesis. *Mol Cancer Ther* 7, 271-279.
- Borghi, L., Schianchi, T., Meschi, T., Guerra, A., Allegri, F., Maggiore, U., and Novarini, A. (2002). Comparison of two diets for the prevention of recurrent stones in idiopathic hypercalciuria. *N Engl J Med* 346, 77-84.
- Bowers, C.Y., Granda, R., Mohan, S., Kuipers, J., Baylink, D., and Veldhuis, J.D. (2004). Sustained elevation of pulsatile growth hormone (GH) secretion and insulin-like growth factor I (IGF-I), IGF-binding protein-3 (IGFBP-3), and IGFBP-5 concentrations during

30-day continuous subcutaneous infusion of GH-releasing peptide-2 in older men and women. *J Clin Endocrinol Metab* 89, 2290-2300.

Bramani, S., Song, H., Beattie, J., Tonner, E., Flint, D.J., and Allan, G.J. (1999). Amino acids within the extracellular matrix (ECM) binding region (201-218) of rat insulin-like growth factor binding protein (IGFBP)-5 are important determinants in binding IGF-I. *J Mol Endocrinol* 23, 117-123.

Brandt, P., Neve, R.L., Kammesheidt, A., Rhoads, R.E., and Vanaman, T.C. (1992). Analysis of the tissue-specific distribution of mRNAs encoding the plasma membrane calcium-pumping ATPases and characterization of an alternately spliced form of PMCA4 at the cDNA and genomic levels. *J Biol Chem* 267, 4376-4385.

Brinkman, A., Groffen, C., Kortleve, D.J., Geurts van Kessel, A., and Drop, S.L. (1988). Isolation and characterization of a cDNA encoding the low molecular weight insulin-like growth factor binding protein (IBP-1). *EMBO J* 7, 2417-2423.

Brisken, C., Ayyannan, A., Nguyen, C., Heineman, A., Reinhardt, F., Tan, J., Dey, S.K., Dotto, G.P., and Weinberg, R.A. (2002). IGF-2 is a mediator of prolactin-induced morphogenesis in the breast. *Dev Cell* 3, 877-887.

Buset, M., Lipkin, M., Winawer, S., Swaroop, S., and Friedman, E. (1986). Inhibition of human colonic epithelial cell proliferation in vivo and in vitro by calcium. *Cancer Res* 46, 5426-5430.

Carboni, J.M., Wittman, M., Yang, Z., Lee, F., Greer, A., Hurlburt, W., Hillerman, S., Cao, C., Cantor, G.H., Dell-John, J., *et al.* (2009). BMS-754807, a small molecule inhibitor of insulin-like growth factor-1R/IR. *Mol Cancer Ther* 8, 3341-3349.

Carro, E., Trejo, J.L., Gomez-Isla, T., LeRoith, D., and Torres-Aleman, I. (2002). Serum insulin-like growth factor I regulates brain amyloid-beta levels. *Nat Med* 8, 1390-1397.

Cashman, K.D. (2002). Calcium intake, calcium bioavailability and bone health. *Br J Nutr* 87 Suppl 2, S169-177.

Chang, Q., Hoefs, S., van der Kemp, A.W., Topala, C.N., Bindels, R.J., and Hoenderop, J.G. (2005). The beta-glucuronidase klotho hydrolyzes and activates the TRPV5 channel. *Science* 310, 490-493.

Chen, Y.Y., Lu, F.I., and Hwang, P.P. (2003). Comparisons of calcium regulation in fish larvae. *J Exp Zool A Comp Exp Biol* 295, 127-135.

- Cheng, X., Jin, J., Hu, L., Shen, D., Dong, X.P., Samie, M.A., Knoff, J., Eisinger, B., Liu, M.L., Huang, S.M., *et al.* (2010). TRP channel regulates EGFR signaling in hair morphogenesis and skin barrier formation. *Cell* *141*, 331-343.
- Chothia, C., Gough, J., Vogel, C., and Teichmann, S.A. (2003). Evolution of the protein repertoire. *Science* *300*, 1701-1703.
- Clancy, D.J., Gems, D., Harshman, L.G., Oldham, S., Stocker, H., Hafen, E., Leever, S.J., and Partridge, L. (2001). Extension of life-span by loss of CHICO, a *Drosophila* insulin receptor substrate protein. *Science* *292*, 104-106.
- Clapham, D.E. (2003). TRP channels as cellular sensors. *Nature* *426*, 517-524.
- Clapham, D.E. (2007). Calcium signaling. *Cell* *131*, 1047-1058.
- Clemmons, D.R. (1997). Insulin-like growth factor binding proteins and their role in controlling IGF actions. *Cytokine Growth Factor Rev* *8*, 45-62.
- Clines, G.A., and Guise, T.A. (2005). Hypercalcaemia of malignancy and basic research on mechanisms responsible for osteolytic and osteoblastic metastasis to bone. *Endocr Relat Cancer* *12*, 549-583.
- Conover, C.A., and Kiefer, M.C. (1993). Regulation and biological effect of endogenous insulin-like growth factor binding protein-5 in human osteoblastic cells. *J Clin Endocrinol Metab* *76*, 1153-1159.
- Constancia, M., Hemberger, M., Hughes, J., Dean, W., Ferguson-Smith, A., Fundele, R., Stewart, F., Kelsey, G., Fowden, A., Sibley, C., *et al.* (2002). Placental-specific IGF-II is a major modulator of placental and fetal growth. *Nature* *417*, 945-948.
- Conus, N.M., Hemmings, B.A., and Pearson, R.B. (1998). Differential regulation by calcium reveals distinct signaling requirements for the activation of Akt and p70S6k. *J Biol Chem* *273*, 4776-4782.
- Cooper, M.S., and Gittoes, N.J. (2008). Diagnosis and management of hypocalcaemia. *BMJ* *336*, 1298-1302.
- Coticchia, C.M., Revankar, C.M., Deb, T.B., Dickson, R.B., and Johnson, M.D. (2009). Calmodulin modulates Akt activity in human breast cancer cell lines. *Breast Cancer Res Treat* *115*, 545-560.
- Crosnier, C., Stamatakis, D., and Lewis, J. (2006). Organizing cell renewal in the intestine: stem cells, signals and combinatorial control. *Nat Rev Genet* *7*, 349-359.

Crosnier, C., Vargesson, N., Gschmeissner, S., Ariza-McNaughton, L., Morrison, A., and Lewis, J. (2005). Delta-Notch signalling controls commitment to a secretory fate in the zebrafish intestine. *Development* *132*, 1093-1104.

Cui, H., Cruz-Correa, M., Giardiello, F.M., Hutcheon, D.F., Kafonek, D.R., Brandenburg, S., Wu, Y., He, X., Powe, N.R., and Feinberg, A.P. (2003). Loss of IGF2 imprinting: a potential marker of colorectal cancer risk. *Science* *299*, 1753-1755.

Dai, W., Kamei, H., Zhao, Y., Ding, J., Du, Z., and Duan, C. (2010). Duplicated zebrafish insulin-like growth factor binding protein-5 genes with split functional domains: evidence for evolutionarily conserved IGF binding, nuclear localization, and transactivation activity. *FASEB J* *24*, 2020-2029.

Danielsen, A., Larsen, E., and Gammeltoft, S. (1990). Chromaffin cells express two types of insulin-like growth factor receptors. *Brain Res* *518*, 95-100.

Dardenne, O., Prud'homme, J., Arabian, A., Glorieux, F.H., and St-Arnaud, R. (2001). Targeted inactivation of the 25-hydroxyvitamin D(3)-1(alpha)-hydroxylase gene (CYP27B1) creates an animal model of pseudovitamin D-deficiency rickets. *Endocrinology* *142*, 3135-3141.

Dardenne, O., Prud'homme, J., Hacking, S.A., Glorieux, F.H., and St-Arnaud, R. (2003). Correction of the abnormal mineral ion homeostasis with a high-calcium, high-phosphorus, high-lactose diet rescues the PDDR phenotype of mice deficient for the 25-hydroxyvitamin D-1alpha-hydroxylase (CYP27B1). *Bone* *32*, 332-340.

Darwish, H.M., Krisinger, J., Strom, M., and DeLuca, H.F. (1987). Molecular cloning of the cDNA and chromosomal gene for vitamin D-dependent calcium-binding protein of rat intestine. *Proc Natl Acad Sci U S A* *84*, 6108-6111.

Daughaday, W.H., and Kapadia, M. (1989). Significance of abnormal serum binding of insulin-like growth factor II in the development of hypoglycemia in patients with non-islet-cell tumors. *Proc Natl Acad Sci U S A* *86*, 6778-6782.

De Santis, T., Casavola, V., Reshkin, S.J., Guerra, L., Ambruosi, B., Fiandanese, N., Dalbies-Tran, R., Goudet, G., and Dell'Aquila, M.E. (2009). The extracellular calcium-sensing receptor is expressed in the cumulus-oocyte complex in mammals and modulates oocyte meiotic maturation. *Reproduction* *138*, 439-452.

DeChiara, T.M., Efstratiadis, A., and Robertson, E.J. (1990). A growth-deficiency phenotype in heterozygous mice carrying an insulin-like growth factor II gene disrupted by targeting. *Nature* *345*, 78-80.

Devlin, R.D., Du, Z., Buccilli, V., Jorgetti, V., and Canalis, E. (2002). Transgenic mice overexpressing insulin-like growth factor binding protein-5 display transiently decreased osteoblastic function and osteopenia. *Endocrinology* 143, 3955-3962.

Diehl, J.A., Cheng, M., Roussel, M.F., and Sherr, C.J. (1998). Glycogen synthase kinase-3 β regulates cyclin D1 proteolysis and subcellular localization. *Genes Dev* 12, 3499-3511.

Dilworth, M.R., Kusinski, L.C., Cowley, E., Ward, B.S., Husain, S.M., Constancia, M., Sibley, C.P., and Glazier, J.D. (2010). Placental-specific *Igf2* knockout mice exhibit hypocalcemia and adaptive changes in placental calcium transport. *Proc Natl Acad Sci U S A* 107, 3894-3899.

Duan, C., and Clemmons, D.R. (1998). Differential expression and biological effects of insulin-like growth factor-binding protein-4 and -5 in vascular smooth muscle cells. *J Biol Chem* 273, 16836-16842.

Duan, C., Liimatta, M.B., and Bottum, O.L. (1999). Insulin-like growth factor (IGF)-I regulates IGF-binding protein-5 gene expression through the phosphatidylinositol 3-kinase, protein kinase B/Akt, and p70 S6 kinase signaling pathway. *J Biol Chem* 274, 37147-37153.

Duan, C., and Xu, Q. (2005). Roles of insulin-like growth factor (IGF) binding proteins in regulating IGF actions. *Gen Comp Endocrinol* 142, 44-52.

Dupont, J., Pierre, A., Froment, P., and Moreau, C. (2003). The insulin-like growth factor axis in cell cycle progression. *Horm Metab Res* 35, 740-750.

Eguchi, S., Numaguchi, K., Iwasaki, H., Matsumoto, T., Yamakawa, T., Utsunomiya, H., Motley, E.D., Kawakatsu, H., Owada, K.M., Hirata, Y., *et al.* (1998). Calcium-dependent epidermal growth factor receptor transactivation mediates the angiotensin II-induced mitogen-activated protein kinase activation in vascular smooth muscle cells. *J Biol Chem* 273, 8890-8896.

Eisen, J.S. (1991). Determination of primary motoneuron identity in developing zebrafish embryos. *Science* 252, 569-572.

Eisen, J.S., Pike, S.H., and Debu, B. (1989). The growth cones of identified motoneurons in embryonic zebrafish select appropriate pathways in the absence of specific cellular interactions. *Neuron* 2, 1097-1104.

Eisen, J.S., and Smith, J.C. (2008). Controlling morpholino experiments: don't stop making antisense. *Development* 135, 1735-1743.

Evans, D.H. (2002). Cell signaling and ion transport across the fish gill epithelium. *J Exp Zool* 293, 336-347.

Feskanich, D., Willett, W.C., and Colditz, G.A. (2003). Calcium, vitamin D, milk consumption, and hip fractures: a prospective study among postmenopausal women. *Am J Clin Nutr* 77, 504-511.

Firth, S.M., and Baxter, R.C. (2002). Cellular actions of the insulin-like growth factor binding proteins. *Endocr Rev* 23, 824-854.

Firth, S.M., Clemmons, D.R., and Baxter, R.C. (2001). Mutagenesis of basic amino acids in the carboxyl-terminal region of insulin-like growth factor binding protein-5 affects acid-labile subunit binding. *Endocrinology* 142, 2147.

Fixemer, T., Wissenbach, U., Flockerzi, V., and Bonkhoff, H. (2003). Expression of the Ca²⁺-selective cation channel TRPV6 in human prostate cancer: a novel prognostic marker for tumor progression. *Oncogene* 22, 7858-7861.

Flik, G., Fenwick, J.C., Kolar, Z., Mayer-Gostan, N., and Wendelaar Bonga, S.E. (1985). Whole-body calcium flux rates in cichlid teleost fish *Oreochromis mossambicus* adapted to freshwater. *Am J Physiol* 249, R432-437.

Flik, G., Verbost, P.M., and S.E., W.B. (1995). Calcium transport process in fishes. In: *Cellular and Molecular Approaches to Fish Ionic Regulation*, edited by Wood, CM and Shuttleworth, TJ San Diego, CA: Academic, 317-342.

Foley, J.E., Maeder, M.L., Pearlberg, J., Joung, J.K., Peterson, R.T., and Yeh, J.R. (2009). Targeted mutagenesis in zebrafish using customized zinc-finger nucleases. *Nat Protoc* 4, 1855-1867.

Forbes, B.E., Hartfield, P.J., McNeil, K.A., Surinya, K.H., Milner, S.J., Cosgrove, L.J., and Wallace, J.C. (2002). Characteristics of binding of insulin-like growth factor (IGF)-I and IGF-II analogues to the type 1 IGF receptor determined by BIAcore analysis. *Eur J Biochem* 269, 961-968.

Force, A., Lynch, M., Pickett, F.B., Amores, A., Yan, Y.L., and Postlethwait, J. (1999). Preservation of duplicate genes by complementary, degenerative mutations. *Genetics* 151, 1531-1545.

Frasca, F., Pandini, G., Scalia, P., Sciacca, L., Mineo, R., Costantino, A., Goldfine, I.D., Belfiore, A., and Vigneri, R. (1999). Insulin receptor isoform A, a newly recognized, high-affinity insulin-like growth factor II receptor in fetal and cancer cells. *Mol Cell Biol* 19, 3278-3288.

Fukada, H., Ozaki, Y., Pierce, A.L., Adachi, S., Yamauchi, K., Hara, A., Swanson, P., and Dickhoff, W.W. (2005). Identification of the salmon somatolactin receptor, a new member of the cytokine receptor family. *Endocrinology* 146, 2354-2361.

Garcia-Echeverria, C., Pearson, M.A., Marti, A., Meyer, T., Mestan, J., Zimmermann, J., Gao, J., Brueggen, J., Capraro, H.G., Cozens, R., *et al.* (2004). In vivo antitumor activity of NVP-AEW541-A novel, potent, and selective inhibitor of the IGF-IR kinase. *Cancer Cell* 5, 231-239.

Garrett, T.P., McKern, N.M., Lou, M., Frenkel, M.J., Bentley, J.D., Lovrecz, G.O., Elleman, T.C., Cosgrove, L.J., and Ward, C.W. (1998). Crystal structure of the first three domains of the type-1 insulin-like growth factor receptor. *Nature* 394, 395-399.

Geling, A., Steiner, H., Willem, M., Bally-Cuif, L., and Haass, C. (2002). A gamma-secretase inhibitor blocks Notch signaling in vivo and causes a severe neurogenic phenotype in zebrafish. *EMBO Rep* 3, 688-694.

Giustina, A., Mazziotti, G., and Canalis, E. (2008). Growth hormone, insulin-like growth factors, and the skeleton. *Endocr Rev* 29, 535-559.

Gkika, D., Mahieu, F., Nilius, B., Hoenderop, J.G., and Bindels, R.J. (2004). 80K-H as a new Ca²⁺ sensor regulating the activity of the epithelial Ca²⁺ channel transient receptor potential cation channel V5 (TRPV5). *J Biol Chem* 279, 26351-26357.

Gronborg, M., Wulff, B.S., Rasmussen, J.S., Kjeldsen, T., and Gammeltoft, S. (1993). Structure-function relationship of the insulin-like growth factor-I receptor tyrosine kinase. *J Biol Chem* 268, 23435-23440.

Hamelers, I.H., van Schaik, R.F., Sipkema, J., Sussenbach, J.S., and Steenbergh, P.H. (2002). Insulin-like growth factor I triggers nuclear accumulation of cyclin D1 in MCF-7S breast cancer cells. *J Biol Chem* 277, 47645-47652.

Hankinson, S.E., Willett, W.C., Colditz, G.A., Hunter, D.J., Michaud, D.S., Deroo, B., Rosner, B., Speizer, F.E., and Pollak, M. (1998). Circulating concentrations of insulin-like growth factor-I and risk of breast cancer. *Lancet* 351, 1393-1396.

Hellstrom, A., Perruzzi, C., Ju, M., Engstrom, E., Hard, A.L., Liu, J.L., Albertsson-Wikland, K., Carlsson, B., Niklasson, A., Sjobell, L., *et al.* (2001). Low IGF-I suppresses VEGF-survival signaling in retinal endothelial cells: direct correlation with clinical retinopathy of prematurity. *Proc Natl Acad Sci U S A* 98, 5804-5808.

Hirose, S., Kaneko, T., Naito, N., and Takei, Y. (2003). Molecular biology of major components of chloride cells. *Comp Biochem Physiol B Biochem Mol Biol* 136, 593-620.

Hoenderop, J.G., Dardenne, O., Van Abel, M., Van Der Kemp, A.W., Van Os, C.H., St - Arnaud, R., and Bindels, R.J. (2002). Modulation of renal Ca²⁺ transport protein genes by dietary Ca²⁺ and 1,25-dihydroxyvitamin D₃ in 25-hydroxyvitamin D₃-1alpha-hydroxylase knockout mice. *FASEB J* 16, 1398-1406.

Hoenderop, J.G., Muller, D., Van Der Kemp, A.W., Hartog, A., Suzuki, M., Ishibashi, K., Imai, M., Sweep, F., Willems, P.H., Van Os, C.H., *et al.* (2001). Calcitriol controls the epithelial calcium channel in kidney. *J Am Soc Nephrol* 12, 1342-1349.

Hoenderop, J.G., Nilius, B., and Bindels, R.J. (2005). Calcium absorption across epithelia. *Physiol Rev* 85, 373-422.

Hoenderop, J.G., van der Kemp, A.W., Hartog, A., van de Graaf, S.F., van Os, C.H., Willems, P.H., and Bindels, R.J. (1999). Molecular identification of the apical Ca²⁺ channel in 1, 25-dihydroxyvitamin D₃-responsive epithelia. *J Biol Chem* 274, 8375-8378.

Hoenderop, J.G., van Leeuwen, J.P., van der Eerden, B.C., Kersten, F.F., van der Kemp, A.W., Merillat, A.M., Waarsing, J.H., Rossier, B.C., Vallon, V., Hummler, E., *et al.* (2003a). Renal Ca²⁺ wasting, hyperabsorption, and reduced bone thickness in mice lacking TRPV5. *J Clin Invest* 112, 1906-1914.

Hoenderop, J.G., Voets, T., Hoefs, S., Weidema, F., Prenen, J., Nilius, B., and Bindels, R.J. (2003b). Homo- and heterotetrameric architecture of the epithelial Ca²⁺ channels TRPV5 and TRPV6. *EMBO J* 22, 776-785.

Holzenberger, M., Dupont, J., Ducos, B., Leneuve, P., Geloën, A., Even, P.C., Cervera, P., and Le Bouc, Y. (2003). IGF-1 receptor regulates lifespan and resistance to oxidative stress in mice. *Nature* 421, 182-187.

Horng, J.L., Lin, L.Y., Huang, C.J., Katoh, F., Kaneko, T., and Hwang, P.P. (2007). Knockdown of V-ATPase subunit A (*atp6v1a*) impairs acid secretion and ion balance in zebrafish (*Danio rerio*). *Am J Physiol Regul Integr Comp Physiol* 292, R2068-2076.

Hovey, R.C., Harris, J., Hadsell, D.L., Lee, A.V., Ormandy, C.J., and Vonderhaar, B.K. (2003). Local insulin-like growth factor-II mediates prolactin-induced mammary gland development. *Mol Endocrinol* 17, 460-471.

Hsiao, C.D., You, M.S., Guh, Y.J., Ma, M., Jiang, Y.J., and Hwang, P.P. (2007). A positive regulatory loop between *foxi3a* and *foxi3b* is essential for specification and differentiation of zebrafish epidermal ionocytes. *PLoS One* 2, e302.

- Hsieh, T., Gordon, R.E., Clemmons, D.R., Busby, W.H., Jr., and Duan, C. (2003). Regulation of vascular smooth muscle cell responses to insulin-like growth factor (IGF)-I by local IGF-binding proteins. *J Biol Chem* 278, 42886-42892.
- Humbert, S., Bryson, E.A., Cordelieres, F.P., Connors, N.C., Datta, S.R., Finkbeiner, S., Greenberg, M.E., and Saudou, F. (2002). The IGF-1/Akt pathway is neuroprotective in Huntington's disease and involves Huntingtin phosphorylation by Akt. *Dev Cell* 2, 831-837.
- Hwang, P.P. (2009). Ion uptake and acid secretion in zebrafish (*Danio rerio*). *J Exp Biol* 212, 1745-1752.
- Hwang, P.P., and Lee, T.H. (2007). New insights into fish ion regulation and mitochondrion-rich cells. *Comp Biochem Physiol A Mol Integr Physiol* 148, 479-497.
- Hylka, V.W., Teplow, D.B., Kent, S.B., and Straus, D.S. (1985). Identification of a peptide fragment from the carboxyl-terminal extension region (E-domain) of rat proinsulin-like growth factor-II. *J Biol Chem* 260, 14417-14420.
- Imai, Y., Busby, W.H., Jr., Smith, C.E., Clarke, J.B., Garmon, A.J., Horwitz, G.D., Rees, C., and Clemmons, D.R. (1997). Protease-resistant form of insulin-like growth factor-binding protein 5 is an inhibitor of insulin-like growth factor-I actions on porcine smooth muscle cells in culture. *J Clin Invest* 100, 2596-2605.
- Imai, Y., Moralez, A., Andag, U., Clarke, J.B., Busby, W.H., Jr., and Clemmons, D.R. (2000). Substitutions for hydrophobic amino acids in the N-terminal domains of IGFBP-3 and -5 markedly reduce IGF-I binding and alter their biologic actions. *J Biol Chem* 275, 18188-18194.
- James, P.L., Stewart, C.E., and Rotwein, P. (1996). Insulin-like growth factor binding protein-5 modulates muscle differentiation through an insulin-like growth factor-dependent mechanism. *J Cell Biol* 133, 683-693.
- Janicke, M., Carney, T.J., and Hammerschmidt, M. (2007). Foxi3 transcription factors and Notch signaling control the formation of skin ionocytes from epidermal precursors of the zebrafish embryo. *Dev Biol* 307, 258-271.
- Jaques, G., Noll, K., Wegmann, B., Witten, S., Kogan, E., Radulescu, R.T., and Havemann, K. (1997). Nuclear localization of insulin-like growth factor binding protein 3 in a lung cancer cell line. *Endocrinology* 138, 1767-1770.

Jensen, J., Pedersen, E.E., Galante, P., Hald, J., Heller, R.S., Ishibashi, M., Kageyama, R., Guillemot, F., Serup, P., and Madsen, O.D. (2000). Control of endodermal endocrine development by Hes-1. *Nat Genet* 24, 36-44.

Jones, J.I., Gockerman, A., Busby, W.H., Jr., Camacho-Hubner, C., and Clemmons, D.R. (1993). Extracellular matrix contains insulin-like growth factor binding protein-5: potentiation of the effects of IGF-I. *J Cell Biol* 121, 679-687.

Jurget, A., Berlato, C., Obrist, P., Ploner, C., Massoner, P., Schmolzer, J., Haffner, M.C., Klocker, H., Huber, L.A., Geley, S., *et al.* (2007). Insulin-like growth factor-binding protein-5 enters vesicular structures but not the nucleus. *Traffic* 8, 1815-1828.

Kajimura, S., Aida, K., and Duan, C. (2005). Insulin-like growth factor-binding protein-1 (IGFBP-1) mediates hypoxia-induced embryonic growth and developmental retardation. *Proc Natl Acad Sci U S A* 102, 1240-1245.

Kakizawa, S., Kaneko, T., Hasegawa, S., and Hirano, T. (1993). Activation of somatolactin cells in the pituitary of the rainbow trout *Oncorhynchus mykiss* by low environmental calcium. *Gen Comp Endocrinol* 91, 298-306.

Kallay, E., Kifor, O., Chattopadhyay, N., Brown, E.M., Bischof, M.G., Peterlik, M., and Cross, H.S. (1997). Calcium-dependent c-myc proto-oncogene expression and proliferation of Caco-2 cells: a role for a luminal extracellular calcium-sensing receptor. *Biochem Biophys Res Commun* 232, 80-83.

Kalus, W., Zweckstetter, M., Renner, C., Sanchez, Y., Georgescu, J., Grol, M., Demuth, D., Schumacher, R., Dony, C., Lang, K., *et al.* (1998). Structure of the IGF-binding domain of the insulin-like growth factor-binding protein-5 (IGFBP-5): implications for IGF and IGF-I receptor interactions. *EMBO J* 17, 6558-6572.

Kamei, H., Lu, L., Jiao, S., Li, Y., Gyrupe, C., Laursen, L.S., Oxvig, C., Zhou, J., and Duan, C. (2008). Duplication and diversification of the hypoxia-inducible IGFBP-1 gene in zebrafish. *PLoS ONE* 3, e3091.

Kanzaki, M., Zhang, Y.Q., Mashima, H., Li, L., Shibata, H., and Kojima, I. (1999). Translocation of a calcium-permeable cation channel induced by insulin-like growth factor-I. *Nat Cell Biol* 1, 165-170.

Kawasaki, H., Nakayama, S., and Kretsinger, R.H. (1998). Classification and evolution of EF-hand proteins. *Biometals* 11, 277-295.

Kimmel, C.B., Ballard, W.W., Kimmel, S.R., Ullmann, B., and Schilling, T.F. (1995). Stages of embryonic development of the zebrafish. *Dev Dyn* 203, 253-310.

- Kimmel, C.B., and Warga, R.M. (1986). Tissue-specific cell lineages originate in the gastrula of the zebrafish. *Science* *231*, 365-368.
- Kimmel, C.B., Warga, R.M., and Schilling, T.F. (1990). Origin and organization of the zebrafish fate map. *Development* *108*, 581-594.
- Kishi, S., Uchiyama, J., Baughman, A.M., Goto, T., Lin, M.C., and Tsai, S.B. (2003). The zebrafish as a vertebrate model of functional aging and very gradual senescence. *Exp Gerontol* *38*, 777-786.
- Kleinjan, D.A., Bancewicz, R.M., Gautier, P., Dahm, R., Schonthaler, H.B., Damante, G., Seawright, A., Hever, A.M., Yeyati, P.L., van Heyningen, V., *et al.* (2008). Subfunctionalization of duplicated zebrafish pax6 genes by cis-regulatory divergence. *PLoS Genet* *4*, e29.
- Komuro, I., Wenninger, K.E., Philipson, K.D., and Izumo, S. (1992). Molecular cloning and characterization of the human cardiac Na⁺/Ca²⁺ exchanger cDNA. *Proc Natl Acad Sci U S A* *89*, 4769-4773.
- Kondo, T., Vicent, D., Suzuma, K., Yanagisawa, M., King, G.L., Holzenberger, M., and Kahn, C.R. (2003). Knockout of insulin and IGF-1 receptors on vascular endothelial cells protects against retinal neovascularization. *J Clin Invest* *111*, 1835-1842.
- Koster, H.P., Hartog, A., Van Os, C.H., and Bindels, R.J. (1995). Calbindin-D28K facilitates cytosolic calcium diffusion without interfering with calcium signaling. *Cell Calcium* *18*, 187-196.
- Kulkarni, R.N., Holzenberger, M., Shih, D.Q., Ozcan, U., Stoffel, M., Magnuson, M.A., and Kahn, C.R. (2002). beta-cell-specific deletion of the Igf1 receptor leads to hyperinsulinemia and glucose intolerance but does not alter beta-cell mass. *Nat Genet* *31*, 111-115.
- Kutuzova, G.D., Sundersingh, F., Vaughan, J., Tadi, B.P., Ansay, S.E., Christakos, S., and Deluca, H.F. (2008). TRPV6 is not required for 1alpha,25-dihydroxyvitamin D3-induced intestinal calcium absorption in vivo. *Proc Natl Acad Sci U S A* *105*, 19655-19659.
- Lamprecht, S.A., and Lipkin, M. (2003). Chemoprevention of colon cancer by calcium, vitamin D and folate: molecular mechanisms. *Nat Rev Cancer* *3*, 601-614.
- Larkin, M.A., Blackshields, G., Brown, N.P., Chenna, R., McGettigan, P.A., McWilliam, H., Valentin, F., Wallace, I.M., Wilm, A., Lopez, R., *et al.* (2007). Clustal W and Clustal X version 2.0. *Bioinformatics* *23*, 2947-2948.

- Lau, M.M., Stewart, C.E., Liu, Z., Bhatt, H., Rotwein, P., and Stewart, C.L. (1994). Loss of the imprinted IGF2/cation-independent mannose 6-phosphate receptor results in fetal overgrowth and perinatal lethality. *Genes Dev* 8, 2953-2963.
- Lawson, N.D., and Weinstein, B.M. (2002). In vivo imaging of embryonic vascular development using transgenic zebrafish. *Dev Biol* 248, 307-318.
- Le Guellec, D., Morvan-Dubois, G., and Sire, J.Y. (2004). Skin development in bony fish with particular emphasis on collagen deposition in the dermis of the zebrafish (*Danio rerio*). *Int J Dev Biol* 48, 217-231.
- Le Roith, D., Bondy, C., Yakar, S., Liu, J.L., and Butler, A. (2001). The somatomedin hypothesis: 2001. *Endocr Rev* 22, 53-74.
- Lee, H., and Kimelman, D. (2002). A dominant-negative form of p63 is required for epidermal proliferation in zebrafish. *Dev Cell* 2, 607-616.
- Lehen'kyi, V., Flourakis, M., Skryma, R., and Prevarskaya, N. (2007). TRPV6 channel controls prostate cancer cell proliferation via Ca(2+)/NFAT-dependent pathways. *Oncogene* 26, 7380-7385.
- Leu, J.I., Crissey, M.A., Craig, L.E., and Taub, R. (2003). Impaired hepatocyte DNA synthetic response posthepatectomy in insulin-like growth factor binding protein 1-deficient mice with defects in C/EBP beta and mitogen-activated protein kinase/extracellular signal-regulated kinase regulation. *Mol Cell Biol* 23, 1251-1259.
- Lewitt, M.S., Saunders, H., Phuyal, J.L., and Baxter, R.C. (1994). Complex formation by human insulin-like growth factor-binding protein-3 and human acid-labile subunit in growth hormone-deficient rats. *Endocrinology* 134, 2404-2409.
- Li, W., Fawcett, J., Widmer, H.R., Fielder, P.J., Rabkin, R., and Keller, G.A. (1997). Nuclear transport of insulin-like growth factor-I and insulin-like growth factor binding protein-3 in opossum kidney cells. *Endocrinology* 138, 1763-1766.
- Li, Y., Xiang, J., and Duan, C. (2005). Insulin-like growth factor-binding protein-3 plays an important role in regulating pharyngeal skeleton and inner ear formation and differentiation. *J Biol Chem* 280, 3613-3620.
- Liao, B.K., Deng, A.N., Chen, S.C., Chou, M.Y., and Hwang, P.P. (2007). Expression and water calcium dependence of calcium transporter isoforms in zebrafish gill mitochondrion-rich cells. *BMC Genomics* 8, 354.

- Lin, L.Y., Horng, J.L., Kunkel, J.G., and Hwang, P.P. (2006). Proton pump-rich cell secretes acid in skin of zebrafish larvae. *Am J Physiol Cell Physiol* *290*, C371-378.
- Linkhart, T.A., and Mohan, S. (1989). Parathyroid hormone stimulates release of insulin-like growth factor-I (IGF-I) and IGF-II from neonatal mouse calvaria in organ culture. *Endocrinology* *125*, 1484-1491.
- Liu, J.P., Baker, J., Perkins, A.S., Robertson, E.J., and Efstratiadis, A. (1993). Mice carrying null mutations of the genes encoding insulin-like growth factor I (Igf-1) and type I IGF receptor (Igf1r). *Cell* *75*, 59-72.
- Lorand, L., and Graham, R.M. (2003). Transglutaminases: crosslinking enzymes with pleiotropic functions. *Nat Rev Mol Cell Biol* *4*, 140-156.
- Luo, H., Yu, G., Tremblay, J., and Wu, J. (2004). EphB6-null mutation results in compromised T cell function. *J Clin Invest* *114*, 1762-1773.
- Lytton, J. (2007). Na⁺/Ca²⁺ exchangers: three mammalian gene families control Ca²⁺ transport. *Biochem J* *406*, 365-382.
- Maures, T., Chan, S.J., Xu, B., Sun, H., Ding, J., and Duan, C. (2002). Structural, biochemical, and expression analysis of two distinct insulin-like growth factor I receptors and their ligands in zebrafish. *Endocrinology* *143*, 1858-1871.
- Mayack, S.R., Shadrach, J.L., Kim, F.S., and Wagers, A.J. (2010). Systemic signals regulate ageing and rejuvenation of blood stem cell niches. *Nature* *463*, 495-500.
- McCarthy, T.L., Centrella, M., and Canalis, E. (1989). Parathyroid hormone enhances the transcript and polypeptide levels of insulin-like growth factor I in osteoblast-enriched cultures from fetal rat bone. *Endocrinology* *124*, 1247-1253.
- McClintock, J.M., Kheirbek, M.A., and Prince, V.E. (2002). Knockdown of duplicated zebrafish *hoxb1* genes reveals distinct roles in hindbrain patterning and a novel mechanism of duplicate gene retention. *Development* *129*, 2339-2354.
- McCormick, S.D. (2001). Endocrine Control of Osmoregulation in Teleost Fish. *American Zoologist* *41*, 781-794.
- McCormick, S.D., Hasegawa, S., and Hirano, T. (1992). Calcium uptake in the skin of a freshwater teleost. *Proc Natl Acad Sci U S A* *89*, 3635-3638.
- McNeil, S.E., Hobson, S.A., Nipper, V., and Rodland, K.D. (1998). Functional calcium-sensing receptors in rat fibroblasts are required for activation of SRC kinase and mitogen-

activated protein kinase in response to extracellular calcium. *J Biol Chem* 273, 1114-1120.

Medema, R.H., Kops, G.J., Bos, J.L., and Burgering, B.M. (2000). AFX-like Forkhead transcription factors mediate cell-cycle regulation by Ras and PKB through p27kip1. *Nature* 404, 782-787.

Meyer, M.B., Watanuki, M., Kim, S., Shevde, N.K., and Pike, J.W. (2006). The human transient receptor potential vanilloid type 6 distal promoter contains multiple vitamin D receptor binding sites that mediate activation by 1,25-dihydroxyvitamin D₃ in intestinal cells. *Mol Endocrinol* 20, 1447-1461.

Miura, M., Surmacz, E., Burgaud, J.L., and Baserga, R. (1995). Different effects on mitogenesis and transformation of a mutation at tyrosine 1251 of the insulin-like growth factor I receptor. *J Biol Chem* 270, 22639-22644.

Miyake, H., Nelson, C., Rennie, P.S., and Gleave, M.E. (2000a). Overexpression of insulin-like growth factor binding protein-5 helps accelerate progression to androgen-independence in the human prostate LNCaP tumor model through activation of phosphatidylinositol 3'-kinase pathway. *Endocrinology* 141, 2257-2265.

Miyake, H., Pollak, M., and Gleave, M.E. (2000b). Castration-induced up-regulation of insulin-like growth factor binding protein-5 potentiates insulin-like growth factor-I activity and accelerates progression to androgen independence in prostate cancer models. *Cancer Res* 60, 3058-3064.

Miyakoshi, N., Richman, C., Kasukawa, Y., Linkhart, T.A., Baylink, D.J., and Mohan, S. (2001). Evidence that IGF-binding protein-5 functions as a growth factor. *J Clin Invest* 107, 73-81.

Mohan, S., Nakao, Y., Honda, Y., Landale, E., Leser, U., Dony, C., Lang, K., and Baylink, D.J. (1995). Studies on the mechanisms by which insulin-like growth factor (IGF) binding protein-4 (IGFBP-4) and IGFBP-5 modulate IGF actions in bone cells. *J Biol Chem* 270, 20424-20431.

Morgan, D.O., Edman, J.C., Standring, D.N., Fried, V.A., Smith, M.C., Roth, R.A., and Rutter, W.J. (1987). Insulin-like growth factor II receptor as a multifunctional binding protein. *Nature* 329, 301-307.

Morison, I.M., Becroft, D.M., Taniguchi, T., Woods, C.G., and Reeve, A.E. (1996). Somatic overgrowth associated with overexpression of insulin-like growth factor II. *Nat Med* 2, 311-316.

- Mueller, T., and Wullimann, M.F. (2002). BrdU-, neuroD (nrd)- and Hu-studies reveal unusual non-ventricular neurogenesis in the postembryonic zebrafish forebrain. *Mech Dev* 117, 123-135.
- Muise-Helmericks, R.C., Grimes, H.L., Bellacosa, A., Malstrom, S.E., Tschlis, P.N., and Rosen, N. (1998). Cyclin D expression is controlled post-transcriptionally via a phosphatidylinositol 3-kinase/Akt-dependent pathway. *J Biol Chem* 273, 29864-29872.
- Murakami, M.S., and Rosen, O.M. (1991). The role of insulin receptor autophosphorylation in signal transduction. *J Biol Chem* 266, 22653-22660.
- Musaro, A., McCullagh, K., Paul, A., Houghton, L., Dobrowolny, G., Molinaro, M., Barton, E.R., Sweeney, H.L., and Rosenthal, N. (2001). Localized Igf-1 transgene expression sustains hypertrophy and regeneration in senescent skeletal muscle. *Nat Genet* 27, 195-200.
- Musaro, A., McCullagh, K.J., Naya, F.J., Olson, E.N., and Rosenthal, N. (1999). IGF-1 induces skeletal myocyte hypertrophy through calcineurin in association with GATA-2 and NF-ATc1. *Nature* 400, 581-585.
- Nef, S., Verma-Kurvari, S., Merenmies, J., Vassalli, J.D., Efstratiadis, A., Accili, D., and Parada, L.F. (2003). Testis determination requires insulin receptor family function in mice. *Nature* 426, 291-295.
- Nemeth, E.F., Steffey, M.E., Hammerland, L.G., Hung, B.C., Van Wagenen, B.C., DelMar, E.G., and Balandrin, M.F. (1998). Calcimimetics with potent and selective activity on the parathyroid calcium receptor. *Proc Natl Acad Sci U S A* 95, 4040-4045.
- Nica, G., Herzog, W., Sonntag, C., and Hammerschmidt, M. (2004). Zebrafish pit1 mutants lack three pituitary cell types and develop severe dwarfism. *Mol Endocrinol* 18, 1196-1209.
- Nicolas, V., Mohan, S., Honda, Y., Prewett, A., Finkelman, R.D., Baylink, D.J., and Farley, J.R. (1995). An age-related decrease in the concentration of insulin-like growth factor binding protein-5 in human cortical bone. *Calcif Tissue Int* 57, 206-212.
- Niemeyer, B.A., Bergs, C., Wissenbach, U., Flockerzi, V., and Trost, C. (2001). Competitive regulation of CaT-like-mediated Ca²⁺ entry by protein kinase C and calmodulin. *Proc Natl Acad Sci U S A* 98, 3600-3605.
- Nilius, B., Prenen, J., Vennekens, R., Hoenderop, J.G., Bindels, R.J., and Droogmans, G. (2001a). Pharmacological modulation of monovalent cation currents through the epithelial Ca²⁺ channel ECaC1. *Br J Pharmacol* 134, 453-462.

- Nilius, B., Vennekens, R., Prenen, J., Hoenderop, J.G., Droogmans, G., and Bindels, R.J. (2001b). The single pore residue Asp542 determines Ca²⁺ permeation and Mg²⁺ block of the epithelial Ca²⁺ channel. *J Biol Chem* *276*, 1020-1025.
- Ning, Y., Hoang, B., Schuller, A.G., Cominski, T.P., Hsu, M.S., Wood, T.L., and Pintar, J.E. (2007). Delayed mammary gland involution in mice with mutation of the insulin-like growth factor binding protein 5 gene. *Endocrinology* *148*, 2138-2147.
- Ning, Y., Schuller, A.G., Bradshaw, S., Rotwein, P., Ludwig, T., Frystyk, J., and Pintar, J.E. (2006). Diminished growth and enhanced glucose metabolism in triple knockout mice containing mutations of insulin-like growth factor binding protein-3, -4, and -5. *Mol Endocrinol* *20*, 2173-2186.
- Niu, T., and Rosen, C.J. (2005). The insulin-like growth factor-I gene and osteoporosis: a critical appraisal. *Gene* *361*, 38-56.
- Oates, A.C., Bruce, A.E., and Ho, R.K. (2000). Too much interference: injection of double-stranded RNA has nonspecific effects in the zebrafish embryo. *Dev Biol* *224*, 20-28.
- Oka, Y., Rozek, L.M., and Czech, M.P. (1985). Direct demonstration of rapid insulin-like growth factor II Receptor internalization and recycling in rat adipocytes. Insulin stimulates ¹²⁵I-insulin-like growth factor II degradation by modulating the IGF-II receptor recycling process. *J Biol Chem* *260*, 9435-9442.
- Okabe, M., and Graham, A. (2004). The origin of the parathyroid gland. *Proc Natl Acad Sci U S A* *101*, 17716-17719.
- Pan, T.C., Liao, B.K., Huang, C.J., Lin, L.Y., and Hwang, P.P. (2005). Epithelial Ca(2+) channel expression and Ca(2+) uptake in developing zebrafish. *Am J Physiol Regul Integr Comp Physiol* *289*, R1202-1211.
- Pandini, G., Frasca, F., Mineo, R., Sciacca, L., Vigneri, R., and Belfiore, A. (2002). Insulin/insulin-like growth factor I hybrid receptors have different biological characteristics depending on the insulin receptor isoform involved. *J Biol Chem* *277*, 39684-39695.
- Pandini, G., Vigneri, R., Costantino, A., Frasca, F., Ippolito, A., Fujita-Yamaguchi, Y., Siddle, K., Goldfine, I.D., and Belfiore, A. (1999). Insulin and insulin-like growth factor-I (IGF-I) receptor overexpression in breast cancers leads to insulin/IGF-I hybrid receptor overexpression: evidence for a second mechanism of IGF-I signaling. *Clin Cancer Res* *5*, 1935-1944.

- Parker, A., Rees, C., Clarke, J., Busby, W.H., Jr., and Clemmons, D.R. (1998). Binding of insulin-like growth factor (IGF)-binding protein-5 to smooth-muscle cell extracellular matrix is a major determinant of the cellular response to IGF-I. *Mol Biol Cell* 9, 2383-2392.
- Parsons, J.A., Brelje, T.C., and Sorenson, R.L. (1992). Adaptation of islets of Langerhans to pregnancy: increased islet cell proliferation and insulin secretion correlates with the onset of placental lactogen secretion. *Endocrinology* 130, 1459-1466.
- Pedone, P.V., Tirabosco, R., Cavazzana, A.O., Ungaro, P., Basso, G., Luksch, R., Carli, M., Bruni, C.B., Frunzio, R., and Riccio, A. (1994). Mono- and bi-allelic expression of insulin-like growth factor II gene in human muscle tumors. *Hum Mol Genet* 3, 1117-1121.
- Peng, J.B., Brown, E.M., and Hediger, M.A. (2001a). Structural conservation of the genes encoding CaT1, CaT2, and related cation channels. *Genomics* 76, 99-109.
- Peng, J.B., Chen, X.Z., Berger, U.V., Vassilev, P.M., Tsukaguchi, H., Brown, E.M., and Hediger, M.A. (1999). Molecular cloning and characterization of a channel-like transporter mediating intestinal calcium absorption. *J Biol Chem* 274, 22739-22746.
- Peng, J.B., Zhuang, L., Berger, U.V., Adam, R.M., Williams, B.J., Brown, E.M., Hediger, M.A., and Freeman, M.R. (2001b). CaT1 expression correlates with tumor grade in prostate cancer. *Biochem Biophys Res Commun* 282, 729-734.
- Perry, S.F., and Wood, C.M. (1985). Kinetics of Branchial Calcium Uptake in the Rainbow Trout: Effects of Acclimation to Various External Calcium Levels. *J Exp Biol* 116, 411-433.
- Pollak, M.N., Schernhammer, E.S., and Hankinson, S.E. (2004). Insulin-like growth factors and neoplasia. *Nat Rev Cancer* 4, 505-518.
- Postlethwait, J., Amores, A., Cresko, W., Singer, A., and Yan, Y.L. (2004). Subfunction partitioning, the teleost radiation and the annotation of the human genome. *Trends Genet* 20, 481-490.
- Powell-Braxton, L., Hollingshead, P., Warburton, C., Dowd, M., Pitts-Meek, S., Dalton, D., Gillett, N., and Stewart, T.A. (1993). IGF-I is required for normal embryonic growth in mice. *Genes Dev* 7, 2609-2617.
- Prince, V.E., and Pickett, F.B. (2002). Splitting pairs: the diverging fates of duplicated genes. *Nat Rev Genet* 3, 827-837.

- Qiu, A., and Hogstrand, C. (2004). Functional characterisation and genomic analysis of an epithelial calcium channel (ECaC) from pufferfish, *Fugu rubripes*. *Gene* 342, 113-123.
- Raber, G., Willems, P.H., Lang, F., Nitschke, R., van Os, C.H., and Bindels, R.J. (1997). Co-ordinated control of apical calcium influx and basolateral calcium efflux in rabbit cortical collecting system. *Cell Calcium* 22, 157-166.
- Radulescu, R.T. (1994). Nuclear localization signal in insulin-like growth factor-binding protein type 3. *Trends Biochem Sci* 19, 278.
- Reeve, A.E., Eccles, M.R., Wilkins, R.J., Bell, G.I., and Millow, L.J. (1985). Expression of insulin-like growth factor-II transcripts in Wilms' tumour. *Nature* 317, 258-260.
- Ren, H., Yin, P., and Duan, C. (2008). IGFBP-5 regulates muscle cell differentiation by binding to IGF-II and switching on the IGF-II auto-regulation loop. *J Cell Biol* 182, 979-991.
- Richman, C., Baylink, D.J., Lang, K., Dony, C., and Mohan, S. (1999). Recombinant human insulin-like growth factor-binding protein-5 stimulates bone formation parameters in vitro and in vivo. *Endocrinology* 140, 4699-4705.
- Rinderknecht, E., and Humbel, R.E. (1978a). The amino acid sequence of human insulin-like growth factor I and its structural homology with proinsulin. *J Biol Chem* 253, 2769-2776.
- Rinderknecht, E., and Humbel, R.E. (1978b). Primary structure of human insulin-like growth factor II. *FEBS Lett* 89, 283-286.
- Rosen, L.B., Ginty, D.D., Weber, M.J., and Greenberg, M.E. (1994). Membrane depolarization and calcium influx stimulate MEK and MAP kinase via activation of Ras. *Neuron* 12, 1207-1221.
- Rozen, F., Yang, X.F., Huynh, H., and Pollak, M. (1997). Antiproliferative action of vitamin D-related compounds and insulin-like growth factor-binding protein 5 accumulation. *J Natl Cancer Inst* 89, 652-656.
- Sakamoto, T., and McCormick, S.D. (2006). Prolactin and growth hormone in fish osmoregulation. *Gen Comp Endocrinol* 147, 24-30.
- Sakatani, T., Kaneda, A., Iacobuzio-Donahue, C.A., Carter, M.G., de Boer Witzel, S., Okano, H., Ko, M.S., Ohlsson, R., Longo, D.L., and Feinberg, A.P. (2005). Loss of imprinting of *Igf2* alters intestinal maturation and tumorigenesis in mice. *Science* 307, 1976-1978.

Salih, D.A., Tripathi, G., Holding, C., Szeszak, T.A., Gonzalez, M.I., Carter, E.J., Cobb, L.J., Eisemann, J.E., and Pell, J.M. (2004). Insulin-like growth factor-binding protein 5 (Igfbp5) compromises survival, growth, muscle development, and fertility in mice. *Proc Natl Acad Sci U S A* *101*, 4314-4319.

Salmon, W.D., Jr., and Daughaday, W.H. (1957). A hormonally controlled serum factor which stimulates sulfate incorporation by cartilage in vitro. *J Lab Clin Med* *49*, 825-836.

Samani, A.A., Yakar, S., LeRoith, D., and Brodt, P. (2007). The role of the IGF system in cancer growth and metastasis: overview and recent insights. *Endocr Rev* *28*, 20-47.

Schedlich, L.J., Le Page, S.L., Firth, S.M., Briggs, L.J., Jans, D.A., and Baxter, R.C. (2000). Nuclear import of insulin-like growth factor-binding protein-3 and -5 is mediated by the importin beta subunit. *J Biol Chem* *275*, 23462-23470.

Schedlich, L.J., Muthukaruppan, A., O'Han, M.K., and Baxter, R.C. (2007). Insulin-like growth factor binding protein-5 interacts with the vitamin D receptor and modulates the vitamin D response in osteoblasts. *Mol Endocrinol* *21*, 2378-2390.

Schedlich, L.J., Young, T.F., Firth, S.M., and Baxter, R.C. (1998). Insulin-like growth factor-binding protein (IGFBP)-3 and IGFBP-5 share a common nuclear transport pathway in T47D human breast carcinoma cells. *J Biol Chem* *273*, 18347-18352.

Schlueter, P.J., Royer, T., Farah, M.H., Laser, B., Chan, S.J., Steiner, D.F., and Duan, C. (2006). Gene duplication and functional divergence of the zebrafish insulin-like growth factor 1 receptors. *FASEB J* *20*, 1230-1232.

Schneeberger, E.E., and Lynch, R.D. (2004). The tight junction: a multifunctional complex. *Am J Physiol Cell Physiol* *286*, C1213-1228.

Schoeber, J.P., Topala, C.N., Wang, X., Diepens, R.J., Lambers, T.T., Hoenderop, J.G., and Bindels, R.J. (2006). RGS2 inhibits the epithelial Ca²⁺ channel TRPV6. *J Biol Chem* *281*, 29669-29674.

Schrier, R.W. (2006). *Diseases of the Kidney and Urinary Tract*. 2320.

Sciacca, L., Mineo, R., Pandini, G., Murabito, A., Vigneri, R., and Belfiore, A. (2002). In IGF-I receptor-deficient leiomyosarcoma cells autocrine IGF-II induces cell invasion and protection from apoptosis via the insulin receptor isoform A. *Oncogene* *21*, 8240-8250.

Scott, J., Cowell, J., Robertson, M.E., Priestley, L.M., Wadey, R., Hopkins, B., Pritchard, J., Bell, G.I., Rall, L.B., Graham, C.F., *et al.* (1985). Insulin-like growth factor-II gene expression in Wilms' tumour and embryonic tissues. *Nature* *317*, 260-262.

Seino, S., and Bell, G.I. (1989). Alternative splicing of human insulin receptor messenger RNA. *Biochem Biophys Res Commun* 159, 312-316.

Semsarian, C., Wu, M.J., Ju, Y.K., Marciniak, T., Yeoh, T., Allen, D.G., Harvey, R.P., and Graham, R.M. (1999). Skeletal muscle hypertrophy is mediated by a Ca²⁺-dependent calcineurin signalling pathway. *Nature* 400, 576-581.

Shand, J.H., Beattie, J., Song, H., Phillips, K., Kelly, S.M., Flint, D.J., and Allan, G.J. (2003). Specific amino acid substitutions determine the differential contribution of the N- and C-terminal domains of insulin-like growth factor (IGF)-binding protein-5 in binding IGF-I. *J Biol Chem* 278, 17859-17866.

Shemer, J., Yaron, A., Werner, H., Shao, Z.M., Sheikh, M.S., Fontana, J.A., LeRoith, D., and Roberts, C.T., Jr. (1993). Regulation of insulin-like growth factor (IGF) binding protein-5 in the T47D human breast carcinoma cell line by IGF-I and retinoic acid. *J Clin Endocrinol Metab* 77, 1246-1250.

Shepard, J.L., Amatruda, J.F., Stern, H.M., Subramanian, A., Finkelstein, D., Ziai, J., Finley, K.R., Pfaff, K.L., Hersey, C., Zhou, Y., *et al.* (2005). A zebrafish bmyb mutation causes genome instability and increased cancer susceptibility. *Proc Natl Acad Sci U S A* 102, 13194-13199.

Shimasaki, S., Gao, L., Shimonaka, M., and Ling, N. (1991a). Isolation and molecular cloning of insulin-like growth factor-binding protein-6. *Mol Endocrinol* 5, 938-948.

Shimasaki, S., Shimonaka, M., Zhang, H.P., and Ling, N. (1991b). Identification of five different insulin-like growth factor binding proteins (IGFBPs) from adult rat serum and molecular cloning of a novel IGFBP-5 in rat and human. *J Biol Chem* 266, 10646-10653.

Shimasaki, S., Uchiyama, F., Shimonaka, M., and Ling, N. (1990). Molecular cloning of the cDNAs encoding a novel insulin-like growth factor-binding protein from rat and human. *Mol Endocrinol* 4, 1451-1458.

Shimizu, M., Swanson, P., Fukada, H., Hara, A., and Dickhoff, W.W. (2000a). Comparison of Extraction Methods and Assay Validation for Salmon Insulin-like Growth Factor-I Using Commercially Available Components. *General and Comparative Endocrinology* 119, 26-36.

Shimizu, M., Swanson, P., Fukada, H., Hara, A., and Dickhoff, W.W. (2000b). Comparison of extraction methods and assay validation for salmon insulin-like growth factor-I using commercially available components. *Gen Comp Endocrinol* 119, 26-36.

Shoback, D. (2008). Clinical practice. Hypoparathyroidism. *N Engl J Med* 359, 391-403.

Sims, N.A., Clement-Lacroix, P., Da Ponte, F., Bouali, Y., Binart, N., Moriggl, R., Goffin, V., Coschigano, K., Gaillard-Kelly, M., Kopchick, J., *et al.* (2000). Bone homeostasis in growth hormone receptor-null mice is restored by IGF-I but independent of Stat5. *J Clin Invest* *106*, 1095-1103.

Singh, B.B., Lockwich, T.P., Bandyopadhyay, B.C., Liu, X., Bollimuntha, S., Brazer, S.C., Combs, C., Das, S., Leenders, A.G., Sheng, Z.H., *et al.* (2004). VAMP2-dependent exocytosis regulates plasma membrane insertion of TRPC3 channels and contributes to agonist-stimulated Ca²⁺ influx. *Mol Cell* *15*, 635-646.

Song, H., Beattie, J., Campbell, I.W., and Allan, G.J. (2000). Overlap of IGF- and heparin-binding sites in rat IGF-binding protein-5. *J Mol Endocrinol* *24*, 43-51.

Song, Y., Kato, S., and Fleet, J.C. (2003a). Vitamin D receptor (VDR) knockout mice reveal VDR-independent regulation of intestinal calcium absorption and ECaC2 and calbindin D9k mRNA. *J Nutr* *133*, 374-380.

Song, Y., Peng, X., Porta, A., Takanaga, H., Peng, J.B., Hediger, M.A., Fleet, J.C., and Christakos, S. (2003b). Calcium transporter 1 and epithelial calcium channel messenger ribonucleic acid are differentially regulated by 1,25 dihydroxyvitamin D₃ in the intestine and kidney of mice. *Endocrinology* *144*, 3885-3894.

Sopjani, M., Kunert, A., Czarkowski, K., Klaus, F., Laufer, J., Foller, M., and Lang, F. (2010). Regulation of the Ca(2+) channel TRPV6 by the kinases SGK1, PKB/Akt, and PIKfyve. *J Membr Biol* *233*, 35-41.

Sternfeld, L., Anderie, I., Schmid, A., Al-Shaldi, H., Krause, E., Magg, T., Schreiner, D., Hofer, H.W., and Schulz, I. (2007). Identification of tyrosines in the putative regulatory site of the Ca²⁺ channel TRPV6. *Cell Calcium* *42*, 91-102.

Strehler, E.E., and Zacharias, D.A. (2001). Role of alternative splicing in generating isoform diversity among plasma membrane calcium pumps. *Physiol Rev* *81*, 21-50.

Streisinger, G., Walker, C., Dower, N., Knauber, D., and Singer, F. (1981). Production of clones of homozygous diploid zebra fish (*Brachydanio rerio*). *Nature* *291*, 293-296.

Stumpf, T., Zhang, Q., Hirnet, D., Lewandrowski, U., Sickmann, A., Wissenbach, U., Dorr, J., Lohr, C., Deitmer, J.W., and Fecher-Trost, C. (2008). The human TRPV6 channel protein is associated with cyclophilin B in human placenta. *J Biol Chem* *283*, 18086-18098.

Suzuki, Y., Kovacs, C.S., Takanaga, H., Peng, J.B., Landowski, C.P., and Hediger, M.A. (2008a). Calcium channel TRPV6 is involved in murine maternal-fetal calcium transport. *J Bone Miner Res* 23, 1249-1256.

Suzuki, Y., Landowski, C.P., and Hediger, M.A. (2008b). Mechanisms and regulation of epithelial Ca²⁺ absorption in health and disease. *Annu Rev Physiol* 70, 257-271.

Tamura, K., Dudley, J., Nei, M., and Kumar, S. (2007). MEGA4: Molecular Evolutionary Genetics Analysis (MEGA) software version 4.0. *Mol Biol Evol* 24, 1596-1599.

Taylor, J.S., Braasch, I., Frickey, T., Meyer, A., and Van de Peer, Y. (2003). Genome duplication, a trait shared by 22000 species of ray-finned fish. *Genome Res* 13, 382-390.

Tfelt-Hansen, J., Chattopadhyay, N., Yano, S., Kanuparthi, D., Rooney, P., Schwarz, P., and Brown, E.M. (2004). Calcium-sensing receptor induces proliferation through p38 mitogen-activated protein kinase and phosphatidylinositol 3-kinase but not extracellularly regulated kinase in a model of humoral hypercalcemia of malignancy. *Endocrinology* 145, 1211-1217.

Tong, P.Y., Tollefsen, S.E., and Kornfeld, S. (1988). The cation-independent mannose 6-phosphate receptor binds insulin-like growth factor II. *J Biol Chem* 263, 2585-2588.

Tonner, E., Barber, M.C., Allan, G.J., Beattie, J., Webster, J., Whitelaw, C.B., and Flint, D.J. (2002). Insulin-like growth factor binding protein-5 (IGFBP-5) induces premature cell death in the mammary glands of transgenic mice. *Development* 129, 4547-4557.

Tripathi, G., Salih, D.A., Drozd, A.C., Cosgrove, R.A., Cobb, L.J., and Pell, J.M. (2009). IGF-independent effects of insulin-like growth factor binding protein-5 (Igfbp5) in vivo. *FASEB J* 23, 2616-2626.

Tseng, D.Y., Chou, M.Y., Tseng, Y.C., Hsiao, C.D., Huang, C.J., Kaneko, T., and Hwang, P.P. (2009). Effects of stanniocalcin 1 on calcium uptake in zebrafish (*Danio rerio*) embryo. *Am J Physiol Regul Integr Comp Physiol* 296, R549-557.

Twigg, S.M., and Baxter, R.C. (1998). Insulin-like growth factor (IGF)-binding protein 5 forms an alternative ternary complex with IGFs and the acid-labile subunit. *J Biol Chem* 273, 6074-6079.

Ueki, I., Ooi, G.T., Tremblay, M.L., Hurst, K.R., Bach, L.A., and Boisclair, Y.R. (2000). Inactivation of the acid labile subunit gene in mice results in mild retardation of postnatal growth despite profound disruptions in the circulating insulin-like growth factor system. *Proc Natl Acad Sci U S A* 97, 6868-6873.

Ueki, K., Okada, T., Hu, J., Liew, C.W., Assmann, A., Dahlgren, G.M., Peters, J.L., Shackman, J.G., Zhang, M., Artner, I., *et al.* (2006). Total insulin and IGF-I resistance in pancreatic beta cells causes overt diabetes. *Nat Genet* 38, 583-588.

Ullrich, A., Gray, A., Tam, A.W., Yang-Feng, T., Tsubokawa, M., Collins, C., Henzel, W., Le Bon, T., Kathuria, S., Chen, E., *et al.* (1986). Insulin-like growth factor I receptor primary structure: comparison with insulin receptor suggests structural determinants that define functional specificity. *EMBO J* 5, 2503-2512.

Urasaki, A., Morvan, G., and Kawakami, K. (2006). Functional dissection of the Tol2 transposable element identified the minimal cis-sequence and a highly repetitive sequence in the subterminal region essential for transposition. *Genetics* 174, 639-649.

Van Abel, M., Hoenderop, J.G., Dardenne, O., St Arnaud, R., Van Os, C.H., Van Leeuwen, H.J., and Bindels, R.J. (2002). 1,25-dihydroxyvitamin D(3)-independent stimulatory effect of estrogen on the expression of ECaC1 in the kidney. *J Am Soc Nephrol* 13, 2102-2109.

van Abel, M., Hoenderop, J.G., van der Kemp, A.W., van Leeuwen, J.P., and Bindels, R.J. (2003). Regulation of the epithelial Ca²⁺ channels in small intestine as studied by quantitative mRNA detection. *Am J Physiol Gastrointest Liver Physiol* 285, G78-85.

Van Buren, J.J., Bhat, S., Rotello, R., Pauza, M.E., and Premkumar, L.S. (2005). Sensitization and translocation of TRPV1 by insulin and IGF-I. *Mol Pain* 1, 17.

Van Cromphaut, S.J., Dewerchin, M., Hoenderop, J.G., Stockmans, I., Van Herck, E., Kato, S., Bindels, R.J., Collen, D., Carmeliet, P., Bouillon, R., *et al.* (2001). Duodenal calcium absorption in vitamin D receptor-knockout mice: functional and molecular aspects. *Proc Natl Acad Sci U S A* 98, 13324-13329.

Van Cromphaut, S.J., Rummens, K., Stockmans, I., Van Herck, E., Dijcks, F.A., Ederveen, A.G., Carmeliet, P., Verhaeghe, J., Bouillon, R., and Carmeliet, G. (2003). Intestinal calcium transporter genes are upregulated by estrogens and the reproductive cycle through vitamin D receptor-independent mechanisms. *J Bone Miner Res* 18, 1725-1736.

van de Graaf, S.F., Chang, Q., Mensenkamp, A.R., Hoenderop, J.G., and Bindels, R.J. (2006a). Direct interaction with Rab11a targets the epithelial Ca²⁺ channels TRPV5 and TRPV6 to the plasma membrane. *Mol Cell Biol* 26, 303-312.

van de Graaf, S.F., Hoenderop, J.G., Gkika, D., Lamers, D., Prenen, J., Rescher, U., Gerke, V., Staub, O., Nilius, B., and Bindels, R.J. (2003). Functional expression of the epithelial Ca(2+) channels (TRPV5 and TRPV6) requires association of the S100A10-annexin 2 complex. *EMBO J* 22, 1478-1487.

van de Graaf, S.F., Hoenderop, J.G., van der Kemp, A.W., Gisler, S.M., and Bindels, R.J. (2006b). Interaction of the epithelial Ca²⁺ channels TRPV5 and TRPV6 with the intestine- and kidney-enriched PDZ protein NHERF4. *Pflugers Arch* 452, 407-417.

van de Graaf, S.F., van der Kemp, A.W., van den Berg, D., van Oorschot, M., Hoenderop, J.G., and Bindels, R.J. (2006c). Identification of BSPRY as a novel auxiliary protein inhibiting TRPV5 activity. *J Am Soc Nephrol* 17, 26-30.

van der Eerden, B.C., Hoenderop, J.G., de Vries, T.J., Schoenmaker, T., Buurman, C.J., Uitterlinden, A.G., Pols, H.A., Bindels, R.J., and van Leeuwen, J.P. (2005). The epithelial Ca²⁺ channel TRPV5 is essential for proper osteoclastic bone resorption. *Proc Natl Acad Sci U S A* 102, 17507-17512.

Van Itallie, C.M., and Anderson, J.M. (2006). Claudins and epithelial paracellular transport. *Annu Rev Physiol* 68, 403-429.

Wang, T.T., Tavera-Mendoza, L.E., Laperriere, D., Libby, E., MacLeod, N.B., Nagai, Y., Bourdeau, V., Konstorum, A., Lallemand, B., Zhang, R., *et al.* (2005). Large-scale in silico and microarray-based identification of direct 1,25-dihydroxyvitamin D₃ target genes. *Mol Endocrinol* 19, 2685-2695.

Wang, X., Lu, L., Li, Y., Li, M., Chen, C., Feng, Q., Zhang, C., and Duan, C. (2009a). Molecular and functional characterization of two distinct IGF binding protein-6 genes in zebrafish. *Am J Physiol Regul Integr Comp Physiol* 296, R1348-1357.

Wang, Y., Nishida, S., Elalieh, H.Z., Long, R.K., Halloran, B.P., and Bikle, D.D. (2006). Role of IGF-I signaling in regulating osteoclastogenesis. *J Bone Miner Res* 21, 1350-1358.

Wang, Y.F., Tseng, Y.C., Yan, J.J., Hiroi, J., and Hwang, P.P. (2009b). Role of SLC12A10.2, a Na-Cl cotransporter-like protein, in a Cl uptake mechanism in zebrafish (*Danio rerio*). *Am J Physiol Regul Integr Comp Physiol* 296, R1650-1660.

Weksberg, R., Shen, D.R., Fei, Y.L., Song, Q.L., and Squire, J. (1993). Disruption of insulin-like growth factor 2 imprinting in Beckwith-Wiedemann syndrome. *Nat Genet* 5, 143-150.

Wessells, R.J., Fitzgerald, E., Cypser, J.R., Tatar, M., and Bodmer, R. (2004). Insulin regulation of heart function in aging fruit flies. *Nat Genet* 36, 1275-1281.

White, M.F., Livingston, J.N., Backer, J.M., Lauris, V., Dull, T.J., Ullrich, A., and Kahn, C.R. (1988a). Mutation of the insulin receptor at tyrosine 960 inhibits signal transmission but does not affect its tyrosine kinase activity. *Cell* 54, 641-649.

- White, M.F., Shoelson, S.E., Keutmann, H., and Kahn, C.R. (1988b). A cascade of tyrosine autophosphorylation in the beta-subunit activates the phosphotransferase of the insulin receptor. *J Biol Chem* *263*, 2969-2980.
- Whitfield, J.F. (2009). Calcium, calcium-sensing receptor and colon cancer. *Cancer Lett* *275*, 9-16.
- Wienholds, E., van Eeden, F., Kusters, M., Mudde, J., Plasterk, R.H., and Cuppen, E. (2003). Efficient target-selected mutagenesis in zebrafish. *Genome Res* *13*, 2700-2707.
- Wilson, P.W., Harding, M., and Lawson, D.E. (1985). Putative amino acid sequence of chick calcium-binding protein deduced from a complementary DNA sequence. *Nucleic Acids Res* *13*, 8867-8881.
- Wissenbach, U., Niemeyer, B.A., Fixemer, T., Schneidewind, A., Trost, C., Cavalie, A., Reus, K., Meese, E., Bonkhoff, H., and Flockerzi, V. (2001). Expression of CaT-like, a novel calcium-selective channel, correlates with the malignancy of prostate cancer. *J Biol Chem* *276*, 19461-19468.
- Wollheim, C.B., and Sharp, G.W. (1981). Regulation of insulin release by calcium. *Physiol Rev* *61*, 914-973.
- Wood, A.W., Duan, C., and Bern, H.A. (2005a). Insulin-like growth factor signaling in fish. *Int Rev Cytol* *243*, 215-285.
- Wood, A.W., Schlueter, P.J., and Duan, C. (2005b). Targeted knockdown of insulin-like growth factor binding protein-2 disrupts cardiovascular development in zebrafish embryos. *Mol Endocrinol* *19*, 1024-1034.
- Wood, R.J., Tchack, L., and Taparia, S. (2001). 1,25-Dihydroxyvitamin D₃ increases the expression of the CaT1 epithelial calcium channel in the Caco-2 human intestinal cell line. *BMC Physiol* *1*, 11.
- Wood, T.L., Rogler, L.E., Czick, M.E., Schuller, A.G., and Pintar, J.E. (2000). Selective alterations in organ sizes in mice with a targeted disruption of the insulin-like growth factor binding protein-2 gene. *Mol Endocrinol* *14*, 1472-1482.
- Wood, W.I., Cachianes, G., Henzel, W.J., Winslow, G.A., Spencer, S.A., Hellmiss, R., Martin, J.L., and Baxter, R.C. (1988). Cloning and expression of the growth hormone-dependent insulin-like growth factor-binding protein. *Mol Endocrinol* *2*, 1176-1185.

- Woods, K.A., Camacho-Hubner, C., Savage, M.O., and Clark, A.J. (1996). Intrauterine growth retardation and postnatal growth failure associated with deletion of the insulin-like growth factor I gene. *N Engl J Med* 335, 1363-1367.
- Xu, Q., Li, S., Zhao, Y., Maures, T.J., Yin, P., and Duan, C. (2004). Evidence that IGF binding protein-5 functions as a ligand-independent transcriptional regulator in vascular smooth muscle cells. *Circ Res* 94, E46-54.
- Yakar, S., Rosen, C.J., Beamer, W.G., Ackert-Bicknell, C.L., Wu, Y., Liu, J.L., Ooi, G.T., Setser, J., Frystyk, J., Boisclair, Y.R., *et al.* (2002). Circulating levels of IGF-1 directly regulate bone growth and density. *J Clin Invest* 110, 771-781.
- Ye, P., and D'Ercole, J. (1998). Insulin-like growth factor I (IGF-I) regulates IGF binding protein-5 gene expression in the brain. *Endocrinology* 139, 65-71.
- Yin, P., Xu, Q., and Duan, C. (2004). Paradoxical actions of endogenous and exogenous insulin-like growth factor-binding protein-5 revealed by RNA interference analysis. *J Biol Chem* 279, 32660-32666.
- Zhang, M., Xuan, S., Bouxsein, M.L., von Stechow, D., Akeno, N., Faugere, M.C., Malluche, H., Zhao, G., Rosen, C.J., Efstratiadis, A., *et al.* (2002). Osteoblast-specific knockout of the insulin-like growth factor (IGF) receptor gene reveals an essential role of IGF signaling in bone matrix mineralization. *J Biol Chem* 277, 44005-44012.
- Zhao, G., Monier-Faugere, M.C., Langub, M.C., Geng, Z., Nakayama, T., Pike, J.W., Chernausek, S.D., Rosen, C.J., Donahue, L.R., Malluche, H.H., *et al.* (2000). Targeted overexpression of insulin-like growth factor I to osteoblasts of transgenic mice: increased trabecular bone volume without increased osteoblast proliferation. *Endocrinology* 141, 2674-2682.
- Zhao, Y. (2007). Insulin-like growth factor binding protein (IGFBP)-5: a protein of two destinations. Doctoral dissertation, The University of Michigan.
- Zhao, Y., Yin, P., Bach, L.A., and Duan, C. (2006). Several acidic amino acids in the N-domain of insulin-like growth factor-binding protein-5 are important for its transactivation activity. *J Biol Chem* 281, 14184-14191.
- Zhou, J., Li, W., Kamei, H., and Duan, C. (2008). Duplication of the IGFBP-2 gene in teleost fish: protein structure and functionality conservation and gene expression divergence. *PLoS One* 3, e3926.

Zhu, Y., Song, D., Tran, N.T., and Nguyen, N. (2007). The effects of the members of growth hormone family knockdown in zebrafish development. *Gen Comp Endocrinol* 150, 395-404.

Zhuang, L., Peng, J.B., Tou, L., Takanaga, H., Adam, R.M., Hediger, M.A., and Freeman, M.R. (2002). Calcium-selective ion channel, CaT1, is apically localized in gastrointestinal tract epithelia and is aberrantly expressed in human malignancies. *Lab Invest* 82, 1755-1764.

Zon, L.I., and Peterson, R.T. (2005). In vivo drug discovery in the zebrafish. *Nat Rev Drug Discov* 4, 35-44.

Zou, S., Kamei, H., Modi, Z., and Duan, C. (2009). Zebrafish IGF genes: gene duplication, conservation and divergence, and novel roles in midline and notochord development. *PLoS One* 4, e7026.